NASA
SPACE VEHICLE
DESIGN CRITERIA
(CHEMICAL PROPULSION)

NASA SP-8109

LIQUID ROCKET ENGINE CENTRIFUGAL FLOW TURBOPUMPS

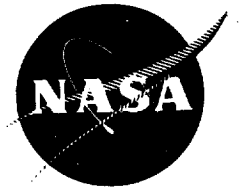

DECEMBER 1973

NATIONAL AERONAUTICS AND SPACE ADMINISTRATION

FOREWORD

NASA experience has indicated a need for uniform criteria for the design of space vehicles. Accordingly, criteria are being developed in the following areas of technology:

Environment
Structures
Guidance and Control
Chemical Propulsion

Individual components of this work will be issued as separate monographs as soon as they are completed. This document, part of the series on Chemical Propulsion, is one such monograph. A list of all monographs issued prior to this one can be found on the final pages of this document.

These monographs are to be regarded as guides to design and not as NASA requirements, except as may be specified in formal project specifications. It is expected, however, that these documents, revised as experience may indicate to be desirable, eventually will provide uniform design practices for NASA space vehicles.

This monograph, "Liquid Rocket Engine Centrifugal Flow Turbopumps", was prepared under the direction of Howard W. Douglass, Chief, Design Criteria Office, Lewis Research Center; project management was by Harold Schmidt. The monograph was written by R. B. Furst of Rocketdyne Division, Rockwell International Corporation, and was edited by Russell B. Keller, Jr. of Lewis. Significant contributions to the text were made by H. Campen and F. Viteri of Aerojet Liquid Rocket Company. To assure technical accuracy of this document, scientists and engineers throughout the technical community participated in interviews, consultations, and critical review of the text. In particular, Mario Messina of Bell Aerospace Company; Glen M. Wood of United Aircraft Corporation; and C. H. Hauser and Dean D. Scheer of the Lewis Research Center individually and collectively reviewed the text in detail.

Comments concerning the technical content of this monograph will be welcomed by the National Aeronautics and Space Administration, Lewis Research Center (Design Criteria Office), Cleveland, OH 44135.

December 1973

For sale by the National Technical Information Service
Springfield, Virginia 22151
Price – $4.50

GUIDE TO THE USE OF THIS MONOGRAPH

The purpose of this monograph is to organize and present, for effective use in design, the significant experience and knowledge accumulated in development and operational programs to date. It reviews and assesses current design practices, and from them establishes firm guidance for achieving greater consistency in design, increased reliability in the end product, and greater efficiency in the design effort. The monograph is organized into two major sections that are preceded by a brief introduction and complemented by a set of references.

The State of the Art, section 2, reviews and discusses the total design problem, and identifies which design elements are involved in successful design. It describes succinctly the current technology pertaining to these elements. When detailed information is required, the best available references are cited. This section serves as a survey of the subject that provides background material and prepares a proper technological base for the *Design Criteria* and Recommended Practices.

The *Design Criteria*, shown in italics in section 3, state clearly and briefly what rule, guide, limitation, or standard must be imposed on each essential design element to assure successful design. The *Design Criteria* can serve effectively as a checklist of rules for the project manager to use in guiding a design or in assessing its adequacy.

The Recommended Practices, also in section 3, state how to satisfy each of the criteria. Whenever possible, the best procedure is described; when this cannot be done concisely, appropriate references are provided. The Recommended Practices, in conjunction with the *Design Criteria*, provide positive guidance to the practicing designer on how to achieve successful design.

Both sections have been organized into decimally numbered subsections so that the subjects within similarly numbered subsections correspond from section to section. The format for the Contents displays this continuity of subject in such a way that a particular aspect of design can be followed through both sections as a discrete subject.

The design criteria monograph is not intended to be a design handbook, a set of specifications, or a design manual. It is a summary and a systematic ordering of the large and loosely organized body of existing successful design techniques and practices. Its value and its merit should be judged on how effectively it makes that material available to and useful to the designer.

CONTENTS

LIST OF FIGURES

LIST OF TABLES

LIQUID ROCKET ENGINE CENTRIFUGAL FLOW TURBOPUMPS

1. INTRODUCTION

The acceptance and highly successful application of centrifugal pumps in chemical as well as nuclear rocket engines result from the simplicity, reliability, light weight, wide operating range, minimal development time, and relatively low costs of these pumps. Usually, other types of pumps become competitive with the centrifugal design only when multistaging is necessary or maximum efficiency of operation is the paramount consideration.

In rocket engine applications, the requirements for light weight and low inlet pressures have resulted in many pump problems. These problems have included impeller rubbing that resulted in oxidizer-pump explosions; bearing failures caused by high axial and radial thrust; excessive cavitation damage; inadequate suction performance; undesirable oscillations in suction and discharge pressure; impeller blade failures; housing ruptures; stress-corrosion cracking; loss of design fits caused by centrifugal or thermal loads; static-seal leakage; and inadequate retention of the components. Additionally, problems have been encountered wherein the structural and dynamic characteristics of the vehicle were involved with those of the pumping system (i.e., POGO effect upon Titan II and Saturn[1]). The solutions to such problems become highly complex.

A particular problem with liquid-hydrogen pumps is the small tip width required for the impeller blade; present designs are rpm-limited and therefore operate normally at lower overall specific speeds than dense-liquid pumps because of the high head rise required. The requirement for small tip width results in fabrication difficulties and lower efficiencies. Improved designs for liquid-hydrogen pumps will require the extension of the current technology for bearings and seals and axial thrust balance systems; increases in critical speed by the use of bearings outboard of the turbine; increases in turbine speed and flow capability; the use of low-speed preinducers to satisfy required inlet pressure limits; and efficient interstage diffusers for multistage pumps.

Some of the pump problems indicated above resulted partially from insufficient background information for application to design analyses. The early axial and radial thrust problems

[1]Symbols, materials, and pumps, engines, and vehicles are identified in Appendix A.

associated with the turbopumps for the Titan I, Atlas, and Thor are attributable to this insufficiency. Also, cracking of cast impeller blades resulted from inadequate information on aluminum casting techniques for production of greatly differing cross-section thicknesses; stress corrosion of aluminum impellers and inducers arose from insufficient background in the influence of heat treatment on different alloys; and limited knowledge of inducer and impeller radial loads resulted in forces sufficient to cause pump inducer and impeller rubbing that led to catastrophic explosions. Some problems occurred because of poor design. For example, the design of cast or drilled bearing-coolant passages that could not be adequately cleaned or inspected resulted in clogging followed by bearing heating; overheated bearings operating in an oxidizer caused explosions or resulted in rubbing of other components that were damaged or that caused explosions.

This monograph presents the useful knowledge derived from these experiences so that similar problems may be avoided in future designs. The material within the monograph is organized along the lines of the pump design sequence. The arrangement and treatment of the subject matter emphasizes that the basic objective of the design effort is to achieve required pump performance within the constraints imposed by the engine/turbopump system. The design must provide this performance while maintaining structural integrity under all operating conditions. Such a design depends on simultaneous solutions of hydrodynamic and mechanical problems, as developed in the monograph.

2. STATE OF THE ART

Centrifugal pumps have generated up to 100 000 feet[1] of head in a single stage; they have been staged to generate even higher heads. Pumps for dense liquids (specific gravity ≥ 1) have been developed with flowrates ranging from 12 gpm at 75 000 rpm to 30 000 gpm at 5800 rpm; liquid-hydrogen pumps have delivered over the range of 800 gpm to 13 000 gpm at 46 000 rpm. The centrifugal pump is capable of operating over a wide range of flowrate without stall or surge. The centrifugal pump with shrouded impellers may operate with relatively large clearances between rotating and stationary parts; this characteristic is particularly advantageous when the pumped fluid is a highly reactive oxidizer. Once the basic pump requirements have been satisfied, the success of the centrifugal flow pump in a rocket engine system depends upon the designer's ability to recognize the cause and suppress the effect of the undesirable, often destructive, dynamic behavior associated with cavitation, start transients, and engine-feed-system oscillations.

Figure 1 illustrates the elements of a typical centrifugal flow pump and provides a basis for the discussions of pump design that follow.

2.1 CONFIGURATION SELECTION

The selection of a pump configuration is influenced by operational, hydrodynamic, and mechanical considerations that include inlet pressure, maximum impeller tip speed, limiting pressure per stage, engine-system compatibility, flow-range requirements, envelope size, pumped fluid, and weight. Many of these factors are interrelated, and some of them are established by the mission or vehicle requirements.

Past experience supports the need for considering limitations on rotating speed, even though the rotating speed should be as great as possible in order to minimize turbopump weight. Maximum pump efficiency, however, may be attained at a speed lower than maximum. The influence of efficiency must then be traded off to minimize equivalent weight (i.e., the increase in vehicle weight for a given loss in efficiency). Shaft critical speed is often a speed-limiting design factor. Critical speed is closely related to the location and size of the bearings and seals, and is influenced by the bearing spring rate. Bearing size must be sufficient to carry required axial and radial loads, and the bearing speed capability decreases as its capacity and size is increased. A relatively large stiff shaft is required to attain high critical speeds; however, the size of the shaft is limited by the maximum rubbing velocity of the shaft seals. The vehicle design considerations set the minimum pump inlet pressures, and the attainable suction specific speed(s) capability of the pump often limits the attainable speed. For high-speed, high-power liquid-hydrogen pumps, the turbine stress limits may

[1]Factors for converting U.S. customary units to the International System of Units (SI units) are given in Appendix B.

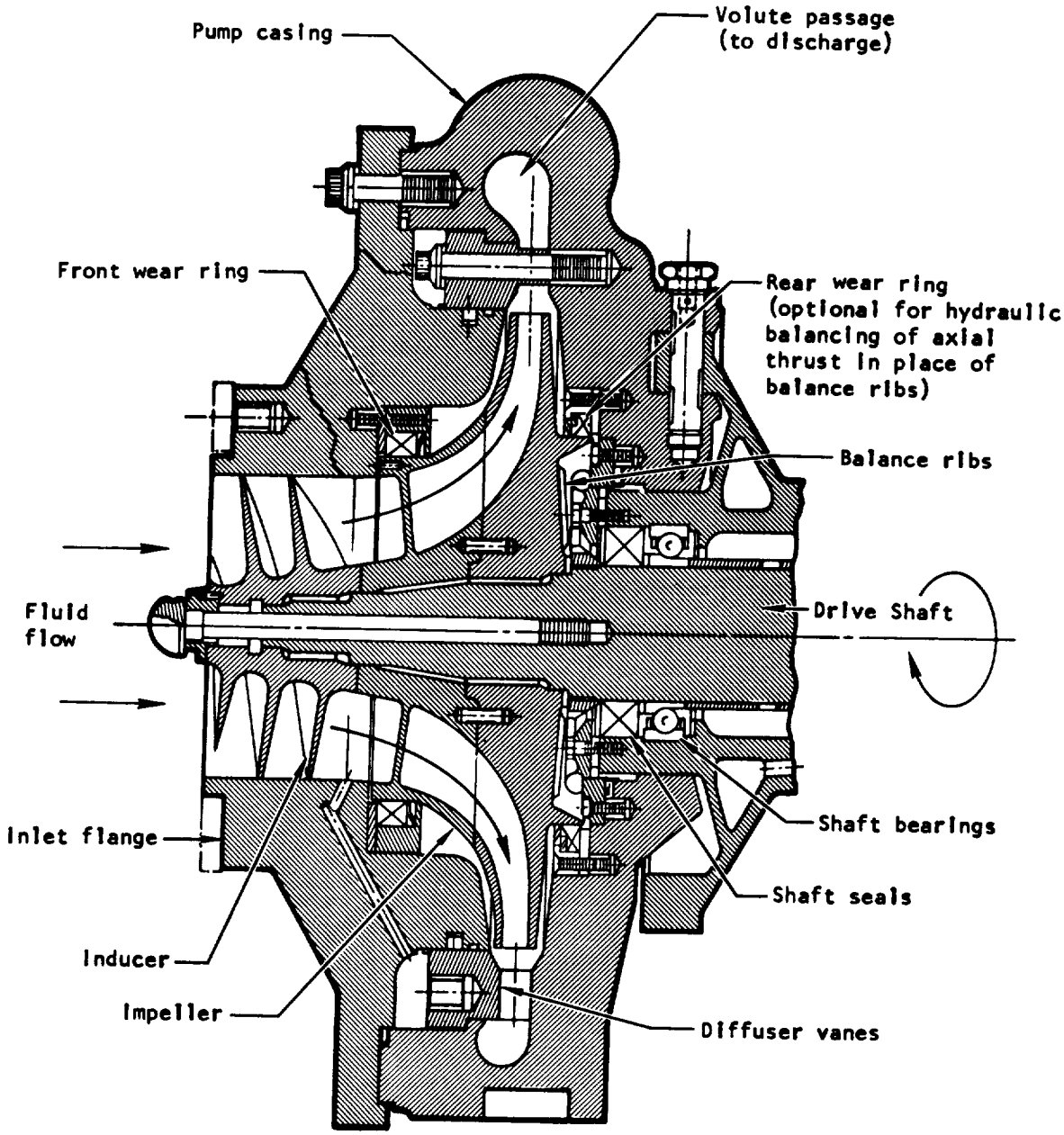

Figure 1. — Elements of a centrifugal flow pump.

determine the maximum operating speed. An example of the influence of the various speed-limiting factors over a range of flowrates for a liquid-oxygen pump is presented in figure 2.

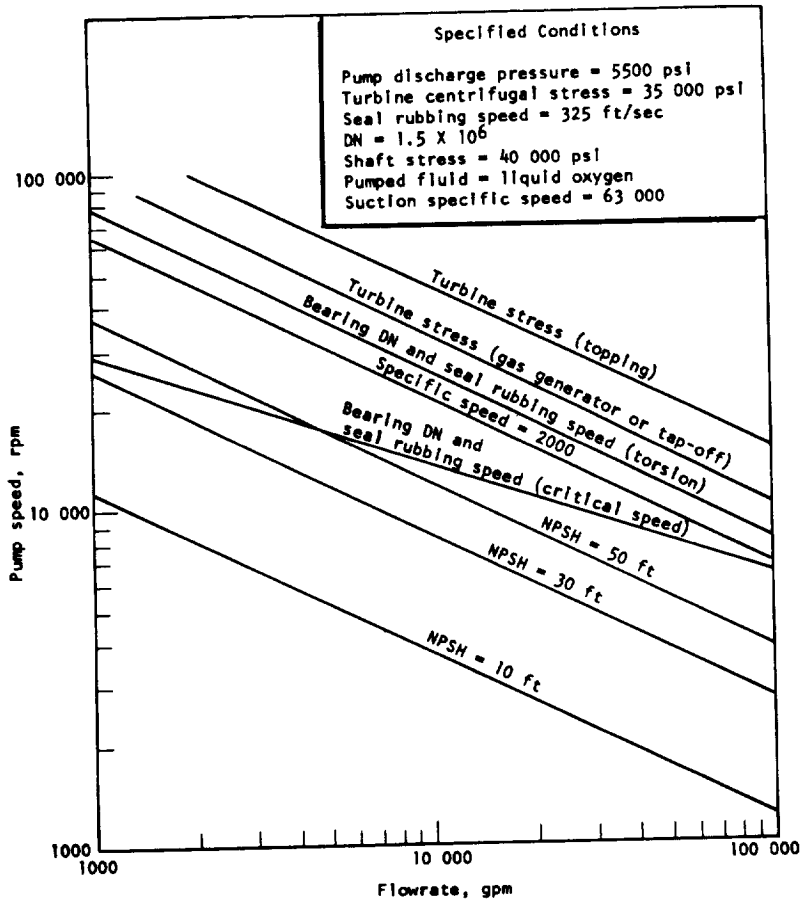

Figure 2. – Various kinds of pump speed limits illustrated for specified conditions.

The rocket engine design establishes the requirements for pump flow and pressure rise; the vehicle tank pressure and turbopump suction-performance limits most often set the pump speed rather than the desire for maximum efficiency. The pump design factors that enter into the final configuration selection are discussed in greater detail in the following sections and in references 1 and 2.

2.2 PUMP PERFORMANCE

The pump design is based primarily on the specified engine operating conditions (i.e., flowrate, headrise, and inlet pressure) and on other requirements such as throttling, system stability, turbine power margin, and the allowable pump development time. The best compromise of all requirements may be achieved at an efficiency point higher or lower than that at the nominal operating flowrate. The best-efficiency point relative to the operating point is established along with the selection of the shape of the headrise/capacity curve. In order to ensure that all information that influences pump performance is considered in design, a design specification is prepared to consolidate the available data and to point out the information that must be supplied by future analyses or tests.

The complexity of a pump increases with the number of stages required; therefore, the maximum pressure rise per stage is a significant design parameter in evaluating configurations for a given application. The impeller stress limits at high impeller tip speeds restrict the maximum headrise per stage to approximately 100 000 ft. A two-stage pump may generate up to 200 000 ft. of head, which is approximately 7000 psi when the fluid is liquid hydrogen. Because of its low density, liquid hydrogen is the only propellant requiring very high headrise and impeller tip speed.

Rocket engine pump efficiencies are lower than those of commercial pumps with comparable specific speeds (ref. 3), as discussed in section 2.2.2. Efficiency is dependent on size rather than on flowrate; therefore, the rocket engine pump flow usually is corrected to a speed corresponding to commercial pump practice before efficiencies at a given specific speed are compared.

2.2.1 Speed

The specific speed N_s and specific diameter D_s are useful parameters for classifying pump types because they indicate the stage characteristics and identify specific areas where the various pump configurations are best suited for the application. In addition, these parameters provide preliminary estimates of pump efficiency and pump size (diameter). The significance of N_s and D_s in pump design is evident in the expressions for the two parameters:

$$N_s = \frac{NQ^{1/2}}{H^{3/4}} \tag{1}$$

$$D_s = \frac{D_{t2} H^{1/4}}{Q^{1/2}} \tag{2}$$

where

N = rotational speed

Q = volumetric flowrate

H = headrise

D_{t2} = discharge tip diameter

Current flight-proven centrifugal flow pumps range from 450 to 2100 in specific speed; some development pumps (e.g., the Mark 14 for the Atlas vehicle) have reached 3000.

Two other parameters of significance in the basic pump design effort are efficiency η and head coefficient ψ. The overall efficiency η is the measure of hydraulic work related to input shaft work:

$$\eta = \frac{P_h}{P_{sh}} = \eta_h \, \eta_v \, \eta_m \tag{3}$$

where

P_h = hydraulic output horsepower

P_{sh} = input shaft horsepower

The hydraulic efficiency η_h is the measure of the actual headrise H compared with the ideal headrise H_i:

$$\eta_h = \frac{H}{H_i} = \frac{\text{actual headrise}}{\text{ideal headrise}} \tag{4}$$

The volumetric efficiency η_v is the measure of the flow losses that occur between the impeller discharge and the volute output:

$$\eta_v = \frac{Q_{\text{delivered}}}{Q_{\text{impeller discharge}}} \tag{5}$$

The mechanical efficiency η_m is the measure of the mechanical losses in the pump:

$$\eta_m = \frac{P_a}{P_{sh}} = \frac{\text{power available for hydrodynamic work}}{\text{shaft horsepower}} \tag{6}$$

where

P_a = shaft horsepower minus mechanical losses

The mechanical losses for pumps with impellers 10 in. in diameter or larger are very small and may be neglected. For pumps with impellers as small as 1.0 in. in diameter, the mechanical losses (seal and bearing power) may be as high as 20 percent of the shaft power.

Head coefficient ψ is a measure of headrise related to impeller discharge tip speed u_{t2}:

$$\psi = \frac{gH}{u_{t2}^2} \tag{7}$$

where

g = acceleration due to gravity

u_{t2} = impeller discharge tip speed

Figure 3 is a representative $N_s - D_s$ diagram relating N_s, D_s, η, and ψ for both centrifugal and axial flow turbopumps; additional information of this kind is presented in references 4 and 5.

2.2.1.1 CRITICAL SPEED

A basic objective in the design of rotating machinery is to avoid operation at a critical speed, i.e., a shaft rotative speed at which a rotor/stator system natural frequency coincides with a possible forcing frequency. Three important critical speeds usually are associated with a turbopump that has a shaft support system with two radial bearings: the shaft bending critical speed, and two speeds that are a function of the nonrigid bearing supports (refs. 6 through 32).

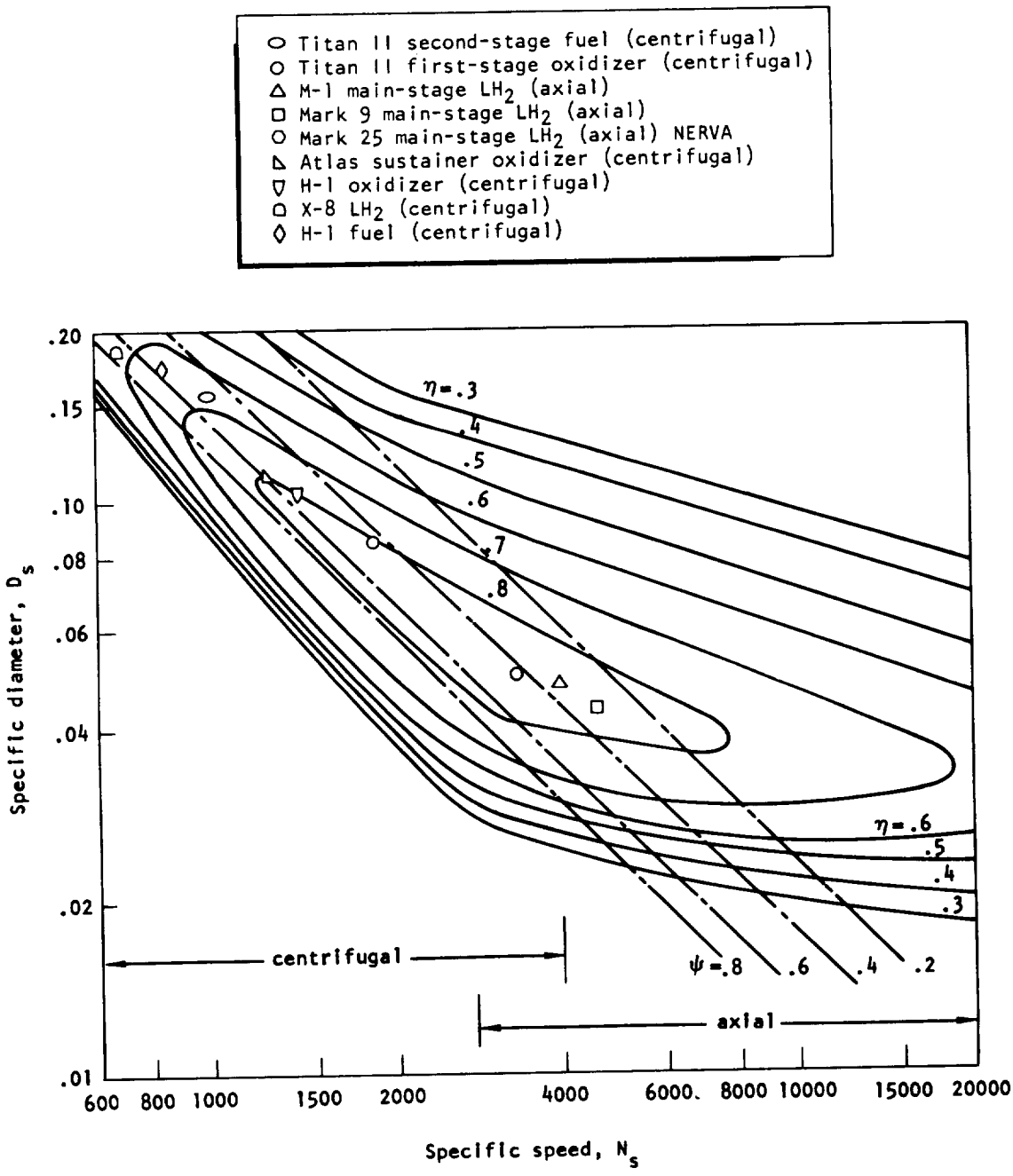

Figure 3. — Representative $N_s - D_s$ diagram for centrifugal and axial flow turbopumps.

There are two distinct design philosophies currently applied in the design of rocket engine turbopumps. In one (ref. 6), the bearing-and-shaft system is designed with all of the turbopump operating speeds kept below the first rigid-body whirl critical speed. To achieve this condition, high bearing spring rates are required. Therefore, roller bearings are often used at both ends of the shaft along with ball bearings if needed for axial thrust.

The other design philosophy (ref. 30) calls for normal pump operation above the first and second whirl critical speeds, but below any mode wherein significant shaft bending occurs. This practice requires lower bearing or bearing-support spring rates and a minimal internal looseness of the bearings. Consequently, only preloaded ball bearings are used. Duplex ball bearings are often used to increase the bearing radial-load capacity.

In both design approaches, a margin of approximately 20 percent is allowed between the shaft operating speed and the nearest calculated whirl critical speed. The disadvantages of operating liquid-hydrogen pumps below the first rigid-body whirl critical speed are the necessary high bearing spring rates and high bearing DN values; as a consequence, when the hydrogen-pump shaft transmits torque through the bearing, the bearing stresses and bearing wear tendencies generally are higher than the acceptable values. The disadvantage of operating above the first rigid-body whirl critical speed is the possibility that subsynchronous whirling instabilities will occur; in addition, machines that operate above the first or second critical speeds of the shaft can incur excessive bearing dynamic loads during partial-speed operation unless sufficient damping is provided (ref. 31).

Nearly all dense-fluid turbopumps operate below the first critical speed. Liquid-hydrogen pumps often operate between two critical speeds, and throttleable pumps may operate at a critical speed for a limited time during start transients or during test. The designer can ease critical-speed difficulties by employing light hardware that is carefully balanced. Axial dimensions are kept short, and the flow passages are shaped to yield optimum bearing spans. Reference 28 presents the important analytical procedures and considerations. For pumps that must operate over a wide speed range, it is necessary to determine whether all operation will be below the first critical speed or between two widely separated critical speeds, or whether some operation at a critical speed will be necessary. Operation below the first critical speed requires a lower maximum design speed. The degree of damping and the energy input, usually set by rotor imbalance, determine the maximum amplitude that will occur at resonance. For many designs, operation through a resonant speed on startup and shutdown transients is acceptable; however, sustained operation during rocket engine mainstage at speeds between 80 and 120 percent of a shaft critical speed set by bearing spring rate is avoided. Limited operation during development tests designed to evaluate amplitudes at critical speed is allowable.

2.2.1.2 SUCTION SPECIFIC SPEED

Suction specific speed S_s is a useful and significant design parameter that relates pump speed, flowrate, and net positive suction head:

$$S_s = \frac{N\,Q^{1/2}}{(NPSH)^{3/4}} \tag{8}$$

where

NPSH = net positive suction head

Corrected suction specific speed S'_s is the suction specific speed of a hypothetical inducer with zero inlet hub diameter that operates with the same inlet axial velocity, inlet tip speed, rotational speed, and minimum required NPSH as the test inducer. The correction is made by numerically increasing the flowrate to compensate for the area blocked by the hub at the inlet:

$$S'_s = \frac{S_s}{(1 - \nu^2)^{1/2}} \tag{9}$$

where

$$\nu = \frac{\text{inlet hub diam.}}{\text{inlet tip diam.}} = \frac{D_{h1}}{D_{t1}}$$

When pumping propellants with vapor pressures similar to that of cold water, rocket engine pumps have been operated with suction specific speed capabilities ranging from 15 000 to over 40 000. The properties of the pumped liquid have a pronounced effect on the suction performance of a pump as shown by the curves in figure 4. The data points plotted on this figure represent test data for the pumps and inducers listed; pump data is for 2-percent head loss, inducer data for 10-percent head loss.

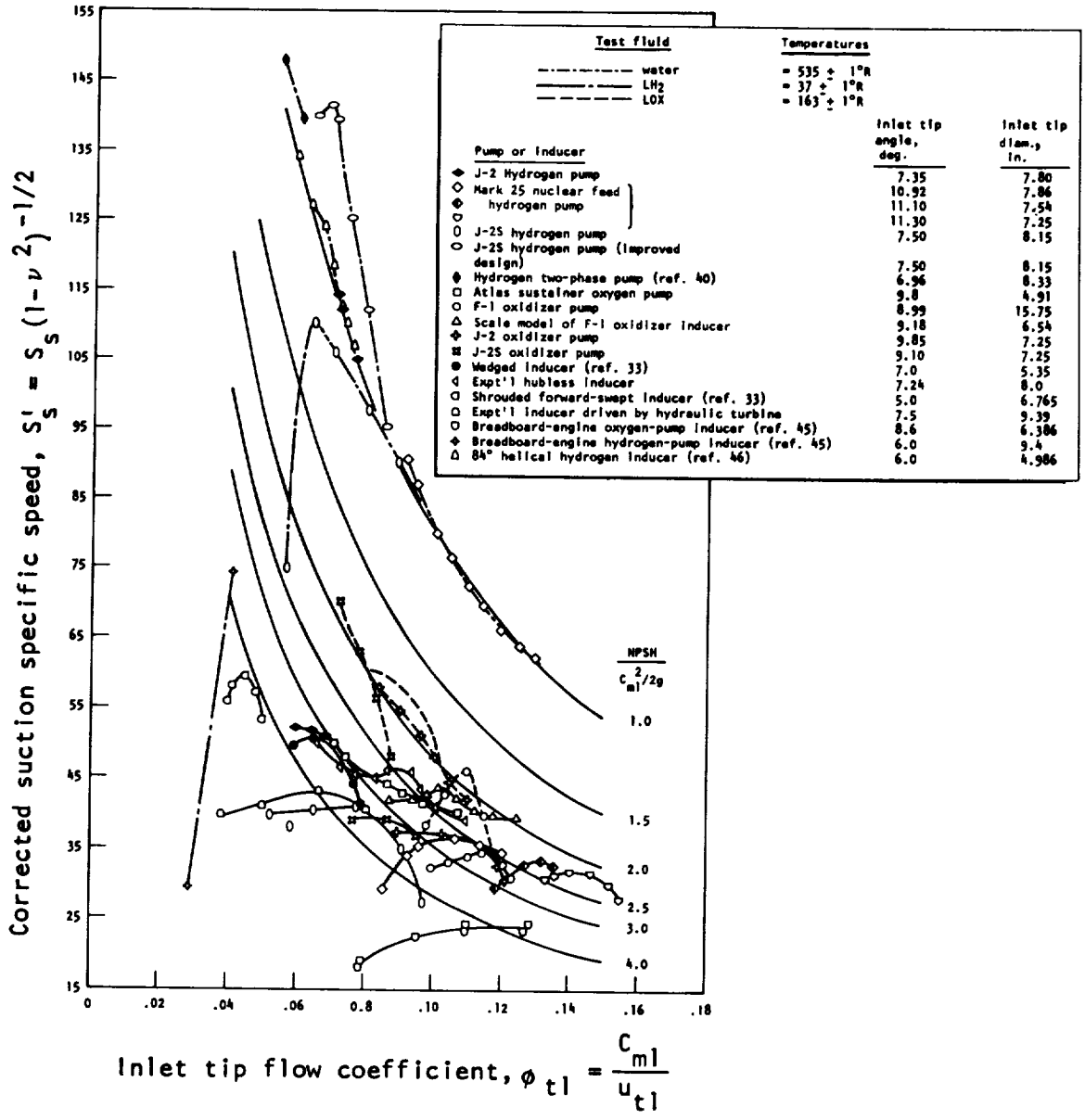

Figure 4. – Summary of empirical data on suction performance of various pumps and inducers.

The inducer inlet tip blade angles β_{t1} presented in figure 4 may be related to the inlet tip flow coefficient ϕ_{t1} by the following relation:

$$\beta_{t1} = \arctan \phi_{t1} + \alpha_{t1} \tag{10}$$

where

ϕ_{t1} = c_{m1}/u_{t1}

c_{m1} = meridional velocity at inlet

u_{t1} = tangential velocity at inlet tip

α_{t1} = inlet tip incidence angle

The usual practice is to strive for a minimum value for α_{t1} (compatible with the blade thickness distribution for structural requirements) so that suction specific speed is maximized (ref. 33).

A pump flowing liquid hydrogen, liquid oxygen, alcohol, or butane is capable of operating at lower NPSH values than the same pump flowing cold water (refs. 33 through 41). These differences in cavitation performance are attributed to the thermodynamic properties of the propellants that result in a thermodynamic suppression head (TSH). The TSH lowers the required NPSH; when liquid hydrogen is pumped, TSH is sufficient to permit pumping a saturated liquid with an acceptable small loss in pump headrise (refs. 38 through 41). The increased suction specific speed capability of cryogenic fluids permits a pump to operate at higher rotating speeds with these fluids than with a low-vapor-pressure liquid such as RP-1 or cold water. The value of TSH is dependent on the inducer or impeller design, on the operating point, and on the fluid properties. Therefore, tests are required to determine the required NPSH.

2.2.1.3 TURBINE LIMITS

For pumped fluids with a density much less than that of water (e.g., LH_2), turbine stress may be a speed-limiting factor on pumps for high-chamber-pressure rocket engines. Turbine blade stresses increase for a given tip speed as the blade height increases. When an increase in turbine power is required, the flowrate of the turbine drive gas must increase, thereby requiring a larger flow area at a given pressure and temperature. The larger annulus area (A_a) may be achieved by increasing the blade height or by increasing the tip diameter. The speed limitations on the turbine may be related to the quantity $N^2 A_a$, the product of the square of the speed N and the rotor blade annulus area A_a. When the stress-limiting value of $N^2 A_a$ is reached, the speed must be reduced as the turbine power is increased.

The quantity $N^2 A_a$ has a maximum value depending upon the materials of fabrication and the operating temperature. The limiting stress relations are explained in greater detail in reference 42. The turbine stress does not limit the rotating speeds for pumps handling fluids with a density approximately that of water.

2.2.1.4 BEARING AND SEAL LIMITS

The bearing required to support the radial and axial loads of a rotating assembly has an upper speed limit that is related to bearing size and to the required operating life. Bearing speed limits are discussed in detail in reference 43. If rubbing shaft seals are required for minimum leakage, the maximum allowable rubbing speed combined with the shaft size as limited by its torque capacity may limit the rotating speed. Reference 44 discusses shaft seal types and their speed limits.

If conventional nose-rubbing shaft seals wear too rapidly because of high rubbing speeds, lift-off seals may be used. When the shaft is not rotating, a lift-off seal provides the low leakage rate typical of the nose-rubbing seal. When the shaft is rotating, the lift-off seal is actuated by a liquid or gas pressure source to separate the sealing surfaces to prevent high-speed rubbing. During this mode of operation, the sealing function is provided by noncontacting seals such as labyrinth seals, floating ring seals, hydrodynamic, or hydrostatic seals. Seal leakage greater than that of rubbing seals must be accepted.

Bearings may be located outboard of the rotating assembly so that the bearing diameter can be smaller than the shaft diameter required by torque or critical speed. Outboard bearing installations have been used on a feed-system turbine for a nuclear rocket engine. To date, outboard bearings have not been used on a complete flight-system turbopump; however, their use is being given serious consideration in advanced designs.

2.2.2 Efficiency

The efficiency of a centrifugal pump is influenced by its operating conditions and by its design. The operating conditions that most strongly contribute to pump efficiency are speed, flowrate, and headrise. As shown in equation (1), these parameters are combined into the pump specific speed N_s.

Specific speed has been used with flowrate Q as a parameter to characterize commercial pump efficiency. Commercial pumps pumping water at certain values for Q and N_s have typical sizes established for the most part by the driving electric motors. Rocket engine pumps, in particular hydrogen pumps, operate at speeds much higher than those of commercial pumps; therefore, for a given flowrate and specific speed, rocket engine pumps

are smaller in size than commercial pumps. This difference contributes to the observed lower efficiency of rocket engine pumps compared with the efficiencies of commercial pumps for the same flowrate. In addition, the higher rotating speeds of rocket engine pumps and the reactive propellants require operating clearances larger than those typical of commercial pumps; the larger clearances result in reduced efficiency. The higher suction specific speeds require increased inlet diameters and thus result in reduced efficiency for a given specific speed, as shown in figure 5. Figure 5 is based on information presented in reference 3 and on test results for the pumps listed in the figure; the cross-hatched areas are discussed in section 2.3.1.1.

Design factors that influence efficiency are the type of impeller (open face or fully shrouded), vaned diffuser or volute, and the requirement for staging. The pump design head coefficient also influences the pump efficiency as indicated in figure 3.

2.2.2.1 PUMP SIZE AND PUMPED FLUID

The size of a pump may influence the pump efficiency by Reynolds-number effects, by relative-surface-roughness effects, and by increased difficulty in maintaining desirable blade, vane, and passage shapes as size is reduced. Reynolds number has little influence on scaling effects with rocket engine pumps, since the number always is high. Roughness of the surface, however, must be minimized for small pumps. Schlichting's formula (ref. 47) for admissible roughness K_{adm} is

$$K_{adm} = \frac{100\,L}{Re_L} \tag{11}$$

where

L = length of the flow passage

Re_L = Reynolds number based on length

Schlichting's criterion is based on keeping the surface irregularities inside the boundary layer.

The pumped fluid influences rocket engine pump performance primarily because oxidizer pumps require large clearances to avoid the possibility of explosion that may result from rubbing. Oxidizer pumps therefore are less efficient than fuel pumps for the same size and specific speed.

		D_{t2}, in.	ψ	η
①	X-8 LH_2	11.0	0.703	0.666
②	Atlas booster RP-1	14.25	0.613	0.720
③	Atlas booster LOX	11.0	0.596	0.785
④	Atlas sustainer RP-1*	8.60	0.589	0.700
⑤	Atlas sustainer LOX	7.7	0.560	0.670
⑥	F-1 RP-1	23.4	0.563	0.760
⑦	F-1 LOX	19.5	0.487	0.745
⑧	J-2 LOX	10.2	0.448	0.815

*No inducer, S_s = 15000

Corrected suction specific speed with coupled inducer

(A) 40000
(B) 20000
(C) 10000
TSH = 0

—·—·— NPSH = $3\frac{C_{m1}^2}{2g}$

— — — — NPSH = $2\frac{C_{m1}^2}{2g}$

——— η (values as noted)

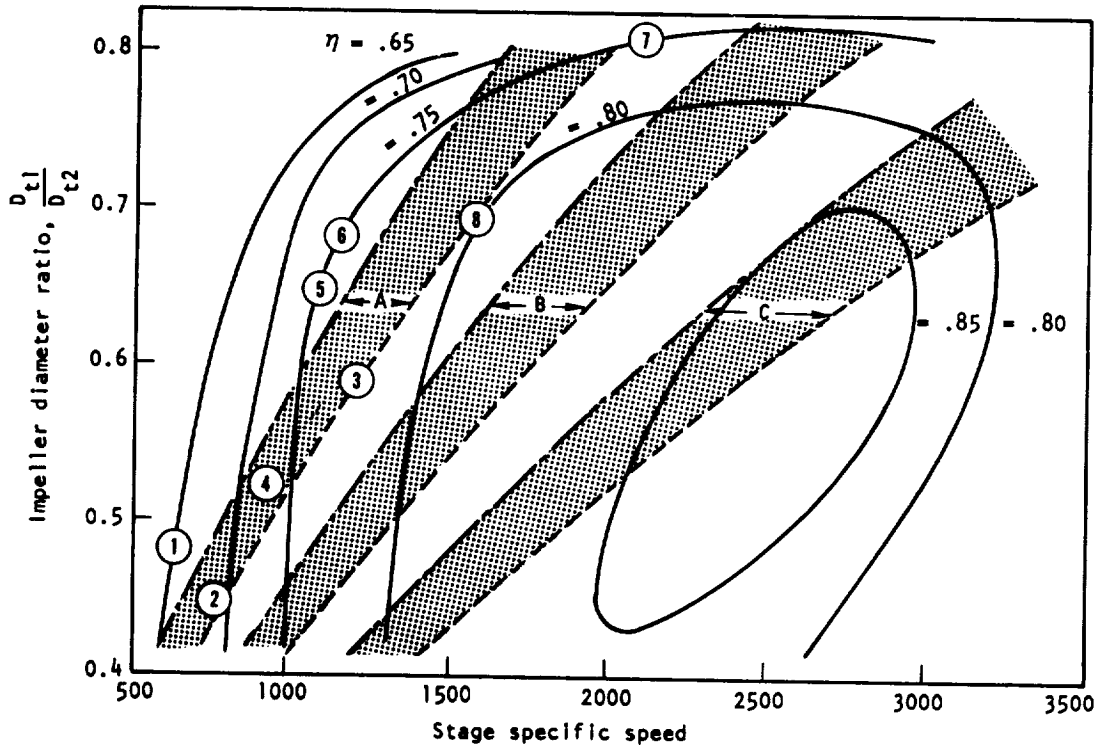

Figure 5. — Influence of impeller diameter ratio on pump performance.

Pump	D_{t2}, in.	Diffuser Geometry	Impeller Geometry
① Expt'l LF_2	1.20	Volute	Shroud
② Atlas Sustainer LOX	7.70	Vaneless Diffuser & Volute	Shroud
③ Atlas Sustainer RP-1	8.60	Volute	Shroud
④ Redstone Oxidizer	9.65	Volute	Shroud
⑤ J-2 LOX	10.20	Volute	Shroud
⑥ XLR-129 LH_2 1st Stage	10.62	Vaneless Diffuser & Volute	Open Face
⑦ Saturn I-B Booster LOX	11.00	Vaned Diffuser & Volute	Shroud
⑧ X-8 LH_2	11.00	Vaned Diffuser & Volute	Shroud
⑨ Redstone Fuel	11.80	Volute	Shroud
⑩ XLR-129 LH_2 2nd Stage	12.60	Vaneless Diffuser & Volute	Open Face
⑪ Saturn I-B Booster RP-1	13.30	Vaned Diffuser & Volute	Shroud

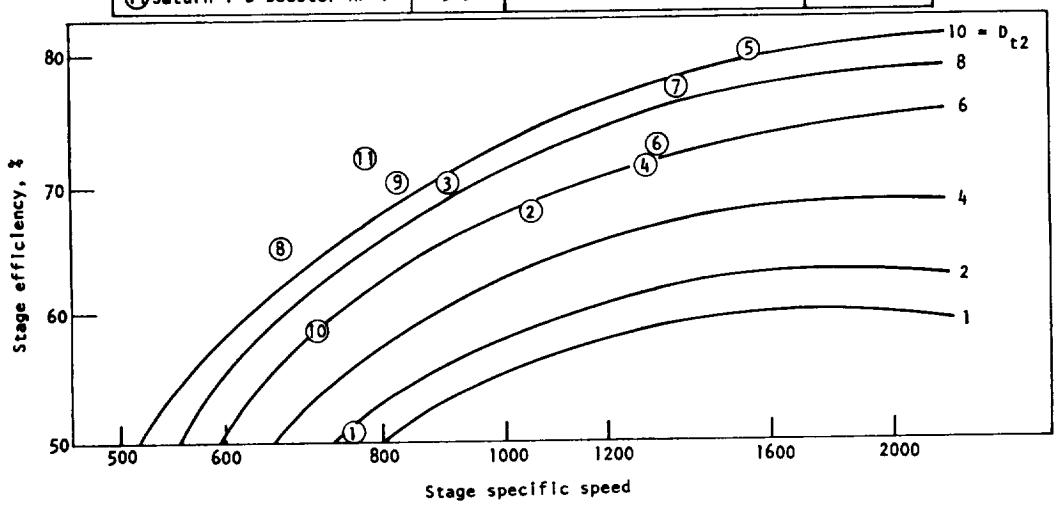

Figure 6. — Influence of pump size on efficiency.

The influences of size and pumped fluid on pump efficiency are presented in figure 6. The impeller discharge tip diameter D_{t2} is used as the characteristic dimension. The curves are based on material from the literature (ref. 48); test results for the pumps listed are superimposed on the curves.

Liquid hydrogen is compressible, and isentropic efficiency therefore is decreased by the temperature rise of the fluid as speed is increased. The temperature at a pump inlet is increased above the bulk liquid inlet temperature by the hot leakage flows, the result being a decrease in the isentropic efficiency by an amount greater than that caused by the recirculating flow. This influence for the J-2S hydrogen pump is presented in figure 7. Approximately 30 percent of the efficiency change with speed results from pressure-induced clearance changes; the remainder is caused by heating effects.

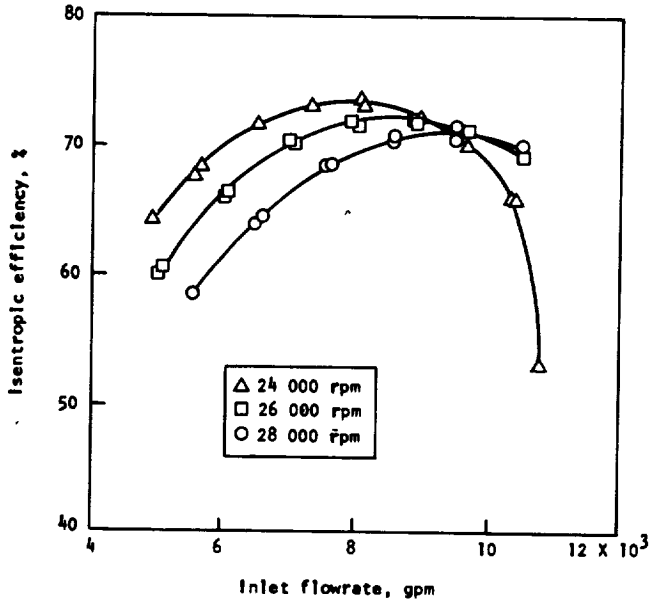

Figure 7. — Influence of speed on hydrogen-pump efficiency (J-2S).

2.2.2.2 GEOMETRY

The single design requirement that most strongly influences the geometry of rocket engine pumps is the necessity for operating at high suction specific speeds. Typical commercial pumps without inducers are designed for suction specific speeds of approximately 10 000 (gpm units); rocket engine pumps are often designed for suction specific speeds in excess of 40 000. Pumps designed for high suction specific speed require increased inlet diameters to reduce the inlet velocity and inducers that are capable of pumping with cavitating flow. Figure 8 compares the geometry of pumps with N_s = 1500 designed for suction specific speeds of 10 000 and 40 000.

As pointed out by Wislicenus (ref. 3), the increased size of the flow passages necessary for low NPSH values or high suction specific speed imposes an efficiency penalty. The efficiency penalty presented in reference 3 was compared with available data to generate the curves in figure 9 showing the influence of increasing design suction specific speeds and specific speeds in limiting rocket engine pump efficiency. These influences, along with the effect of the ratio of impeller inlet tip diameter to discharge tip diameter, are presented in figure 5.

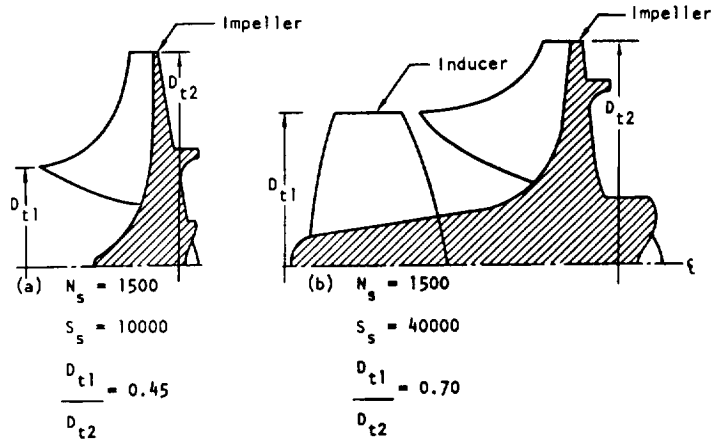

Figure 8. – Influence of suction specific speed on pump geometry.

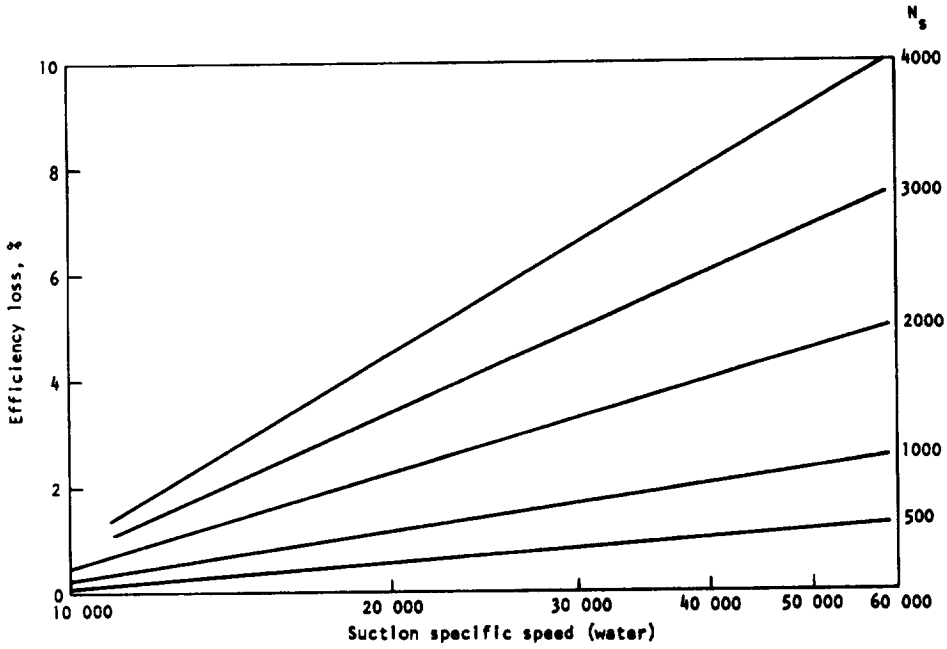

Figure 9. – Influence of suction specific speed on efficiency.

The use of vaned diffusers in centrifugal pumps results in increased efficiency over pumps with vaneless diffusers or pumps discharging the impeller flow directly into a volute. The use of vaned diffusers increases the overall pump diameter unless a folded volute is used. Pump efficiency is increased by reducing the velocity in the pump volute. The velocity is reduced in the vaned diffusers in a short length, and therefore the flow-path length subject to the high velocity leaving the impeller is greatly reduced. Vaned diffusers contribute a greater efficiency increase when the pump head coefficient is high ($\psi > 0.5$) and when the specific speed is low ($N_S < 1500$). Examples of pump efficiency with volutes only and volutes following vaneless or vaned diffusers are presented in figure 6. Vaneless diffusers result in the lowest efficiency and generally are not used for pumps. The geometry of the different diffuser types is presented in figure 10.

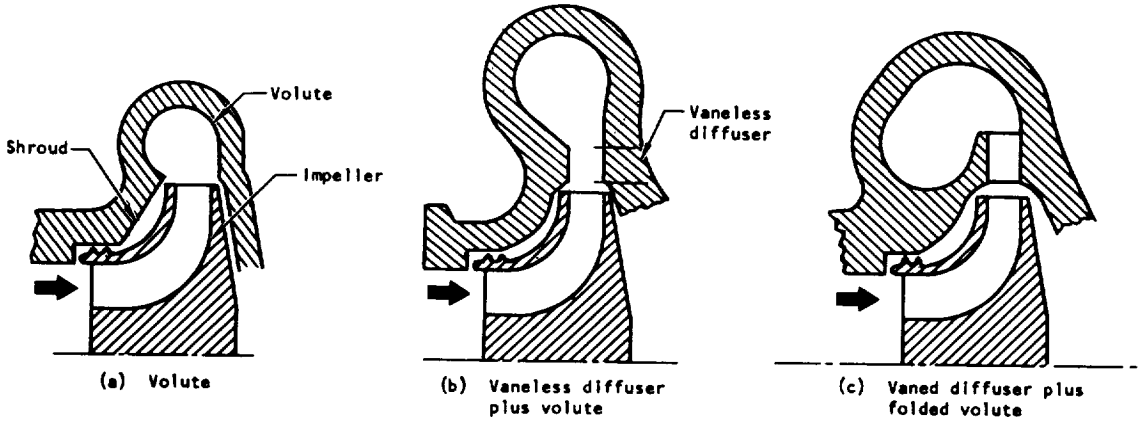

Figure 10. – Geometries for three types of diffusing systems.

2.2.2.3 STAGING

The low density of liquid hydrogen requires that high headrises be produced for a given pressure rise. High impeller tip speeds and low specific speeds thus are necessary. The impeller tip speeds may be reduced and the stage specific speed may be increased by producing the required pressure rise in more than one stage. This practice results in increased pump efficiency and reduced impeller stresses.

The problems that occur with staging are associated with the large velocity difference between the impeller discharge velocity of a given stage and the impeller inlet velocity of the following stage. The ratio of the impeller discharge velocity to impeller inlet velocity may be as high as six. The high velocity ratio has resulted in nonuniform impeller inlet velocities caused by excessive diffusion in the flow passages leading from one impeller to a following impeller.

The two basic types of interstage flow passages are the external diffusing passage and the internal crossover (fig. 11). Only the external passage type has been incorporated in a production rocket engine pump (the RL10 hydrogen pump). The internal-crossover type most generally is used for high-pressure commercial pumps as it leads to reduced weight and high efficiency. These same factors promise that the internal-crossover type of multistage pump will find applications in high-pressure hydrogen pumps.

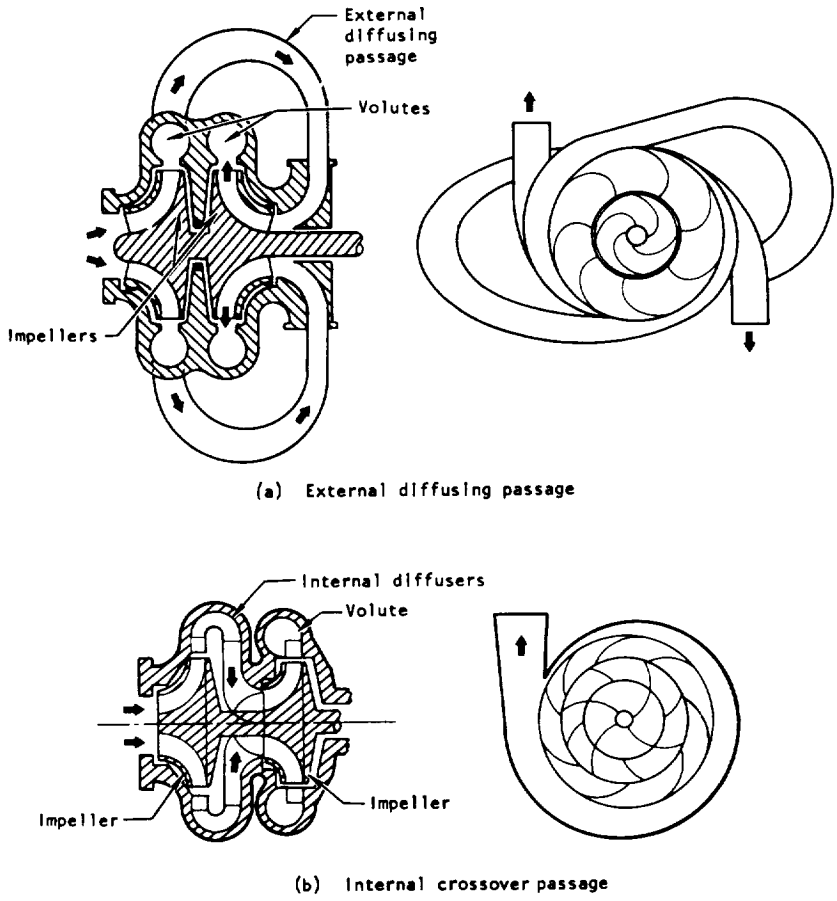

Figure 11. – Basic types of interstage flow passages.

Design limits for interstage diffusing systems have not been published in detail, although many high-efficiency multistage pumps have been developed by the commercial pump

industry. A performance comparison of two widely differing sizes of commercial pumps, as indicated by the different Q/N values, is presented in figure 12 (ref. 49). The subscript d on symbols in figure 12 indicates the value of the parameter at the design point.

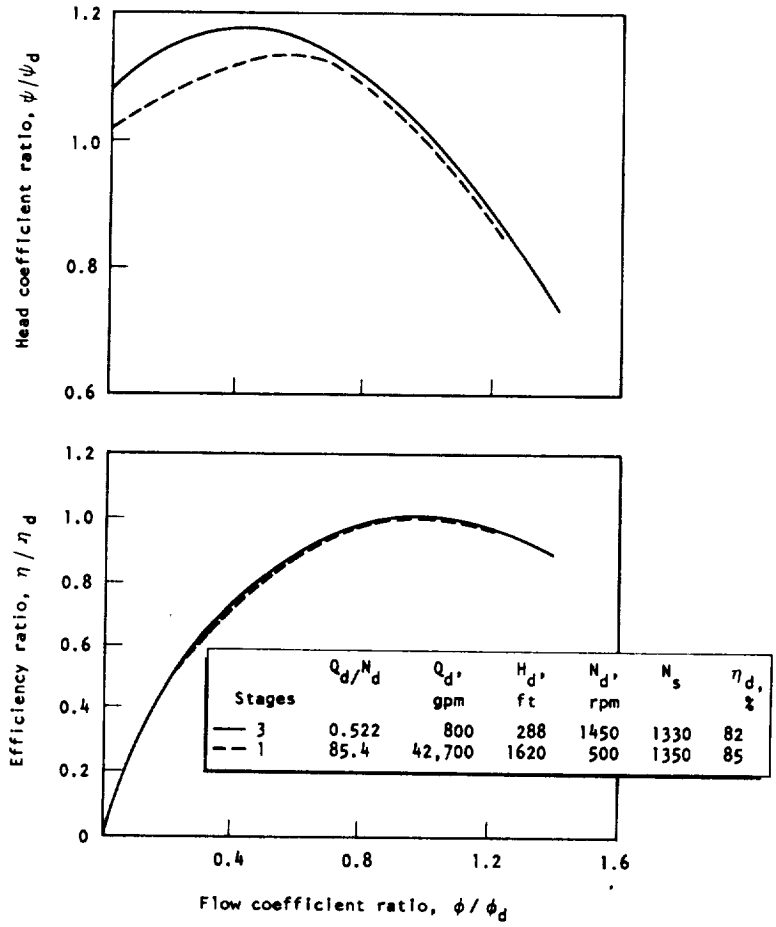

Figure 12. – Performance comparison of internal-crossover pumps differing greatly in size.

2.2.3 Flow Range

The range of flowrates over which a centrifugal pump will operate with stability in the rocket engine system determines the engine's throttling capability. The flow-range capability depends on the flow resistance, inductance, and capacitance of the rocket engine flow

system and on the pump head-vs-flow characteristic. The stability of a pump in a rocket engine system is calculated by the use of an analog or digital computer program that incorporates mathematical models of both the pump and the rocket engine flow system. In general, the pump with the steepest negative slope of the head-vs-flow curve is most stable in a given rocket engine system and therefore will operate over the widest flow range.

Experimental studies by Hansen (ref. 50) with impellers having full-length blades show that the widest flow range with a negative H-vs-Q slope is obtained with a small number of blades and a moderate head coefficient (ψ = 0.5). The head coefficient for a 7-blade impeller with rising-head-to-shutoff was 0.523 at the best-efficiency point for a vaned diffuser and volute. For a vaneless diffuser and volute, the blade number was reduced to 4 before a rising-head-to-shutoff could be obtained, and a head coefficient of 0.388 resulted. The impeller discharge blade angle was 20.75° in both cases. Reduction of the impeller blade number to 4 resulted in a substantial sacrifice of efficiency. Hansen's tests evaluated radial-flow centrifugal impellers with a limited specific speed range from 700 to 1300. Experiments conducted on experimental F-1 oxidizer pumps demonstrated that the number of blades at the impeller discharge could be doubled from 6 to 12 and that the best-efficiency head coefficient could be increased from 0.42 to 0.49 while maintaining or even improving the negative-slope flow range and obtaining a slight increase in efficiency.

It has been suggested by Anisimov (ref. 51) that the use of partial-length blades between full-length blades can improve flow range by virtue of reducing the boundary-layer thickness that exists with all full blades. Test results obtained by the rocket engine industry with an impeller with such partial-length blades agree with test results presented by Anisimov and verify his premise. The state-of-the-art practice is to use a small number of inlet blades (8 or less) with additional blades at the discharge as required to meet the design head coefficient.

Tests of impellers with comparable inlet flow coefficients and tip blade angles have indicated that the pump with the smaller hub diameter will have the superior flow range. Light hydrodynamic loading in the inlet region of the blades also appears to improve the flow range. With pump fluids such as liquid hydrogen, the internal heating caused by high headrise and low efficiency at reduced flowrates may cause loss of pumping ability. This loss is due to the backflow of internally generated gaseous hydrogen toward the inlet by the impeller centrifugal field. Increased inlet pressures delay such loss of pumping ability. Pump bypass as a means to improve flow range is limited to the amount that will result in 20 percent, by volume, of gas flowrate at the pump inlet (refs. 39 and 40).

Typical pump performance as related to pump geometry is presented in figure 13.

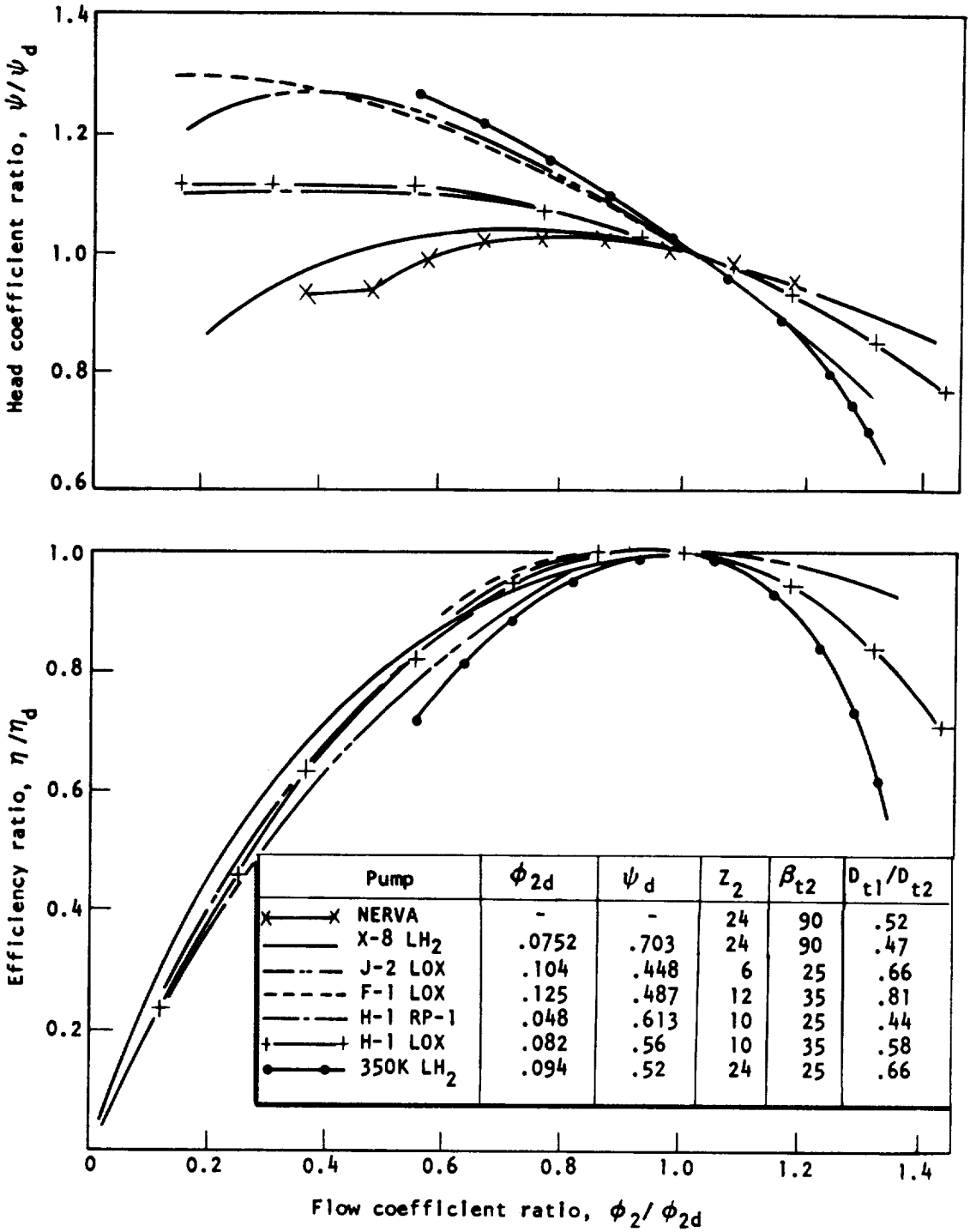

Figure 13. — Pump performance as a function of pump geometry.

2.3 IMPELLER

The impeller of a centrifugal pump converts the input shaft power into the static pressure rise and velocity energy of the pumped fluid. The velocity energy leaving the impeller is converted, for the most part, to static pressure in the pump housing. The impeller must deliver the design discharge flowrate plus any internal leakage or auxiliary flows and provide sufficient pressure rise to overcome the internal pump pressure losses while achieving the design pressure rise. The impeller must operate at the inlet pressure available from the vehicle, from a direct-coupled inducer, or from a separate low-pressure pump. The materials from which the impeller is fabricated must be compatible with the pumped fluids, the torque loads, and the tip speeds required to generate the pressure rise. The impeller axial and radial clearances during operation must be sufficient to avoid rubbing. The impeller may incorporate an integral inducer, a separate inducer, or no inducer at all. The impeller may be fully shrouded, open faced, or completely unshrouded. Completely unshrouded impellers have had limited use. The considerations involved in successful impeller design are discussed in detail in the following sections.

2.3.1 Hydrodynamic Design

Once the pump speed has been selected, the impeller design can then be accomplished. The overall pump head-vs-flow characteristics are largely dependent upon the impeller design that establishes the pump head coefficient ψ (eq. (7)). The pump head coefficient ψ is determined by the impeller discharge flow coefficient ϕ_2 ; discharge blade angle β_2 ; and the impeller discharge blade number Z_2 , which itself is a function of shroud stress, tip speed, β_2 , and fabrication method; thus

$$\psi = f(\phi_2, \beta_2, Z_2) \qquad (12)$$

The impeller suction specific speed S_s is determined by the inlet flow coefficient ϕ_1 , the inlet angle β_1 , the inlet-hub-to-inlet-tip diameter ratio ν, and the inlet blade thickness t_1 :

$$S_s = f(\phi_1, \beta_1, \nu, t_1) \qquad (13)$$

The impeller and overall pump efficiency are influenced by the surface finish of impeller flow path, the ratio of inlet tip to discharge tip diameter, and impeller seal and rotor clearances.

Efficient impeller designs such as those for the pumps in the Atlas and Titan booster engine systems have been developed by considering one-dimensional flow theory supplemented with empirical data. In more recent work, however, quasi-three-dimensional analyses are

Table I. - Impeller Geometry and Pump Performance

Pump identification[1]	Discharge blade angle β_2, deg	Number of blades Z_2	Z_2/β_2	Tip diameter, in.	Tip width, in.	Best-efficiency specific speed	Best pump efficiency
Titan							
87-5 fuel	35	12	0.343	10.75	0.74	1130	0.72
87-5 oxidizer	28	9	.322	9.42	1.00	1860	.75
91-5 fuel	28	8	.285	4.93	0.44	1750	.74
91-5 fuel (exptl)	28	9	.322	4.75	.48	1590	.68
91-5 oxidizer	35	12	.343	8.75	.53	945	.62
87-3 fuel	22.5	8	.355	10.99	.67	980	.55
87-3 oxidizer	22.5	8	.355	9.87	.94	1650	.65
91-3 fuel	22.5	6	.266	4.35	.40	1864	.60
91-3 oxidizer	22.5	8	.355	8.33	.64	1169	.65
Titan IIA fuel	28	9	.322	6.97	.48	1440	.68
NERVA							
Mark III Mod III	90	18	.20	12.25	.49	914	.65
Mark III Mod IV	90	48	.533	12.25	.49	960	.70
Mark III Mod IV	90	24	.266	12.25	.49	1000	.70
M-1							
M-1 oxygen	35	12	.343	10.70	.81	1125	.66
Atlas and H-1							
Mark 3 fuel	25	10	.40	14.25	.85	760	.72
F-1							
Mark 10 oxidizer	25	6	.24	19.5	2.7	2140	.74
Mark 10 fuel	25	6	.24	23.4	1.7	1200	.76
J-2							
Mark 15-0 oxygen	25	6	.24	10.2	0.74	1600	.81
X-8							
Mark 19 hydrogen	90	24	.266	11.0	.43	670	.67
J-2S							
Mark 29-F hydrogen	60	24	.40	11.5	.53	1000	.76

[1]87-5 = LR-87-AJ-5 engine system
91-5 = LR-91-AJ-5 engine system
87-3 = LR-87-AJ-3 engine system
91-3 = LR-91-AJ-3 engine system

used to estimate more accurately the velocity distributions within the impeller. The velocity gradients then are evaluated for the possible occurrence of flow eddies or flow separation. The impeller blade angle distribution and the blade number are adjusted until desired design limits are achieved.

Representative impeller geometries and associated pump performance are presented in table I.

2.3.1.1 DIAMETER RATIO

The ratio of impeller inlet tip diameter to impeller discharge tip diameter D_{t1}/D_{t2} (= δ) influences the pump efficiency. At a given value for N_s, the increase in inlet diameter required for an increase in suction specific speed results in reduced efficiency. This influence is presented in figure 5. The cavitation performance presented therein in the cross-hatched bands was calculated from the following equation (ref. 33):

$$S'_s = \frac{8147}{\varphi_1} \left(\frac{NPSH}{c^2_{m1}/2g} \right)^{-3/4} \qquad (14)$$

The relation of flow coefficient to attainable $\frac{NPSH}{c^2_{m1}/2g}$ is presented in figure 14.

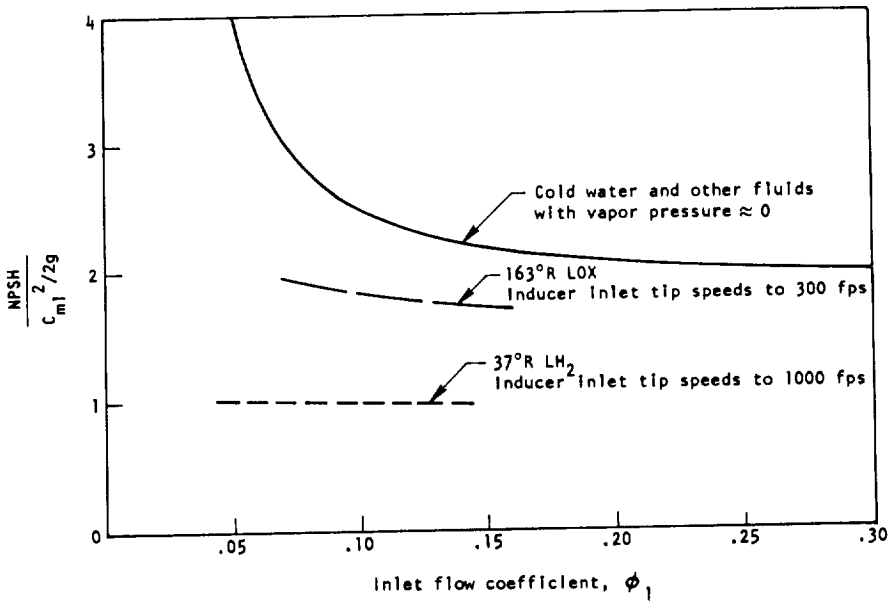

Figure 14. – Influence of impeller flow coefficient on NPSH (various fluids).

The higher values for δ result in a higher inlet relative velocity caused by the higher peripheral velocity. The higher inlet relative velocity increases the impeller diffusion and results in lower efficiency. Efficiency of most rocket engine pumps is compromised to permit operation at low inlet pressures. The use of a low-pressure boost pump permits optimization of main pump efficiency.

2.3.1.2 HEAD AND FLOW COEFFICIENTS

The pump head coefficient and the resulting impeller discharge diameter can have a wide range of values depending upon the flowrate, required suction performance, the required pump efficiency, and the head-vs-flow slope. Centrifugal-pump head coefficients vary from approximately 0.35 to more than 0.70. The lower head coefficients are obtained with a small number of blades (3 to 5); the higher head coefficients require many blades (20 to 60). More blades are required at a given head coefficient if the impeller discharge flow coefficient is decreased; this relation is covered in more detail in section 2.3.1.3. Head coefficient is not limited by flow coefficient. Higher head coefficients are generally used for low-specific-speed applications, since efficiency is thereby maximized and the small inlet diameter permits maximum blade length. With high-specific-speed pumps, low head coefficients are accepted in order to achieve the blade length along the shroud needed for good efficiency over a wide flow range.

The longer blade length results from the increased tip diameter associated with decreased head coefficient and from the reduced blade angle required to achieve the lower head coefficient. Both the impeller inlet and discharge flow coefficients may vary from as low as 0.05 to 0.30. The impeller inlet flow coefficient ϕ_1 is selected to satisfy the required suction performance, whereas the impeller discharge flow coefficient ϕ_2 is determined by the impeller blade angle as limited by stress and the desired head coefficient. The higher flow coefficients are possible only for high-specific-speed, high-NPSH pumps.

The NPSH required as a function of inlet flow coefficient is presented in figure 14 for sharp-leading-edge impellers (coupled inducers). The discharge flow coefficient is established by the desired head coefficient and a practical blade number based on fabrication limits. The discharge meridional component of velocity $c_{m\,2}$ may vary from 1 to 1.5 times the impeller inlet velocity. The impeller inlet velocity is considered to be the velocity at the exit of a coupled inducer or at the equivalent exit of an integral inducer.

The off-design performance requirements of the engine system during starts or throttling often govern the selection of the head coefficient, because this coefficient largely determines the nature of the pump head-vs-capacity curve. To verify system stability over the entire operating range, the slope of the head/capacity curve is compared with the engine system pressure drop characteristics and capacitance. An analog computer is often used for

this purpose as discussed in reference 1. The pump head/capacity curve is determined largely by head coefficient (fig. 13). For pumps with a given head coefficient, an impeller with the largest blade number will result in the steepest slope.

The impeller head coefficient may be increased or decreased by underfiling or overfiling the impeller trailing edge as shown in figure 15. The pump head and horsepower can be varied by as much as 10 percent in this manner with little or no change in efficiency.

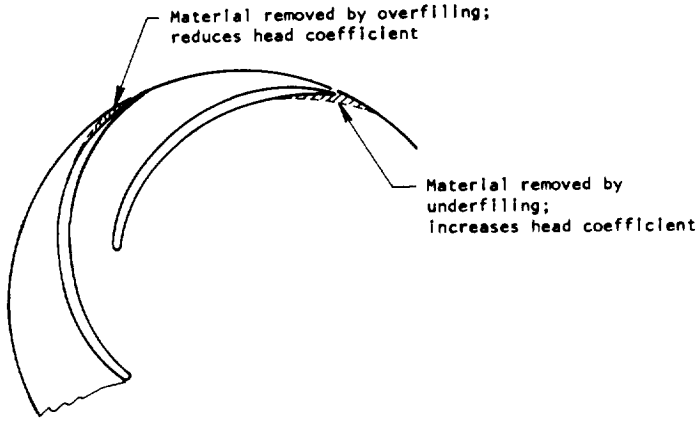

Figure 15. – Effect of filing impeller trailing edge.

2.3.1.3 BLADE NUMBER AND BLADE GEOMETRY

Discharge blade angles on impellers for rocket engine pumps have ranged from 22.5° to 90°, and blade numbers from 6 to 48 have been tested (table I). From the fabrication standpoint, the minimum number of blades is desired. Backswept impellers (blade angles less than 90°) with low head coefficients tend to have wider and more stable operating range than radial-bladed impellers. The range of high efficiency for pumps with low-head-coefficient impellers is, however, smaller than the range for pumps with high-head-coefficient impellers. This characteristic is evidenced by the normalized pump performance curves for pumps with both radially bladed and backswept impellers shown in figure 13.

The impeller blade number and blade angle that result in a desired pump head coefficient are also related to the impeller discharge flow coefficient. The blade number must be such that impeller diffusion or suction-surface velocity-gradient limits are not exceeded. The minimum number of blades that can satisfy impeller velocity-gradient limits is presented in figure 16. Test results for several pumps substantiate the analytically derived curves. As noted, the curves presented are for shrouded impellers with $\delta = 0.65$. The influence of th

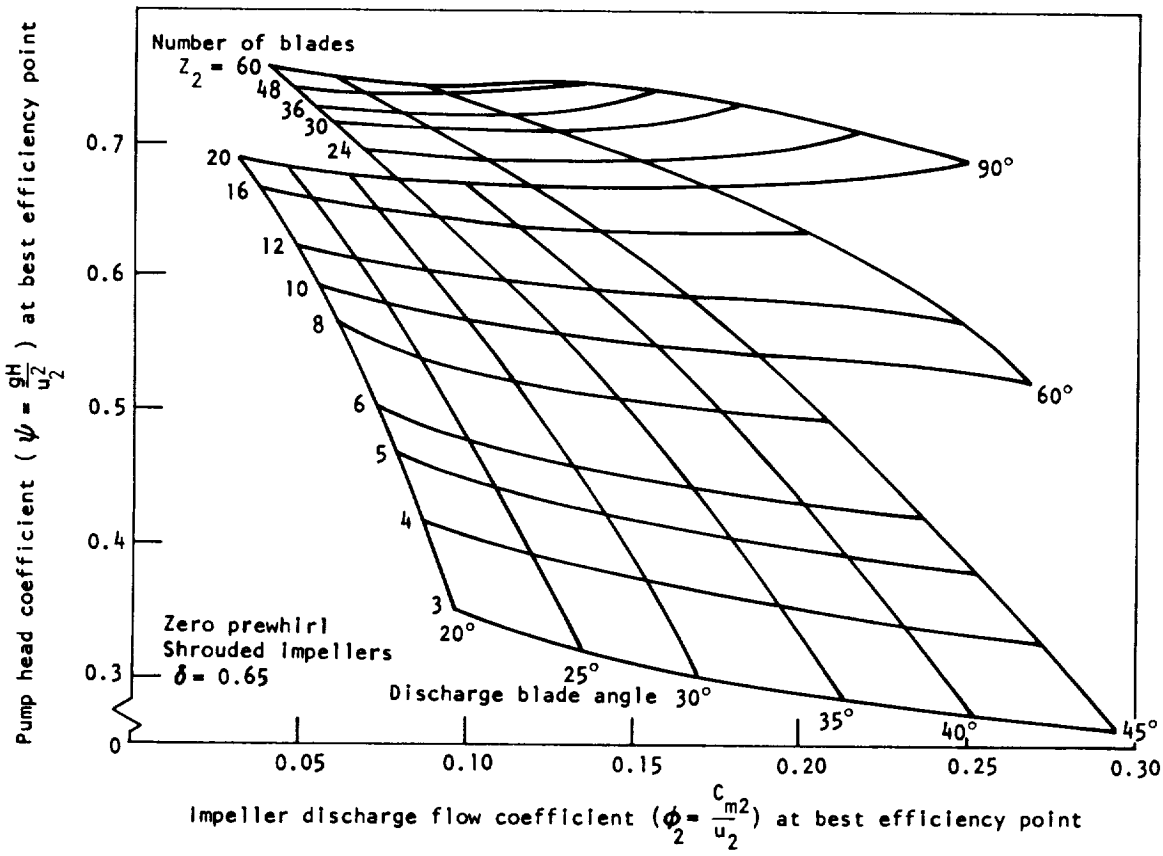

Figure 16. — Impeller blade number and discharge angle related to discharge flow coefficient and head coefficient.

value for δ on head coefficient may be evaluated by use of the slip equation given below (eq. (17)). Open-face impellers also generate less head than shrouded impellers (sec. 2.3.1.4).

Velocity Gradients. — The impeller suction-surface relative-velocity gradient G at any meridional length L_m along the blade surface may be represented by

$$G = \frac{W^2_{S2} - W^2_{S1}}{\overline{W}_S^{\,2} \left(\frac{\Delta L_m}{L_m} \right)} \tag{15}$$

where W_{S2} and W_{S1} are relative velocities on the suction surface spaced a distance ΔL_m apart, and $\overline{W}_S$ is the arithmetic average of W_{S1} and W_{S2}; the spacing ΔL_m is selected sufficiently small that the gradient is nearly a constant in the region being analyzed. Values

for G as high as 3.5 have resulted in acceptable performance when the pressure surface relative velocity is simultaneously in the direction of flow and greater than zero.

The relative velocities on the impeller blade surface are calculated by procedures presented in references 52 through 54. Examples of acceptable gradients are presented in figures 17 (ref. 55) and 18; an unacceptable gradient is presented in figure 19, which shows both a rapid drop in suction surface velocity near the inlet and a reversed velocity on the pressure side of the blades.

Slip Coefficient. – The inability of an impeller with a finite number of blades to impart the same tangential whirl to the fluid as an impeller with an infinite number of blades is represented by the slip coefficient M:

$$M = \frac{c_{u2\infty}}{c_{u2}} \tag{16}$$

where

$c_{u2\infty}$ = tangential velocity with infinite number of blades

c_{u2} = tangential velocity with a given number of blades

A review of the literature shows that many proposed methods for predicting slip exist (ref. 56); however, no universal equation has been formulated. The methods of Buseman, Pfliederer, Stanitz, and Stodola are still widely accepted (ref. 4). The empirically derived expression for M:

$$M = 1 + \frac{(1.37 + 0.23 \sin \beta_2)(\phi_2 + 0.05)^{0.6}}{0.5\, Z_2 (X_L)^{0.6} (1 + X_L/2)(1 - 0.12\delta)} \tag{17}$$

where $X_L = \dfrac{\text{axial distance from midpoint of impeller inlet to impeller discharge}}{\text{impeller discharge diameter}}$

was used along with hydrodynamic loading limits and velocity gradients established by quasi-three-dimensional flow analyses of several impeller designs to develop the impeller design influence on head coefficient presented in figure 16.

A small number of blades Z_2 reduces the tangential velocity c_{u2} leaving the impeller and therefore reduces the head coefficient. A low head coefficient obtained by use of a small number of blades and a large slip coefficient may not result in a steep head/flow characteristic. The steepest head/flow characteristic for a given head coefficient is obtained with a value for M closely approaching unity, a condition that occurs when the number of blades is large ($Z_2 > 20$).

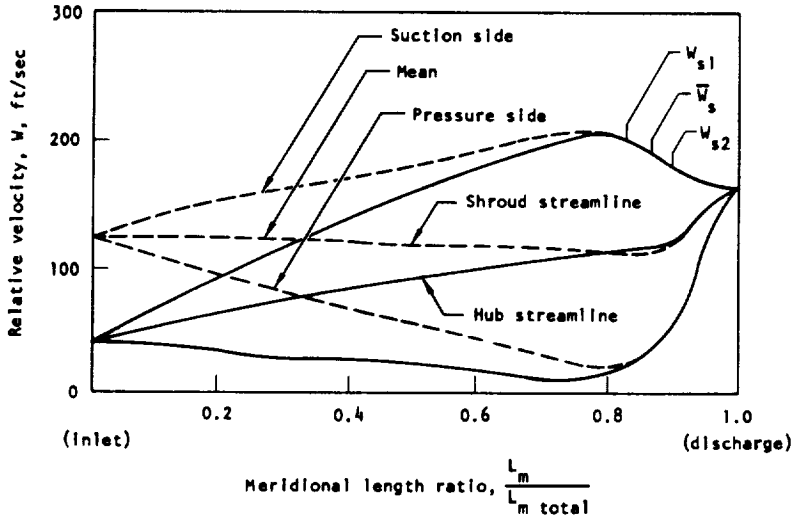

Figure 17. – Calculated relative velocities along hub and shroud streamlines for 12-gpm LF_2-pump impeller.

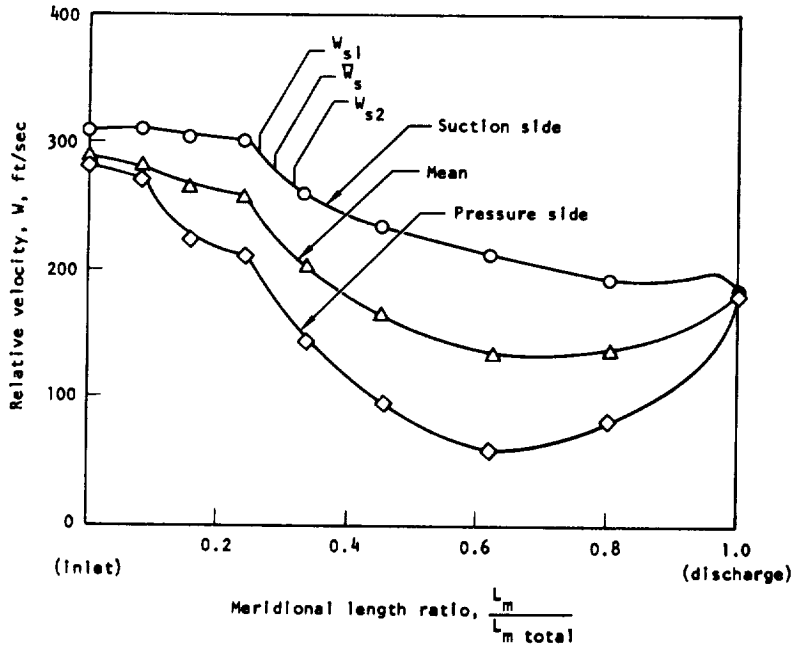

Figure 18. – Calculated relative velocities along streamlines for experimental F-1 fuel impeller with six full blades and six splitters.

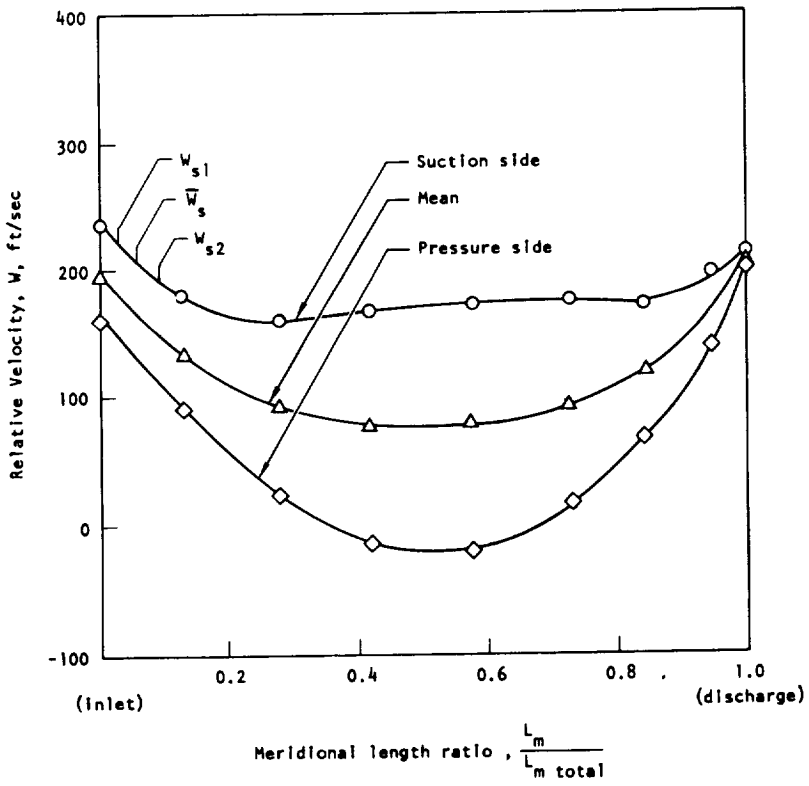

Figure 19. – Calculated relative velocities along streamlines for experimental F-1 LOX impeller with eight full blades.

2.3.1.4 SHROUDING

The effect of a shroud on the hydrodynamic performance of an impeller depends upon the relative influence of (1) the increased shaft power required by the rotating shroud disk friction, (2) shrouded-impeller seal leakage vs open-impeller blade clearance losses, and (3) the reduced head coefficient due to friction losses on the stationary shroud of an open impeller. The shrouded impeller permits more housing deflection without problems in critical clearances or rubbing; this characteristic generally results in lower overall pump weight. For normal operating clearances, the shrouded impeller with the same geometry produces higher efficiency and pressure.

Figure 20 shows typical shrouded and unshrouded impellers. Figure 21 presents the ratios of efficiency and head for three open-face and three shrouded impellers with the same blade shape. The curves in figure 21 were based on data presented in references 57 and 58.

Shrouded titanium impeller - J-2S

Open-face titanium impeller-XLR129

Figure 20. – Shrouded and open-face impellers.

In shrouded impellers, a radial clearance inlet seal is used to minimize leakage. For oxidizer pumps, the impeller seals are fabricated from nonreactive, nonsparking materials so that close clearances are allowable. The seal clearance can be held to 0.0005 times the impeller tip diameter, a value that, for the J-2 oxidizer pump, results in an efficiency approximately 95 percent of the zero-clearance efficiency at a specific speed of 1500. Values for impeller seal flow coefficient K for several tested configurations are presented in figure 22.

2.3.2 Mechanical Design

Impeller mechanical design is based on hydrodynamic requirements, structural requirements, fabrication methods, and the properties of selected materials. The structural design of the impeller must provide for axial retention, accurate radial piloting, reliable torque transmission, strength to resist centrifugal and fluid-induced stresses, and resistance to dynamic forces for adequate fatigue life. Fabrication must be accomplished by a method that satisfies the hydrodynamic and structural requirements with minimum cost. The impellers may be fabricated by casting, machining, diffusion bonding, or combinations of procedures (ref. 59). The method of fabrication should be such that balancing adequate for

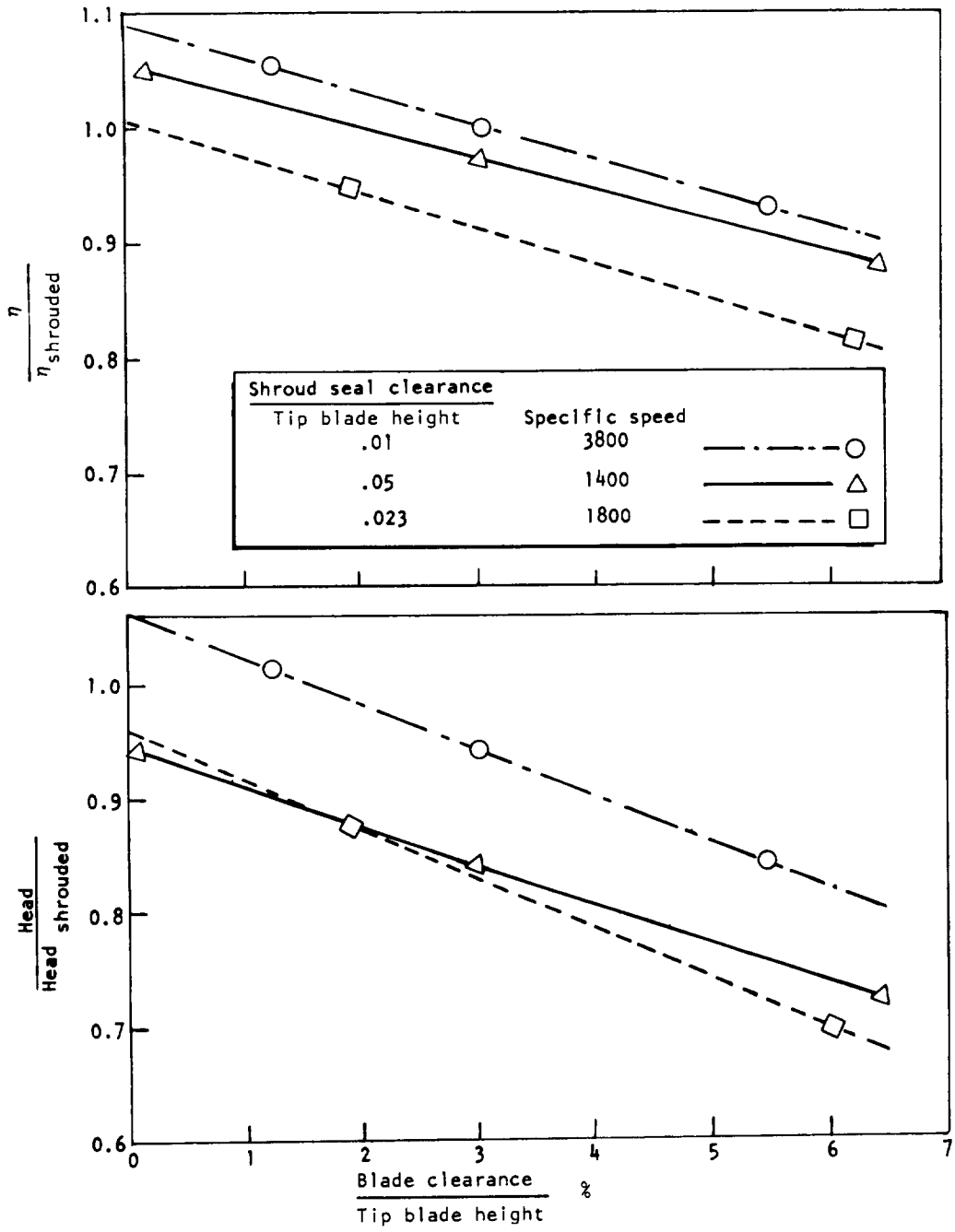

Figure 21. – Relative performance of open-face and shrouded impellers.

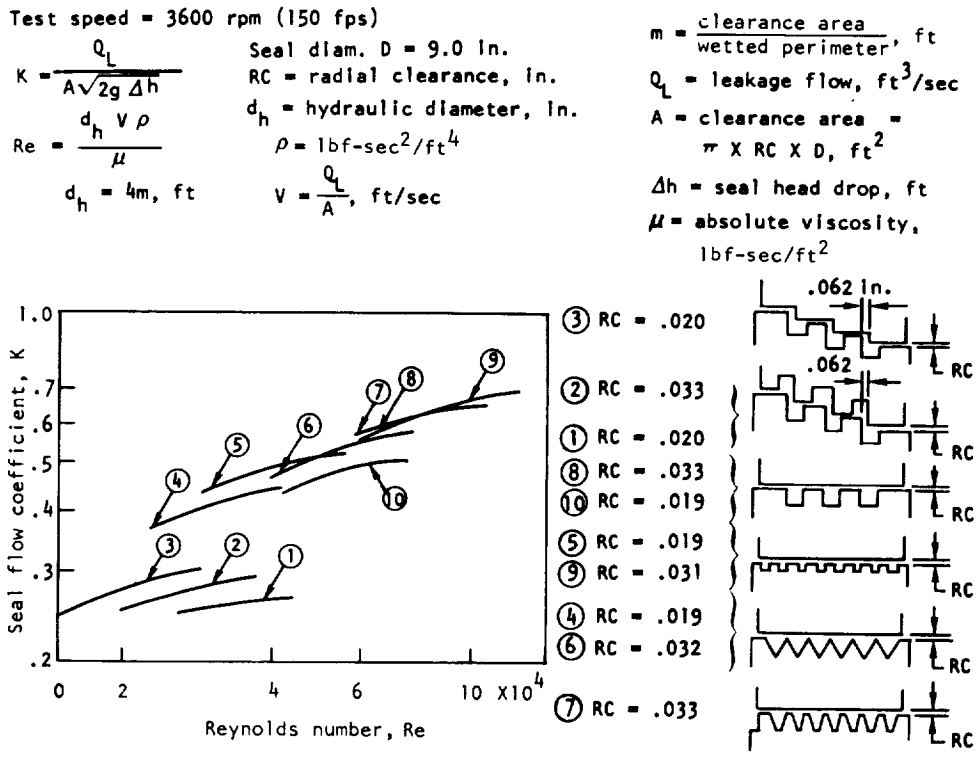

Figure 22. – Variation of seal flow coefficient with Reynolds number (various seal configurations).

the required rotor tip speed can be achieved. The materials selected must be structurally adequate and chemically compatible with the pumped fluid; the selected material should contribute to ease of fabrication and minimum cost. Improper heat treatment of some alloys has resulted in cracks in castings or stress corrosion in forged alloys. These problems have been solved; however, caution is exercised when new processes or new materials are contemplated.

Structural design factors that have caused problems with rocket engine impellers include thermal shrinkage, Poisson deformation, loss of piloting from centrifugal stress, casting cracks, and fatigue cracking. Thermal shrinkage, particularly of aluminum impellers on steel shafts, has resulted in loss of axial retention, which can result in a lowered shaft critical speed. This effect has been eliminated by use of thermal-compensating spacers, sufficient bolt stretch, and short axial-retention length. Poisson deformation results in axial shortening of the impeller as the tip diameter grows; detailed attention to the problem has resulted in successful solutions similar to those for thermal shrinkage. Loss of radial piloting caused by centrifugal stress has resulted in imbalance that produced excessive bearing loads and loose

spline fits that resulted in fretting corrosion. Radial piloting has been ensured by use of interference fits and by design of impeller hubs to reduce centrifugal growth in pilot and spline areas. Casting cracks that resulted from residual stresses have been eliminated by proper casting techniques (e.g., use of chills) and by heat treating. Fatigue failures in castings have been caused by high residual stresses from casting and by high local stresses; both kinds of stresses are relieved by heat treatment or overspeed. Endurance limits have been increased 40 percent by shot peening to induce surface compressive stress.

The current limit of tip speed for shrouded cast impellers pumping liquid hydrogen is 1400 fps for Inconel 718 and for vacuum-melt, vacuum-cast aluminum. An open-face titanium impeller (Ti-5Al-2.5Sn) with a smooth central hole has been operated in liquid hydrogen to a tip speed of 2500 fps (ref. 45). A shrouded diffusion-bonded titanium impeller (Ti-5Al-2.5Sn) with an impeller discharge blade angle 37° from tangential was spun to 2870 fps at room temperature (ref. 60). Care is exercised with high-speed impellers to minimize superimposing of drive torque loads on the hub regions where the centrifugally induced stresses are highest.

The present state of the art of impeller structural design permits the prediction of the minimum required material thicknesses for most of the shroud, blades, and disk. However, regions where stress concentrations exist are difficult to analyze, and spin tests in air using stress coat and strain gages are required to determine the magnitude of these local stresses in high-speed hydrogen-pump impellers. Tests are necessary to detect stress-concentration regions in low-tip-speed impellers that are highly stressed by hydraulic loads imposed by a dense liquid. The burst margin of the impeller disk, deflections of the disk and blades affecting fits and clearances, and the blade stresses are calculated, so that structural adequacy can be assessed. Disk stresses are determined by the finite-element technique (ref. 61). The analysis includes the level and distribution (uniformity) of material tensile strength and ductility; it also accounts for centrifugal, pressure, and thermal stresses as well as stress concentrations. The pricipal criterion for evaluating the configuration is burst speed based on average tangential stress and acceptable deflections.

Blade stresses are calculated on the basis of centrifugal and steady-state pressure loads, cyclic pressure loads, and the effect of operation at the minimum margin from blade natural frequencies. Stresses are calculated at maximum speed and maximum pressure loading (maximum flowrate), a cyclic pressure loading of ±30 percent of the steady-state value being applied. Structural adequacy is assessed by comparing calculated stresses with the allowable stress as determined from a modified Goodman diagram (fig. 23). The impeller blade bending stresses from centrifugal loading may be minimized by use of radial-element blades. Blade angles measuring less than 90° from the meridional plane may be generated by radial elements if the angle of the back shroud, or hub, relative to the axis at the impeller exit is less than 90°. The impeller axial length is increased when the hub and shroud angles at the impeller exit are less than 90°; therefore, this geometry is used only for maximum tip speeds.

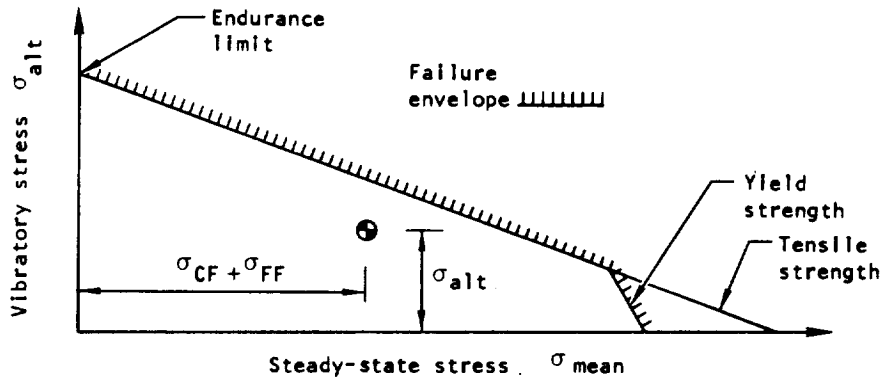

Figure 23. – Typical modified Goodman diagram.

2.3.3 Fabrication

Impellers are fabricated by casting, machining, and diffusion bonding. The highest-tip-speed impellers, used for pumping liquid hydrogen, are open-face impellers machined from a forged titanium alloy (ref. 62). Shrouded impellers for dense fuels or oxidizer service are cast, since cast material properties are adequate for the required tip speeds of less than 1000 fps. Open-face impellers for oxidizer service may be cast or machined. Shrouded impellers for use in liquid hydrogen have been machined from forgings; they have also been fabricated by generating all the components separately from a titanium alloy, diffusion bonding them, and finishing internal passages by chemical milling (refs. 59 and 60).

The maximum blade number for machined blades in shrouded impellers is limited to approximately 28 sin β_2 by required cutting tool clearance and limits on tool length-to-diameter ratio. The existence of the shroud imposes obvious restrictions on blade shapes that can be machined. Open-face impellers, however, may be machined easily with no serious limits imposed upon the blade shape or blade number by machine-tool limitations.

Aluminum impellers cast in ceramic-shell core molds can be made with a 63 μ in. per inch surface finish for diameters up to 10 in. and a 125 μ in. per inch finish for diameters of 10 to 20 in. Similar finishes have been obtained with investment castings of Inconel 718 and stainless steels.

Impeller balance requirements are a function of the speed and weight of the rotating assembly, since both variables influence the forces imposed on the bearings. A residual balance that has proven acceptable in practice may be calculated by the equation presented in section 3.3.3. In calculating acceptable production balancing requirements, allowance

must be made for manufacturing and assembly errors that result in offset of rotors from true center. Normality control and piloting influence the rotor rotating center after assembly. Provisions for final balance after assembly can be used to minimize imbalance in very-high-speed machines.

In the assembly of built-up rotors, the possibility of misassembly exists whenever a part can be mounted in more than one position. Various practices are used to preclude the possibility of misassembly. These usually take the form of minor modifications to the hardware that prevent mating the parts when they are not in the correct position.

All the various components of a rotating assembly obviously must be designed for the same direction of rotation. It is an established practice to coordinate design efforts and avoid problems of mismatched direction of rotation by making a preliminary axonometric projection of the assembly that shows clearly the direction of rotation. Copies are furnished to all designers on the job.

High-speed impellers are proof tested by prespinning each part during the fabrication process to provide partial quality assurance. Prespinning each impeller has additional benefits in that local yielding occurs at areas of high strain concentration such as bolt holes, splines, and keyways. This yielding produces favorable residual stresses that effectively prestress the part and prevents the occurrence of yielding during operation.

2.3.4 Materials

Impeller materials that have been used successfully with rocket propellants are shown in table II. Materials that are not listed as cast were forged. The materials are chemically compatible with the pumped fluid, have satisfactory strength and ductility at the operating temperatures, and can be used to fabricate impellers with existing technology.

2.4 HOUSING

The pump housing is the physical structure that forms the containing envelope for the pump. It consists of the casing (the part of the pump that surrounds the impeller), the diffusing system and volute for single-stage pumps, and the crossover system for multistage pumps. The diffusing system may include vaned or vaneless diffusers upstream of the volute and a conical diffuser or duffusers downstream of the volute. In addition, the housing contains and mounts the bearings that support the rotating assembly and the seals that prevent leakage of the pumped fluid. Consideration is given to both the mechanical and hydraulic factors in selecting a particular housing configuration, because the housing not

Table II. - Materials Successfully Used for Impellers

Impeller material	Pumped fluid						
	LH_2, CH_4	IRFNA, N_2O_4	LOX	LF_2	FLOX	RP-1	N_2H_4, UDMH, or 50/50 mixture
Aluminum							
A356 (cast)		X	X				X
A357 (cast)			X		X	X	
2014-T6	X						
6061-T6			X			X	X
7075-T73	X	X	X			X	X
7079			X				
Steel							
AM 350		X					X
304L (cast)		X	X				
304L		X					X
310			X			X	
347 (cast)			X				
Inconel 718 (cast)			X	X	X		
"K" Monel			X				
Ti-5Al-2.5Sn	X					X	

Note: X indicates that the material was used successfully with the fluid shown; absence of X means either that no data on the use are available or that the material was incompatible with the fluid. Materials not shown as cast were forged.

only represents the major segment of pump weight but has a most significant effect upon pump efficiency. It is commonly accepted that the housing determines the operating point where the best efficiency occurs (refs. 63 and 64).

Housings have been successfully fabricated using two basic processes: casting in one or more pieces, or welding together forged, formed, cast, or machined elements. Materials have included cast aluminum alloys, cast stainless steels, and high-strength wrought aluminum alloys and steels. Sometimes, separate liners are used to provide an inert material as an interface with the impeller to achieve configuration flexibility or to simplify fabrication.

Duffuser vanes can be integral or separate. Reinforcing bolts through diffuser or guide vanes have provided structural aid.

Housing structures must be designed to sustain mounting loads as well as internal pressure loads. External loads on parts such as the volute may be minimized by incorporating flexible ducts that minimize bending loads.

2.4.1 Hydrodynamic Design

The hydrodynamic design of the housing components is based on a combination of theoretical and empirical considerations. A systematic experimental background similar to that for axial pump and compressor cascades is not available, because the greater geometric and analytical complexity of the centrifugal pump makes the experimental task more difficult and because to date there has been less emphasis on this approach.

2.4.1.1 CASING

Major considerations in the design of the casing involve the shape and smoothness of the interior walls that form the flow path from the inlet to the diffiuser (fig. 1). The shape must follow closely the exact contour of the impeller, particularly for an open-face impeller where this wall contour establishes the size and uniformity of the tip clearance. The roughness of the casing inner wall – due either to surface finish or to fasteners and attachment points – influences the radial pressure gradient and thereby the axial thrust balance. Furthermore, increasing roughness of the wall increases the impeller disk friction loss. Current practice is to achieve a surface finish of about 63 μ in./in.; necessary fasteners and attachment points are located as close as possible to the pump center line where the impeller relative velocity – and therefore fluid velocity – is at its lowest.

2.4.1.2 DIFFUSION SYSTEM

The pump diffusion systems of interest for both single and multistage pumps are the vaneless and vaned diffuser upstream of the volute and the conical diffuser downstream of the volute. For multistage pumps, the diffusing system between stages may consist of a vaned diffuser followed by an internal crossover passage with no volute, or a volute followed by external crossover tubes.

2.4.1.2.1 Vaneless Diffuser

The gap between the impeller discharge and the vaned diffuser inlet or the volute tongue (referred to as a vaneless diffuser) acts as a mixing zone for the impeller blade wakes; this

mixing can significantly suppress pressure-perturbation effects (ref. 65). Figure 24 shows this gap expressed as the ratio of diametral clearance to impeller diameter plotted against impeller discharge flow angle. The available mixing length is approximately the radial clearance divided by the sine of the impeller discharge flow angle. Current practice is to maintain a constant ratio of mixing length to impeller diameter by increasing the spacing as the impeller discharge flow angle increases.

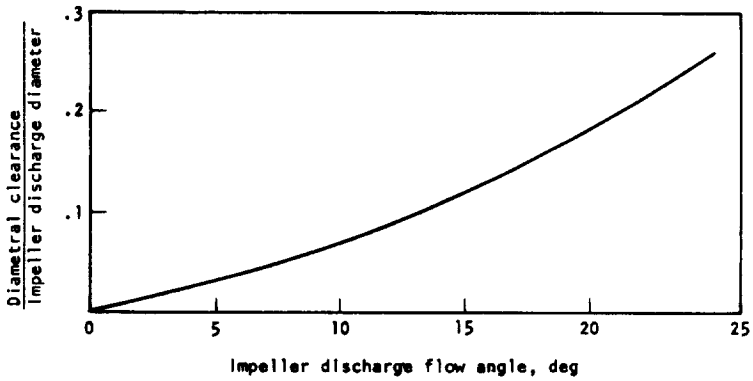

Figure 24. – Impeller-to-stator spacing as a function of discharge flow angle.

As an example of the influence of this gap size, a gain of 1.8 percent in the efficiency of the NERVA pump (at a specific speed of 980) was obtained by trimming the impeller and thereby increasing the ratio of diametral clearance to impeller diameter from 0.03 to 0.06.

It should be noted that any increase in gap size above the minimum values necessary for suppression of pressure perturbations (fig. 24) reduces efficiency and increases weight. In addition, pressure losses in the vaneless diffuser increase as pump specific speed decreases; these pressure losses may be calculated by procedures presented in reference 66. The required radial clearance may be reduced by design of the impeller to produce a minimum thickness of the boundary layer.

2.4.1.2.2 Vaned Diffuser

A vaned diffuser provides volute flow-matching over a wide flow range and also a lower volute velocity that reduces the pressure differences caused by manufacturing variations.

Both the volute flow-matching and reduced volute velocity reduce impeller radial loads. Vaned diffusers are also used to obtain maximum pump efficiency. The reduced volute velocity results in a 3-percent increase in pump efficiency at a specific speed of 1200 and greater improvement as specific speeds are decreased (ref. 4). However, vaned diffusers designed for radial-vaned impellers in low-specific-speed pumps have exhibited discontinuities in the head/capacity curve at flow rates of 45 to 50 percent of the best-efficiency operating point (fig. 13). Operation at or near this region of head discontinuity (diffuser stall) usually is unstable and is avoided. The design-point efficiency of pumps with vaned diffusers generally is higher and remains higher with decreasing flow, but falls more rapidly with increasing flow than that for pumps with a vaneless volute.

Most investigators (refs. 63, 64, 67, and 68) agree that the diffuser throat area is the most important parameter for determining a match with the impeller discharge flow. Figure 25

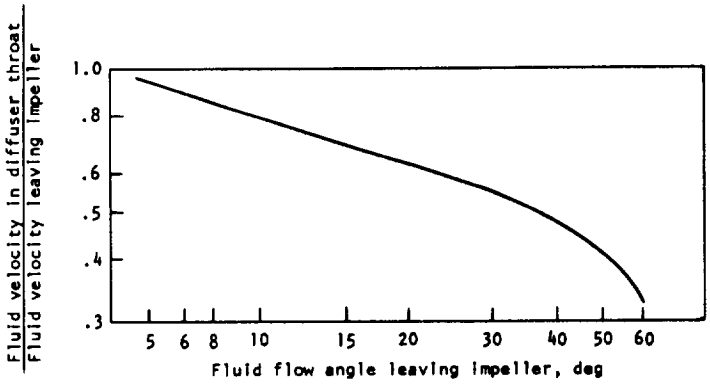

Figure 25. — Relative velocities in diffuser throat and at impeller discharge as a function of fluid flow angle.

presents the ratio of diffuser throat velocity to impeller discharge velocity that may be used to calculate the diffuser throat area. The diffuser inlet angle and shape also influence the slope of the characteristic curves; however, systematic design information is not available.

The rate of diffusion described by the effective cone angle of the vaned diffuser strongly influences the number of diffuser vanes required. Eckert and Schnell (ref. 66) present an equation that relates the required number of circular arc diffuser vanes to the diffuser equivalent cone angle θ, radius ratio R_4/R_3, discharge-to-inlet area ratio A_4/A_3 of the vaned diffuser, and vane inlet angle β_3. The results of calculations for several area ratios are presented in figure 26; the equivalent cone angle used in the calculations was 8°. A small number of diffuser vanes minimizes blockage, and so each diffuser passage is fed by more than one impeller passage (ref. 69).

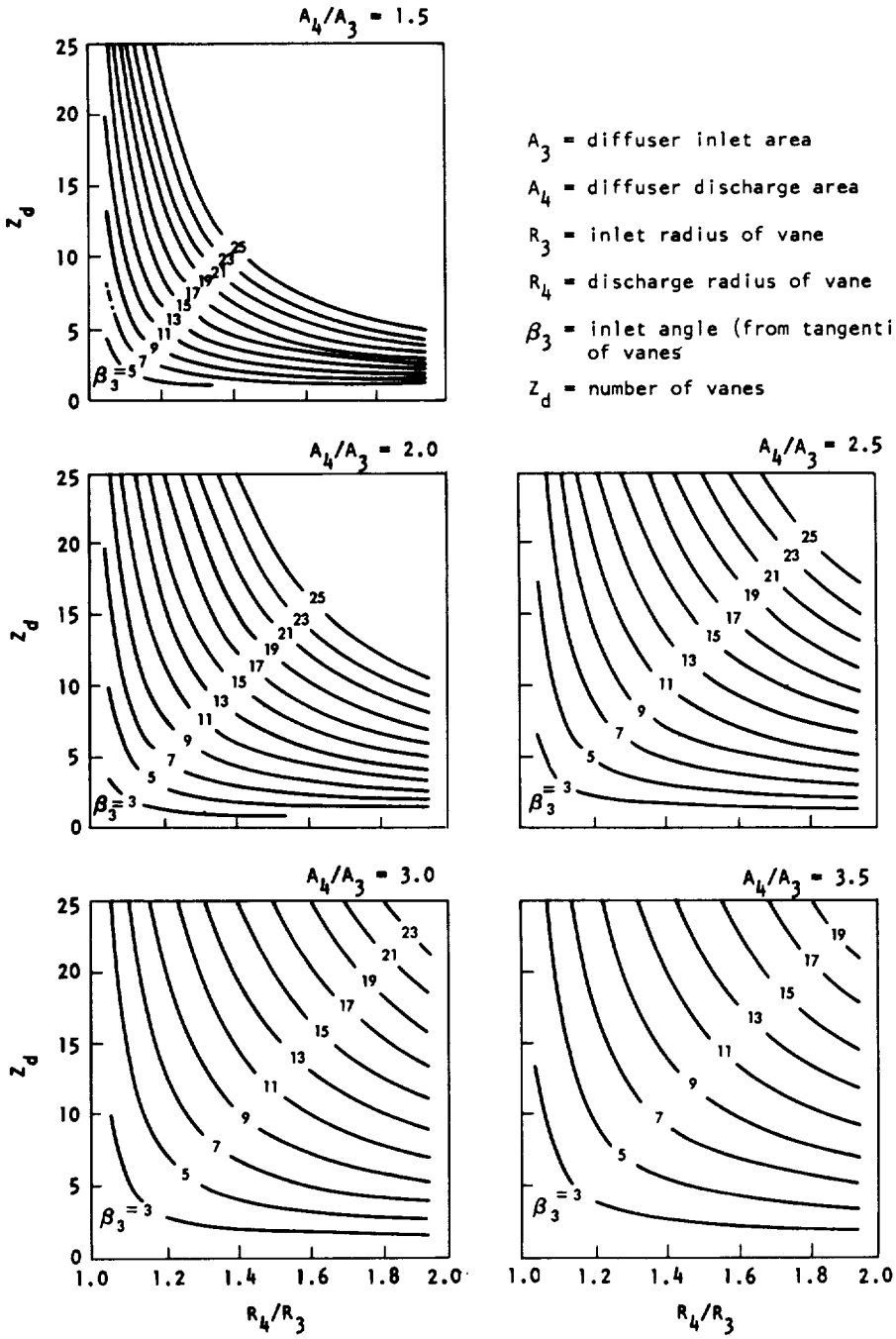

Figure 26. — Required number of circular arc diffuser vanes Z_d as a function of R_4/R_3, A_4/A_3, and β_3 for $\theta = 8°$.

For minimum losses, the diffuser vane inlet angle, β_3, is designed to match the entering fluid flow angle at the design flow rate. If the pump is required to operate at reduced flow rates (as in a throttled engine), the diffuser vane inlet angle may be designed to match the inlet flow angle at a flow coefficient as low as 80 percent of the nominal value for maximum engine thrust.

The influence of various diffuser area distributions may be evaluated by means of a computer program such as that presented in reference 70; this evaluation permits comparison of velocity gradients with previously tested successful diffusers.

When diffusers are required to carry casing structural forces, a vane island type of diffuser (fig. 27(a)) may be used. The inlet angle and throat area requirements for the vane island diffuser are the same as those for vaned diffusers (fig. 27(b)). The relation between throat area and discharge area is described by the cone angle, which normally is 7° to 10° (ref. 71).

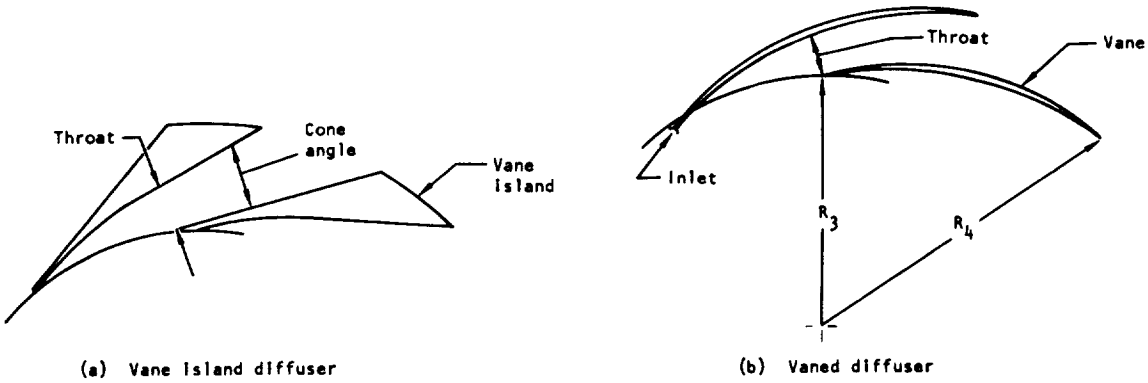

Figure 27. – Vaned diffuser designs.

For all types of diffusers, the diffusion factor D for a single stage of diffusion is maintained less than or equal to 0.6. D can be expressed as

$$D = \frac{P_{s3} - P_{s\,min}}{P_{t3} - P_{s\,min}} \tag{18}$$

where

P_{s3} = static pressure at diffuser inlet

$P_{s\,min}$ = minimum pressure in diffuser

P_{t3} = total pressure at diffuser inlet

The width of a diffuser vane b_3 is made approximately equal to the impeller tip width b_{t2}, i.e.,

$$b_3 = (.9 \text{ to } 1.0)\, b_{t2} \tag{19}$$

and the side walls are rounded or faired. These practices minimize flow separation even under conditions of axial misalignment with the impeller and produce an efficient energy conversion in the diffuser.

2.4.1.2.3 Interstage Flow Passage

Interstage flow passages (fig. 11) are required in multistage pumps to guide the fluid from the discharge of one stage to the inlet of the next stage and to provide velocity matching. Limited design information is available for multistage rocket pumps because only a few have been designed and tested. Examples are the J-2S fuel pump, which has vaned interstage passages, and the breadboard liquid-hydrogen pump (ref. 62), which had a double-discharge volute with two external crossover tubes. Some of the concepts and practices for the design of interstage flow passages used in the commercial pump and compressor industry are presented in references 66 and 72.

An additional objective when using a vaned diffuser with a volute is to avoid the possibility of wave reinforcement of the pressure waves that result from the interaction of the impeller blade wakes with the diffuser vanes. The impeller discharge blade number Z_2, diffuser vane number Z_d, and volute flow-path length πD_v are important design parameters. Superposition of pressure waves can result in large amplitude oscillations in discharge pressure. This superposition, or reinforcement, of waves is avoided by proper matching of the number of impeller blades and the number of diffuser vanes. Reinforcement of the j^{th} harmonic of the waves will occur whenever the reinforcement index m is an integer, where m is given by the expressions (refs. 65 and 73)

$$m = j\,\frac{Z_2}{Z_d}\left\{\frac{Z_d - Z_2}{Z_2} + \frac{\pi D_v N}{(a + W)}\right\} \quad \text{if } Z_2 > Z_d \tag{20}$$

and

$$m = j\,\frac{Z_2}{Z_d}\left\{\frac{Z_d - Z_2}{Z_2} - \frac{\pi D_v N}{(a + W)}\right\} \quad \text{if } Z_d > Z_2 \tag{21}$$

where

- j = order of the harmonic of the fundamental wave frequency
- D_v = average distance from center of pump to center of volute passage
- a = velocity of sound in liquid
- W = average relative velocity of fluid in volute passage

2.4.1.3 VOLUTE

The object of volute design is to provide a distribution of cross-sectional area with respect to wrap angle that will yield a constant impeller discharge static pressure at the design point of the pump; the radial load on the shaft and the impeller vibrations are thereby minimized. An asymmetric volute cross section is preferred because it produces a single vortex that is stable and that improves the efficiency of the conical diffuser at the exit (refs. 66 and 71). The conical diffuser at the volute exit will operate efficiently when the included angle for circular cross sections is between 7° and 9°; for square cross sections, 6°; and for two parallel walls, 11°.

The inlet angle of the volute tongue is designed for zero incidence angle at the design flow in order to reduce the losses associated with the volute, to minimize local pressure differences, and to reduce the amplitude of the pressure oscillations in the pump discharge. If a vaned diffuser precedes the volute, the transition from the vaned diffuser to the volute tongue must be designed to avoid an interaction that would lead to an unstable (e.g., bi-stable) pump head-versus-flow characteristic. Stable flow is achieved by fairing one diffuser vane into the volute tongue or by leaving a large clearance between the vane discharge and the tongue.

2.4.1.3.1 Cross-Sectional Area

Two methods are in use for sizing the volute cross-sectional area: constant moment of momentum, and constant mean velocity.

Constant moment of momentum. – The fluid tangential velocity is assumed to be inversely proportional to the radius. After the volute shape has been established, the volute cross-sectional area satisfying the given flow requirement is determined at each circumferential station. The constant-moment-of-momentum method was applied to the design of Titan I and Titan II pump housings; corrected for friction losses (ref. 74), the method was used in the design of the J-2S Mark 29 fuel pump, which experienced very light radial bearing loads.

Constant mean velocity. – The velocity is assumed to be constant, and therefore the cross-sectional area is increased proportionally as the central volute wrap angle increases. The method was developed as a simplification in volute design.

Although there are only minor differences in pump efficiency between the two methods (ref. 64), the unsymmetrical pressure (with its associated radial hydraulic forces upon the impeller) around the volute passage has been found to be higher in designs based on the constant-mean-velocity method (ref. 63).

2.4.1.3.2 Off-Design Radial Load

Splitter vanes or multiple tongues and vaned diffusers in the volute housing or double-outlet volutes (fig. 28) are used to reduce radial thrust over a wide flow range and to provide structural support to the housing. The greater the number of symmetrically located splitter vanes, the better is the balance of radial thrust. This is an advantage of the multiple-tongue volute. Vaned diffusers reduce the velocity of the fluid and control the flow angle at the entrance to the volute tongue and therefore produce a uniform impeller discharge pressure with a resultant low radial load. The impeller discharge pressure as a function of angular distance from the tongue is presented for three types of volutes and a range of flowrates in figure 29 (ref. 75).

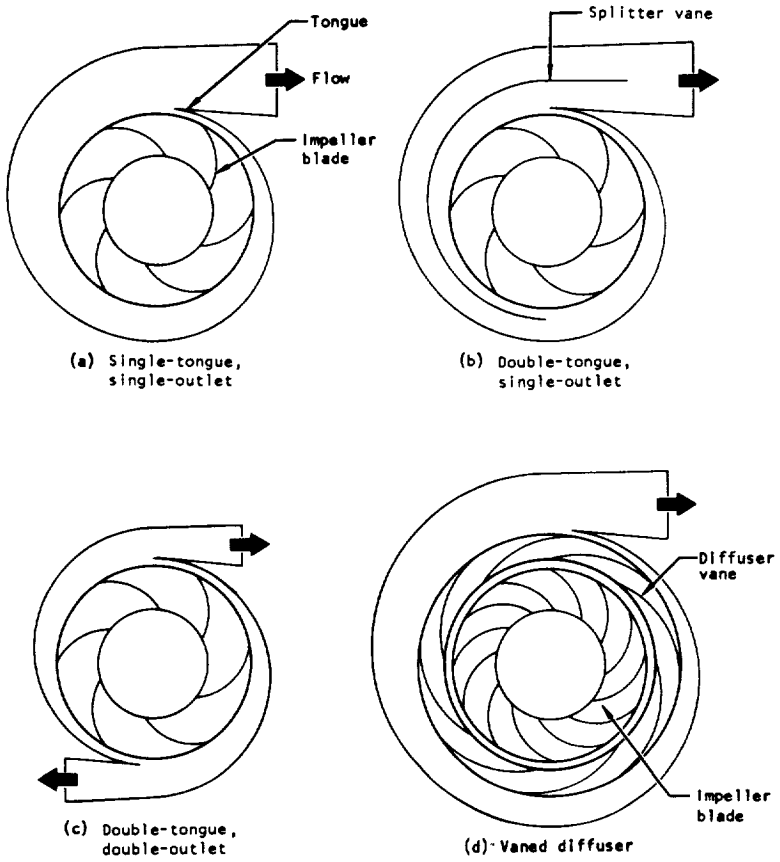

Figure 28. – Volute configurations.

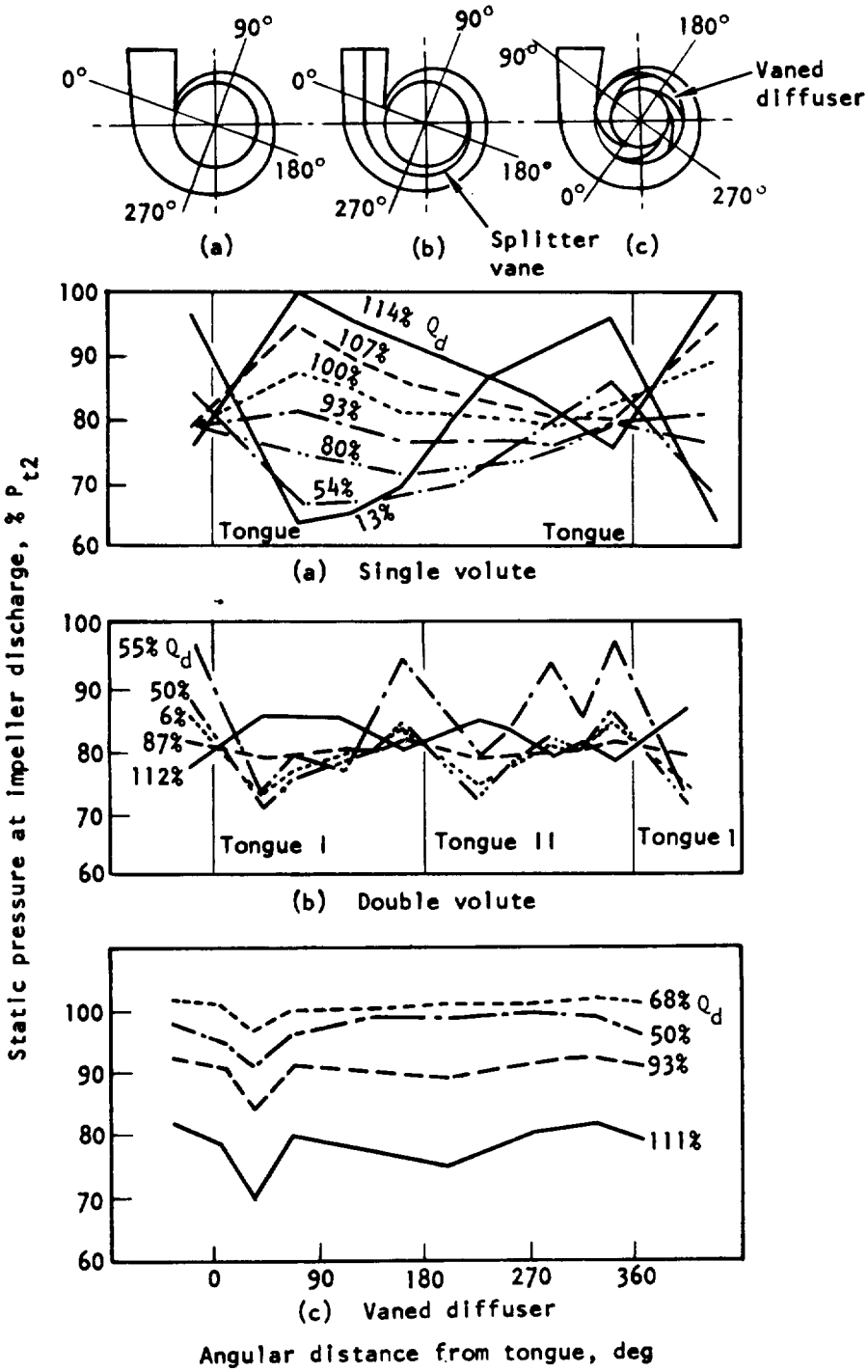

Figure 29. – Impeller discharge pressure as a function of volute design and percent design flowrate.

2.4.2 Structural Design

The housing structure must be capable of withstanding external mounting loads as well as loads due to internal pressures, and deformation must be limited so that sealing surfaces will remain effective and bearing supports will not be distorted. The housing structure must be adequate to accommodate access for instrumentation.

A major concern in housing design is the integrity of the volute tongue that withstands a large volute-separating load. The tongue must be ductile; when the volute is cast of aluminum, provisions are made to chill the tongue region rapidly during casting to provide both high ductility and strength. The volute structure is proof-pressure tested to produce tongue yielding. This practice results in lower tongue stress and improved fatigue life during normal pump operation. Figure 30 presents several successful structural design solutions.

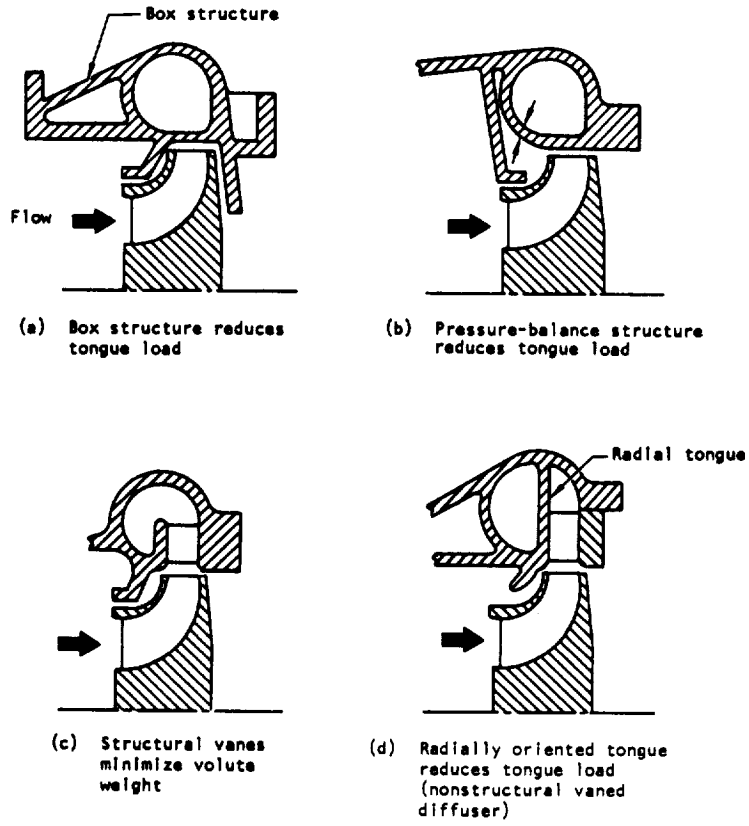

Figure 30. – Volute structural geometries.

Figure 30(a) utilizes a box structure to minimize the volute tongue deformation. The design in figure 30(b) pressure balances much of the volute to minimize tongue deformation. In figure 30(c), structural diffuser vanes support volute separating forces and thereby minimize weight. The design of figure 30(d) utilizes a long radially oriented tongue in conjunction with nonstructural diffuser vanes in a folded volute; the long radial tongue is loaded in bending rather than in tension so that the loads are minimized.

In order to minimize external forces upon the pump housing, the inlet and discharge ducting may be connected to the engine by flexible bellows. Another method for keeping external loads low is to utilize the discharge duct as part of the mounting structure to the engine in conjunction with hinged mounting points on the housing. This design requires the use of only a low-pressure bellows at the pump inlet and so is adaptable to high pump-discharge pressures. For minimum volute separating forces, a circular cross section is used. Housing stresses and deflection may be calculated by procedures presented in references 61 and 76. The steady state and dynamic stresses calculated for the pump housing are evaluated by means of a modified Goodman diagram (fig. 23) in order to establish the capability of the design to meet the required life. Safety factors are applied to compensate for uncertainties in material properties and analytical techniques. The values of the safety factors vary with the type of material control, quality control, and structural development program and with the expected application. Current practices in the use of structural design safety factors are summarized in table III.

2.4.3 Mechanical Design

The mechanical design of the pump housing must satisfy the hydrodynamic requirements and in addition provide reliable structure, leak-free joints and static seals, reliable fasteners and attachments, materials compatible with the propellants, and fabrication feasibility. Provision for anticipated special instrumentation is made during the design phase to ensure access and structural reliability.

2.4.3.1 JOINTS AND STATIC SEALS

Joints serve to connect housing components and to carry loads. A joint also may be required to prevent a leak from a region of high pressure to one of lower pressure internally or to the environment surrounding the pump.

Bolt and stud-nut and clamp-type flange configurations have been used successfully. For high-pressure pumps (>1000 psi), bolts or studs with nuts to connect mating flange joints have been used. Face-to-face contact is preferred in order to control contact loads, minimize relative motion and so avoid fretting, and provide reliable dimensional control. The joint

Table III. - Current Practices in Structural Design

Basic safety factors	Practice
Minimum yield factor of safety	≥ 1.1
Minimum ultimate factor of safety	≥ 1.4
Design loads	Most critical combined conditions
Material properties	Minimum guaranteed, based on maximum operating temperature, environment, and service life
Primary stresses	Maintain yield and ultimate safety factors
Secondary stresses	Local yielding allowed; maintain ultimate safety factor on total strain
Fatigue factors	
Low-cycle fatigue	4X predicted cycles
High-cycle fatigue	10X predicted cycles
Accumulation damage	Sum of 4X low-cycle fatigue damage + 4X creep damage + 10X high-cycle fatigue damage ≤ 1.0
Service life	Consider operating condition profile for total design life
Special pressure vessel factors	
Verification pressures	
Proof pressure	Proof factor X limit pressure at design temperature
Burst pressure	1.5X limit pressure at design temperature
Limit pressure	Maximum expected operating pressure including surges, accelerations, and oscillations
Proof factor	Value established by fracture mechanics analysis, or 1.2, whichever is greater
Checkout pressures	
Proof pressure	1.5X checkout pressure
Burst pressure	2.0X checkout pressure
Checkout pressure	System checkout pressure permitted with personnel present

design is influenced by the static-seal configuration and by assembly and installation requirements. Flange static seals that have been successfully used are O-rings, spring-loaded O-rings, K-seals, and conoseals (ref. 77). The welded seal is of particular interest for very low leakage and light weight. With welded seals, lightweight flexible lips are sealed by welding at assembly; load transmission is provided by bolted flanges.

Static-seal mating surfaces in the housing must be free from distortions that exceed the seal capability for conformance. The seal materials must be capable of maintaining an effective seal after a long shelf life. Materials that relax under prolonged load are not satisfactory seal

materials, because they may not be able to conform to joint deformation after lengthy storage periods. The pressure differential to which external seals are subjected normally are minimized by the use of a double-seal arrangement with a drain to a low-pressure point provided between the two seals. Further information on the design of static seals may be found in reference 77.

2.4.3.2 FASTENERS AND ATTACHMENTS

Fasteners and attachments used in housings are almost always of special design because of the chemical or thermal unsuitability of most materials available commercially. Although these special designs are custom made, the cost usually remains competitive because of the detailed stress analysis, chemical compatibility and strength certification, material and fabrication traceability, and configuration control that must be applied to all fasteners and attachments. The use of special designs can avoid the inadvertent substitution of a different material or the same material with a different heat treatment. Fasteners are designed to permit repeated assembly and disassembly without damage. Sufficient material allowances are made to allow repair by installation of thread inserts or use of oversized studs. Fastener and attachments are designed so that thorough cleaning is possible.

Positive locking devices are provided for all fasteners and attachments to prevent loosening by vibration; snap rings are avoided unless positive retention can be ensured.

Fastener preload is controlled carefully in order to minimize fretting and to maintain consistent housing-assembly spring rates.

2.4.3.3 ASSEMBLY PROVISIONS

Certain provisions are made in design to ensure that assembly of the housing does not introduce problems and difficulties. For example, housing liners used to minimize the explosion hazard due to inadvertent rubbing with adjacent rotating components are vented to low-pressure regions to eliminate the possibility that the liner may deviate from the housing contour and rub a rotating component.

Also, the dimensions and significant characteristics of all parts and components are carefully controlled. Detailed logs are kept so that measurements and checks can be repeated exactly as specified.

Finally, provisions are made to minimize any possibility of misassembly of parts. As in the case of the impeller, these provisions usually take the form of minor changes to the hardware that preclude incorrect mating of parts.

2.4.4 Fabrication

Housings may be cast, machined from forgings, or welded from components that were machined, forged, or cast. Cast surface finishes with irregularities of 63 μ in. or less are allowed for pump housings with impeller diameters up to 12 in.; irregularities less than 125 μ in. are allowed for housings for impellers 12 to 24 in. in diameter.

Care is exercised in casting or fabricating housings to avoid brittleness or stress concentrations that can lead to fatigue failures. Proper chilling and heat treatment of castings is important for long fatigue life. Good welds and proper heat treatment are required for welded housings to achieve long life.

2.4.5 Materials

Materials that have been successfully used in housings for centrifugal-flow pumps with various pumped fluids are presented in table IV. The materials are selected for compatibility with the fluid, ease of fabrication, and reliability (ref. 78).

Table IV. - Materials Successfully Used in Pump Housings

Material	Pumped fluid				
	LH_2	LOX	RP-1	N_2O_4	50/50 UDMH/N_2H_4
Aluminum					
A356 (cast)	X	X	X	X	X
A357 (cast)	X	X	X		
6061	X	X			
7075	X	X	X	X	X
7079	X	X			
Steel					
AM350				X	X
304L (cast)	X	X			
310 (cast)	X				
310	X	X	X		
347 (cast)		X			
Inconel 718	X	X			
"K" Monel	X	X	X		
"KR" Monel		X	X		
Ti-5Al-2.5Sn (ELI)	X				

Note: X means that the material has been used successfully with the fluid shown; absence of an X means either that no data on the specific use are available or that the material cannot be used with the fluid. Materials not shown as cast were wrought.

2.5 THRUST BALANCE SYSTEM

The thrust balance system of a turbopump balances the forces resulting from fluid pressure and fluid momentum changes originating in the turbine and the pump. The forces must be balanced to a residual value that can be reliably sustained by the turbopump bearings (ref. 43).

Devices for balancing axial thrust include impeller balance ribs, impeller seals, anti-vortex ribs, self-compensating balance pistons, and thrust bearings (figs. 31 and 32). In most cases, combinations of devices have been used. A large effort in pump development programs has

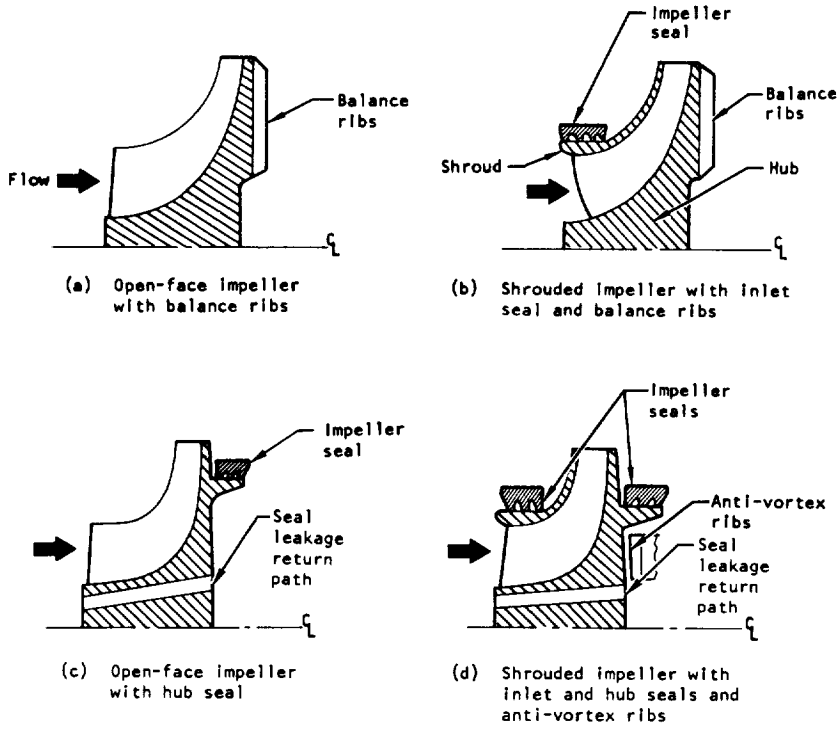

Figure 31. – Methods for balancing axial thrust.

been directed to solving axial-thrust problems. The chief difficulty lies not in designing systems for balancing thrust, but in predicting accurately the magnitude of the unbalanced forces. The usual approach is to utilize the initial analytical results to design test setups for measuring pressures and forces and operating clearances accurately. Then the design is refined on the basis of the test results.

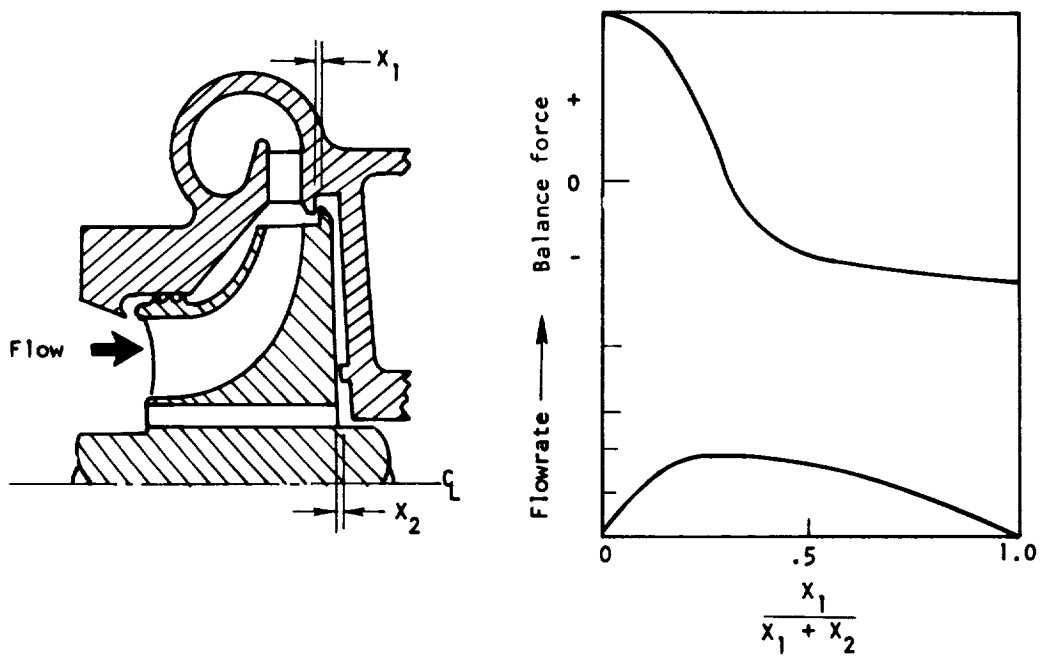

(a) Integral series-flow balance piston

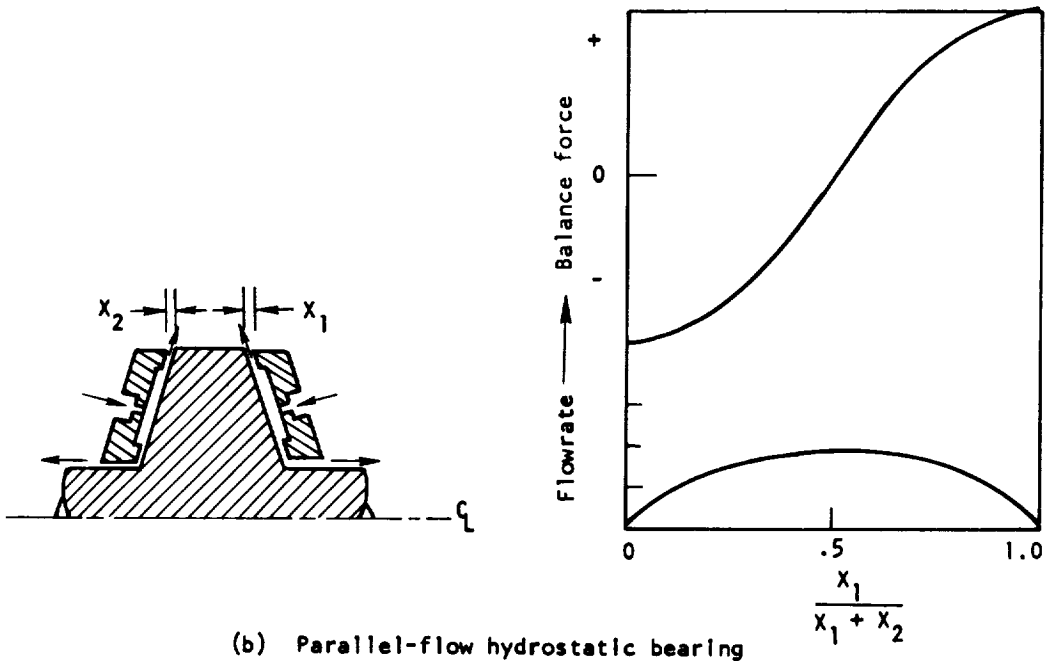

(b) Parallel-flow hydrostatic bearing

Figure 32. – Schematics and force diagrams for typical balance piston and hydrostatic bearing.

2.5.1 Unbalanced Forces

Turbine forces are balanced by the pump axial-thrust system in state-of-the-art turbopumps. Procedures for calculating turbine pressures and axial forces are presented in reference 42. Model turbine tests are used to measure internal pressures so that thrust balance forces may be more accurately estimated. Since nozzle spouting velocities are very high, flow steps in the stream can produce large axial forces on rotors. Rotor/stator alignment and the shape of the turbine rotor downstream of the nozzle are controlled to maintain these forces within the capability of the hardware.

In the pump, pressure gradients occur on the smooth nonpumping impeller hub and shroud surfaces as well as on the open faces of impellers. The pressure gradients on the nonpumping surfaces caused by viscous forces may be calculated by the procedures presented in reference 79. The pressures on the face of an open impeller may be calculated by procedures presented in references 53, 54, and 80.

2.5.2 Methods of Thrust Balance

2.5.2.1 IMPELLER WEAR RINGS

Impeller wear rings, also called impeller seals, are used on the front shroud and hub of shrouded impellers for control of axial thrust (figs. 31(b) and (d)). The area at a diameter smaller than the hub wear ring is held at a pressure slightly above the impeller inlet value by directing the leakage flow from the wear ring to the impeller inlet through holes in the impeller or through external passages. The relative diameters of the two wear rings are sized to produce the required balance force. The J-2 oxidizer pump, which is thrust balanced by use of wear rings, utilizes anti-vortex ribs at a diameter smaller than the hub wear ring to influence the radial pressure gradient in that area. Control of the pressure gradient in that region by trimming the ribs permits adjusting the axial thrust of the impeller without changing the diameters of the impeller wear rings.

The fuel turbopump in the F-1 engine had lead-plated impeller wear rings. When the wear ring rubbed during operation, the relatively soft lead "rolled up" and caused wear on the back disk of the impeller and shroud. The problem was minimized by improving the bond of the lead to the base metal and by enlarging the clearances to reduce the degree of rubbing.

2.5.2.2 IMPELLER BALANCE RIBS

Impeller balance ribs are blades located on the back of the impeller hub (fig. 31(a)). They form a low- or zero-flow impeller that provides a large pressure gradient where they are

located. The rib pumping action reduces the pressure at the smaller diameter to counteract the low pressure at the impeller inlet. Holes may be provided through the impeller into the inside diameter region of the balance ribs to vent that region statically and to provide a positive coolant flow into the balance ribs to prevent cavitation caused by fluid heating that results from the pumping work of the balance rib. Balance ribs have been used on many successful turbopumps; however, usually more development work is required to obtain a configuration that is as effective as wear rings.

The gear-driven Titan pumps utilized open-face impellers with balance ribs on the impeller hub that reduced the axial force to a value that could be sustained by a split-inner-race ball bearing. The F-1 turbopump had shrouded impellers; for control of axial thrust, the oxidizer pump impeller incorporated an inlet wear ring and balance ribs, while the fuel pump impeller incorporated inlet and hub wear rings. The pump forces balanced the direct-drive turbine forces such that tandem split-inner-race ball bearings could sustain the unbalanced axial force.

2.5.2.3 BALANCE PISTONS AND HYDROSTATIC BEARINGS

When pumps operate at very high speeds, ball bearings are not capable of sustaining the normal operating unbalanced axial forces. For these applications, balance pistons and hydrostatic bearings are used. The two types that have been used for rocket engine centrifugal pumps are the series-flow balance piston integral with the impeller (fig. 32(a)) and the separate parallel-flow hydrostatic bearing (ref. 45 and fig. 32(b)). Both types are self-compensating bearings that seek an operating clearance such that the bearings that radially locate the rotor operate with an acceptable axial force. These bearings are designed to operate with a sufficient effective spring rate to avoid axial resonances of the rotating assembly. The design of balance pistons and hydrostatic bearings usually is based on procedures like those presented in reference 81.

The J-2S fuel pump incorporated a series-flow balance piston integral with the hub of the second-stage impeller; this piston reduced the axial load to values that could be sustained by ball bearings that were axially located by springs. The ball bearings positioned the rotating assembly and sustained the spring-limited axial forces until pump pressures increased to values allowing the balance piston to sustain the axial loads. The first stage, an integral-inducer mixed-flow impeller, provided the axial force to balance the turbine force. The balance piston used a rub ring of fiberglas-reinforced Teflon to minimize possible galling of the orifices. The material delaminated, and the orifices opened up. The problem was solved by using lead-filled porous bronze for the rub rings. The J-2 axial fuel pump initially used carbon rub rings; the rings cracked, causing the orifices to open up. The problem also was solved by use of lead-filled porous bronze rub rings.

The breadboard liquid-hydrogen pump (ref. 45) used back-to-back open-face impellers of different diameters to react the turbine thrust, with a pump-discharge-fed, double-acting hydrostatic bearing for axial force balance. The pump roller bearings could support only radial loads.

2.5.2.4 BALL BEARINGS

When the density of the pumped fluid exceeds that of water, ball bearings frequently are the preferred method for sustaining unbalanced loads. The higher fluid density results in lower required pump speeds and lower impeller disk areas for a given pressure rise. The lower speed allows use of larger bearings, and the lower impeller disk area results in lower forces. Both factors permit ball bearings to sustain the resulting unbalanced loads. When bearing DN values are sufficiently low, single or multiple ball bearings can carry substantial loads when adequately cooled. Split-inner-race and angular-contact bearings are capable of sustaining larger axial loads than are deep-groove bearings. Bearing applications are discussed in reference 43.

2.5.3 Materials

Materials for thrust balance systems (table V) are selected for compatibility with the propellant, adequate strength at the required rotating speed, and minimum explosion hazard

Table V. - Materials for Thrust Balance Systems

Component	Material				
Balance ribs	Same material as impeller				
Anti-vortex vanes	Same material as housing				
Impeller seals	KEL-F*, stainless steels*, fiberglas-reinforced Teflon, silver*, leaded bronze, impeller materials, housing materials				
Balance piston	Al 2024 anodized	Al 7075-T73	Inconel 718*	"K" Monel*	Ti-5Al-2.5Sn
Balance-piston orifice	Flame-plated tungsten carbide on 310 stainless	304 stainless	Silver-plated 310 stainless; silver	Leaded bronze	Leaded bronze

*Material suitable for use with LOX.

in the event of an inadvertent rub. Plastic materials such as Kel-F, Teflon, and fluorinated polyvinyl chloride resist burning if rubbed on the impeller in liquid-oxygen pumps and therefore are safe stationary sealing materials when the seal pressure differential is not excessive. The same materials are also satisfactory in liquid-hydrogen pump service.

Materials for the balance-piston orifice are selected to resist galling if rubbed against balance piston rotor or impeller materials. To date, balance piston experience has been almost solely limited to hydrogen pumps. Future oxygen-pumps with balance pistons must limit orifice materials to those that can be LOX-cleaned, resist explosion or ignition upon impact, and are chemically and physically stable in liquid oxygen.

3. DESIGN CRITERIA and Recommended Practices

3.1 CONFIGURATION SELECTION

The pump system shall be based on the interactions and tradeoffs of equivalent performance (efficiency, weight, and size), effort to achieve required reliability, and operational flexibility.

It is recommended that system tradeoff factors be evaluated as discussed in reference 1. Tradeoff of performance factors should result in maximum engine specific impulse for the required vehicle missions.

Select a centrifugal pump when a ratio of maximum-to-minimum stable specific speed N_s greater than 1.2 is required. An N_s-vs-D_s diagram containing representative data, as presented in figure 3, should be used for preliminary selection activities.

Evaluate the parameters presented in figure 2 to ensure that mechanical and fluid-mechanics limitations are observed.

Examine pump configurations critically to ensure that the manufacturing process, the prescribed precision, and resulting costs are justified. Use tolerances, surface finishes, and configurations that result in minimum manufacturing costs when the resulting performance and weight meet the rocket engine requirements.

3.2 PUMP PERFORMANCE

The pump design point shall satisfy the required engine operating range and provide the desired performance characteristics.

The design point should be selected on the basis of (1) the required stall margin under starting, throttling, or other excursions, and (2) the desired shape of the headrise and efficiency curves, including the stall or surge point. The number of stages should be the minimum that can supply the required pressure and efficiency.

The pump design specification should include the following information (the primary source of the information is indicated in the parentheses):

- Nominal design point requirements and tolerances imposed by the engine (Mission Studies)

- Extreme off-design flowrate, headrise, and net positive suction pressure requirements including tolerances for component performance predictions and tolerances imposed by the engine (Engine Computer Model)

- Bearing, seals, and balance-piston flow (Preliminary Design Analysis)

- Future upgrading requirements (Mission Studies)

- Flight vehicle and static-test operating environment (Mission and Development Test Requirements)

- Handling and flight "g" loads (Mission and Development Test Requirements)

- Pump attitudes under static and flight conditions (Mission and Development Test Requirements)

- Duty-cycle definitions including nominal, minimum, and maximum operating duration; start transient, shutdown transient, and restart conditions; and chilldown requirements (Mission and Development Test Requirements)

- Pump test and calibration requirements (Mission and Development Test Requirements)

- Design safety factors (Mission and Development Test Requirements)

- Instrumentation requirements (Mission and Development Test Requirements)

- Tradeoff parameters (i.e., change in the engine specific impulse per point of efficiency, per pound of pump weight, and per inch of length) (Mission Studies)

- Reliability and safety requirements (Mission and Development Test Requirements)

It is recommended that the items listed above be surveyed at the outset of the design effort to ensure that the information is available or will be forthcoming from the primary sources indicated. It is recommended also that these items be kept current and consistent with the engine and turbopump requirements. In addition, the adequacy of the design should be continuously assessed against these requirements.

3.2.1 Speed

The pump speed shall maximize pump efficiency within the limits of hydrodynamic and structural constraints.

Optimize specific speed while observing other limits such as critical speed, suction specific speed, required pressure rise and flowrate, and other limits previously discussed. Consult figures 2, 3, 5, and 9, and observe the guidelines presented below.

3.2.1.1 CRITICAL SPEED

The pump shall not operate continuously at a critical speed.

It is recommended that preliminary critical-speed studies be made to ensure that the selected pump speed is at least 20 percent removed from any calculated critical speed. Reference 32 should be consulted for more precise information. Observe the analytical procedures and practices reported in reference 28.

Critical-speed calculations should consider bearing and bearing-support stiffness including nonlinearities; rotor imbalance forcing functions; shear deformation; gyroscopic effects; and viscous or Coulomb damping as well as bearing dynamic loads and shaft deflection amplitudes in regions where control of critical clearances is required (refs. 2, 6, and 28).

3.2.1.2 SUCTION SPECIFIC SPEED

The design pump speed shall not reach the level at which head loss due to cavitation occurs.

For a pump with an integral inducer, maximum suction specific speed of 40 000 for the inducer is recommended. Without an integral inducer, limit the S_s value to 12 000. Use a low-speed turbopump (boost pump) to increase pump inlet pressure when the available inlet pressure is too low to permit reaching the speed required for efficiency and light weight.

In order to provide for manufacturing variations and for instrumentation errors, the pump inlet NPSH should not be less than $3c^2_{m1}/2g$ for low-vapor-pressure fluids such as water and RP-1, $2.3c^2_{m1}/2g$ for fluids such as LOX and LF_2, and $1.3c^2_{m1}/2g$ for liquid hydrogen.

Observe the limits on suction specific speed prescribed in reference 33 and in figure 4.

3.2.1.3 TURBINE LIMITS

The design pump speed shall not exceed the speed at which turbine stresses become excessive.

Observe the turbine speed-limiting factors presented in reference 42 to ensure that turbine stress limits are not exceeded at the design pump speed and power.

3.2.1.4 BEARING AND SEAL LIMITS

The pump design speed shall not exceed the speed limits for the bearings and seals.

Observe the bearing speed limits presented in reference 43 for the radial and axial loads imposed on the bearing by rotor dynamics and fluid forces.

Observe the seal speed and pressure limits presented in reference 44. Noncontacting seals are recommended when rubbing seals cannot satisfy speed and life requirements.

3.2.2 Efficiency

3.2.2.1 PUMP SIZE AND PUMPED FLUID

The values for pump efficiency shall account for the effect of pump size and pumped fluid.

It is recommended that figure 6 be used for preliminary estimates of the influence of size on pump efficiency.

When a scaled-model pump or substitude fluids are used to obtain design data, the effects of differences in Reynolds number, relative roughness, and relative clearances should be taken into account. Observe Schlichting's formula for admissible roughness (eq. (11)).

The influence of increased seal clearances or impeller blade clearances required by oxidizer pumps should be evaluated when comparing performances of similar pump designs. The influence of fluid compressibility and internal leakage on efficiency of liquid-hydrogen pumps should be evaluated with the use of fluid enthalpy and entropy as a function of pressure and temperature.

3.2.2.2 GEOMETRY

Values for pump efficiency shall account for the effects of (1) the geometry required to attain high suction specific speed and (2) the geometry of the diffusing system.

The efficiency variation due to differences in suction specific speed may be calculated from the data in figure 9, which presents the efficiency change as a function of the specific-speed parameter. Figure 5 is used for a preliminary calculation of the impeller inlet diameter.

The information presented in figure 6 and in reference 4 can be used to estimate the influence of volutes and conical diffusers, vaned diffusers, and vaneless diffusers on pump efficiency.

3.2.2.3 STAGING

Values of pump efficiency shall account for the effects of staging.

Design for the minimum number of stages that (1) can supply the minimum efficiency compatible with the engine system requirements and (2) will result in a pump that does not exceed the impeller tip speed limits in any stage.

Vaned diffusers with internal crossover passages (fig. 11(b)) should be used for minimum envelope and maximum efficiency. The external-diffusing-passage type may be used to take advantage of its simpler geometry when the larger envelope and lower effiency are acceptable.

3.2.3 Flow Range

3.2.3.1 HEAD-VS-FLOW CHARACTERISTIC

The pump head-vs-flow characteristic shall provide the flow range required by the engine system.

The head-vs-flow characteristic of the pump should have a negative slope with respect to head-vs-flow characteristic of the engine liquid flow system at all flowrates. The engine liquid flow system may be considered as extending from the pump discharge to the thrust-chamber injector discharge.

To provide rising head to the lowest possible flowrate, when the impeller discharges into a vaned diffuser, the pump head coefficient should be equal to or less than 0.5.

3.2.3.2 IMPELLER BLADE NUMBER

The impeller blade number shall produce the required flow range.

The impeller inlet blade number should be small enough that the impeller inlet free area is more than 80 percent of the inlet annular area. The impeller discharge blade number should be sufficient to provide the design head coefficient as shown by figure 16. Refer to section 3.3 for further considerations affecting blade number.

3.3 IMPELLER

3.3.1 Hydrodynamic Design

3.3.1.1 DIAMETER RATIO

The ratio of the impeller inlet tip diameter to discharge tip diameter shall maximize efficiency consistent with the required suction performance.

The value for δ should be established from the guides presented in figure 5. The required inlet diameter should be calculated by use of the suction performance information presented in figure 4 supplemented by the guidelines in reference 33.

3.3.1.2 HEAD AND FLOW COEFFICIENTS

The impeller shall produce the required head-vs-flow characteristic while operating at the flow coefficient that satisfies suction performance.

The impeller inlet flow coefficient compatible with the available NPSH should be calculated on the basis of the information presented in figure 14 or on the information in reference 33. Establish discharge flow coefficient by selecting the discharge meridional velocity to be 1 to 1.5 times that at the inlet. For a given ϕ_2, the number of impeller blades Z_2 should be equal to or greater than that shown on figure 16. The head-vs-flow slope of the pump is then calculated with use of an impeller slip coefficient M and pump hydraulic efficiency η_h based on experience to cover the flow range of interest.

The blade number, angle, and tip diameter are adjusted until the required head-vs-flow characteristic is achieved. The pump head/flow characteristic required for engine-system stability is determined by means of an engine-system analysis as discussed in reference 1.

To match final requirements, adjust the impeller head coefficient after fabrication by underfiling or overfiling as shown in figure 15.

3.3.1.3 BLADE NUMBER AND BLADE GEOMETRY

Blade number and blade geometry shall be consistent with the flow coefficient and the meridional passage shape.

Smooth blade shapes and relative-velocity distributions should be established by means of a one-dimensional analysis followed by a quasi-three-dimensional analysis. For a given ϕ_2, the blade number at the impeller discharge should be greater than the minimum number shown in figure 16, and the value for suction-surface relative-velocity gradient G [eq. (15)] should not exceed 3.5, as noted previously. The impeller blade pressure-surface velocity should be greater than zero and in the direction of the discharge.

Inlet blade angle and thickness distribution should be designed for minimum suction-surface velocity for suction performance, wide flow range, and good efficiency. The suction-surface relative velocity for the first 20 percent of the impeller meridional length should not exceed the inlet relative velocity by more than 20 percent at zero-incidence conditions.

To ensure that the pump flowrate is stable over the desired engine operating range (off-design), it is recommended that the discharge blade angle be selected for a characteristic of decreasing headrise with increasing flowrate. It also is recommended that the zero-slope point on the characteristic H-Q curve be at least 10 percent below the lowest required flowrate and the stall point be at least 15 percent below the lowest required flowrate. The relationship of discharge blade angle to number of blades is presented in figure 16.

It is recommended that the slip coefficient approach a value of one by the use of a large number of impeller blades to produce the steepest head/flow slope for a given impeller tip speed. A large slip coefficient may result in a flat head/flow slope with a low head coefficient.

The number of blades at the inlet should be related to the thickness so that the free area is greater than 80 percent of the annulus area; the number of blades at the exit should be related to the thickness so that the free area is greater than 85 percent of the annulus area. Greater inlet or discharge blockage reduces efficiency; greater inlet blockage reduces flow range and suction performance. Four to eight inlet blades are recommended.

3.3.1.4 SHROUDING

The choice of shrouded or unshrouded impellers shall be based on the relative capability to produce maximum efficiency, achieve minimum pump weight, avoid rubbing, satisfy tip speed limits, and satisfy shaft critical speeds.

It is recommended that shrouded impellers be selected for maximum efficiency, freedom from rubbing problems except at the seals, and minimum pump weight. Use seal materials that can tolerate light rubbing without reacting with the propellant or galling the impeller or seal. Open-face impellers should be selected when tip speeds in excess of 2200 fps are required.

3.3.2 Mechanical Design

3.3.2.1 AXIAL RETENTION

Impeller axial retention shall be maintained under all test and operating conditions.

Poisson shortening due to centrifugal-stress-induced radial growth and thermal shrinkage should be calculated so that this influence is included in the design of the axial retention method. Control bolt stretch to maintain a prescribed minimum axial load during operation. Invar spacers may be used to compensate for differential thermal shrinkage. Short axial-length shoulders on the impeller clamped against a shaft shoulder can be used to reduce both thermal and Poisson effects.

3.3.2.2 PILOTING

Impeller radial piloting shall not result in imbalance or fretting corrosion.

Maintain radial piloting by using sufficient interference fit during static assembly so the minimum required load is achieved at the maximum pump rotating speed. By appropriate analysis or test, ensure that any increase in static interference during chilling will not result in yielding that can reduce the interference fit and result in loss of piloting. The impeller hub should be designed so that radial pilot diameters are not subject to large centrifugal stresses.

It is recommended that the mechanical arrangement be selected so that stresses and distortions are minimized, fits and pilots are retained, and attachment stresses kept within acceptable limits. Particular attention should be given to light-alloy impeller pilots on steel shafts and impeller blade-to-hub joints in rapidly chilled cryogenic pumps. The selection of pilot fit should allow for the effects of differences in coefficients of thermal expansion (transient and steady-state temperature) and for operating-stress-induced deformation.

3.3.2.3 FATIGUE MARGIN

The impeller shall not fail from fatigue.

Avoid impeller fatigue failures due to stress concentration by use of appropriate design and manufacturing procedures. Eliminate residual stresses in castings or forgings by heat treating. High-speed impellers should be spun to produce higher deflections than will occur during normal pump operation so that the material is yielded in areas of local stress concentration. This yielding results in an initial compressive stress at low speeds and a lower maximum stress at high speeds. Detect regions of stress concentration by means of brittle lacquer or ceramic coatings that crack in regions of high deflection when the impeller is loaded by spinning or pumping. Combined steady and dynamic forces should produce stresses lower than those that will result in long-time failure as shown by a modified Goodman diagram (fig. 23).

For ductile materials, the endurance limit is reduced by stress-concentration effects on the alternating stress but is not reduced by their effects on the mean stress. Therefore, the stress-concentration factor for blade-root fillet radius or other discontinuities should be applied to the blade alternating stress before using the modified Goodman diagram to determine the blade structural adequacy.

3.3.2.3.1 Fillet Radii and Surface Finish

Blade-fillet radii and surface finish shall minimize stress concentration.

The fillet radii at the blade-to-hub, blade-to-shroud, and blade-to-backplate junctions should be equal to 1.5 times the blade thickness. This ratio will reduce the stress-concentration factor in the area to a value approximating 1. It is recommended that the leading-edge cross section be a 2:1 to 3:1 ellipse.

Blade surface finish grossly affects the fatigue life of an impeller. If the impeller is cast, a 125 μ in. rms finish is readily obtainable on all surfaces; hand finishing should be performed in the high stress and alternating stress areas to improve the surface finish until a 63 μ in. rms finish is attained on all surfaces.

When necessary, shot peen the surface to remove the detrimental residual tensile stress, machining marks, and surface imperfections and to put the surface into a state of residual compression stress.

3.3.2.4 TIP SPEED

Maximum tip speeds shall be consistent with impeller material properties, hydrodynamic design, and construction.

Calculate allowable tip speed limits for the required hydrodynamic design. Impeller disk stresses and deflections should be calculated by procedures similar to those presented in references 61, 82, and 83. For preliminary analysis, the blade thickness for an impeller pumping fluid with a specific gravity near 1 may be approximated as follows:

$$t \approx \frac{.087\, b_{t2}\, u_{t2}}{\sqrt{\sigma_{\text{allowable}}}} \sin \beta_{t2} \qquad (22)$$

where

t = blade thickness

b_{t2} = impeller tip width

u_{t2} = impeller tip speed

β_{t2} = impeller tip blade angle

$\sigma_{allowable}$ = allowable stress

Calculation of blade stresses should include a cyclic pressure loading 30 percent of the steady-state hydraulic loading calculated by means of hydrodynamic analyses. Other factors that strongly influence stress such as shroud thickness, blade angle, tip width, and propellant loads must be included as part of the detailed analysis.

It is recommended that the selection of a hub-to-tip radius ratio be based on a compromise between blade tip speed and blade root stress. Large values of hub-to-tip radius ratio result in larger tip diameters and fluid loads but smaller root stresses; small values of hub-to-tip radius ratio result in smaller tip diameters and fluid loads but relatively large root stresses.

3.3.2.5 SHAFT TORQUE CAPABILITY

The impeller shaft shall transmit the required torque without failure and without fretting.

The shaft torque capacity should be adequate for off-design operation and should include allowances for errors in estimating component efficiency and efficiency shift with the change in flow coefficient that results from increases in speed necessary to meet increased pressure drops in the engine. Torque should be transmitted into regions of the impeller where the combined loads can best be withstood without failure. Contact forces of the torque-transmitting devices (splines, curvics, pins, or bolts) should be large enough to prevent fretting, which has caused explosions; lubricants that are compatible with the propellant can be used to minimize fretting.

It is recommended that wrench flats or wrench-type surfaces and torque-wrench access or turbine-drive access be provided to facilitate breakaway-torque and drag-torque measurements. Provide instructions in the assembly procedure with limits based upon measurement data from new, damaged, and used but undamaged comparison units.

3.3.2.6 CLEARANCES

Impeller-to-housing clearances shall be sufficient to avoid any possibility of metal-to-metal rubbing that can cause rotor side loads, generate heat, or generate metal particles.

It is recommended that shrouded impellers with nonmetallic wear rings be selected whenever tip speed limits are not high enough to prohibit this design. The use of shrouded impellers permits large axial and radial clearances except for the wear ring. The larger housing deflections tolerable with shrouded impellers can result in minimum pump weight.

For propellants such as LF_2, the wear-ring radial clearance must be sufficient to preclude rubbing. For less reactive propellants, light wear-ring rubbing is allowable if side loads are small, particles are not generated, and chemical reaction as a result of heat rise cannot occur. Inert wearing materials such as Teflon, Kel-F, and silver are recommended for oxidizer pumps.

It is recommended that unshrouded impeller tip clearances be minimized within practical mechanical limits, distortion and thrust excursions being taken into account. The influence of tip clearance ratio on efficiency is presented in figure 21.

3.3.3 Fabrication

Techniques for fabricating and assembling the impeller shall be consistent with the required life, performance, and reliability.

The fabrication method depends on the intended tip speed and on the impeller material. Tip speed limits are discussed in section 2.3.2.1; materials that may be selected are presented in table II.

Casting is the preferred method of fabrication for impellers with tip speeds below 1400 fps, because it permits optimization of the hydrodynamic design, is less expensive, and results in excellent shroud-to-blade strength and cleanliness. High-tip-speed impellers (>1400 fps) with open faces should be machined from forgings. Shrouded high-tip-speed impellers for tip speeds to 2200 fps may be machined or, if fabricated from titanium, may be diffusion

bonded. Shrouded machined impellers should be limited to stage specific speeds over 1000 and tip diameter-to-width ratios less than 20. The maximum impeller blade number that can be machined is approximately $28 \sin \beta_2$. The cutter length-to-diameter ratio that establishes the blade spacing should not exceed 10 for aluminum and 8 for titanium parts.

A separate inducer should be selected for use with shrouded impellers because of the impeller fabrication complexity. Separate inducers allow more latitude in blade configuration.

The direction of rotation should be clearly specified on design layouts. The detail and assembly drawings should be checked against this control document. In addition, direction should be verified at assembly.

It is recommended that, as part of the manufacturing procedure, impellers expected to operate at tip speeds above 1000 fps be spun to a speed at least 20 percent above the maximum anticipated operating speed; this procedure will result in local yielding without failure. The speed should be corrected for temperature influence on material properties if the overspeed run is conducted at a temperature different from that for normal operation.

Precautions should be observed in machining high-speed impellers to avoid large values of imbalance. Cutting tools should be changed to produce weight symmetry as cutters wear. Cutters should be changed every 60°, 90°, or 180°, for example, rather than after a certain amount of cutter wear, so that the dimensional changes resulting from cutter wear will be minimized.

Location, amount, and procedure for removing or adding balance correction material should be specified. It is recommended that careful attention be given to fixturing and arbor problems along with consideration of room-temperature fits relative to operating fits on cryogenic pumps.

The following formula is recommended for estimating permissible imbalance of rotating assemblies and rotating assembly components:

$$\text{Residual imbalance, oz-in.} \approx \frac{4 \times \text{rotor weight in lb}}{\text{speed in rpm}}$$

It is recommended that the effects of assembly misalignment upon residual imbalance be minimized for parts that are balanced separately or for parts that are removed and reassembled after balancing. Misalignment as a result of centrifugal growth or thermal distortion should be avoided. Special design provisions (e.g., double registers, conical registers, and dowel pins) or fixtures could be necessary. In general, it is recommended that the disassembly of the rotating assembly after balancing be kept to a minimum.

3.3.4 Materials

Impeller materials shall be compatible with the propellants and shall be capable of satisfying the required tip speeds.

Materials compatible with commonly used rocket engine propellants may be selected from table II. Materials for high-stress application should be selected for ductility to permit relief of stress concentrations by local yielding. Materials for high-tip-speed impellers are discussed in section 2.3.2.1.

The effect of the modulus of elasticity, density (weight), ductility, fatigue strength, damping characteristics, propellant compatibility, and the coefficient of thermal contraction should be evaluated prior to final material selection. Strength-to-weight ratio should not be the dominant criterion.

If ductility is lower than 5 percent, structural analysis and design must consider notch sensitivity, stress raisers, defect propagation, and other failure characteristics of brittle material.

Aluminum alloys A357, 2014, 6061, 7075, and 7079; K-monel; and Inconel 718 are recommended candidates for liquid-oxygen service.

Titanium will produce the highest allowable tip speed impellers. High-purity (ELI) Ti-5Al-2.5Sn is recommended for cryogenic applications because of its relatively high ductility at low temperatures. Titanium is not acceptable for liquid-oxygen service.

Casting is the most feasible method of producing a complex impeller, and hence aluminum A357 is recommended for such applications; this alloy exhibits a good strength-to-weight ratio and is compatible with most propellants including fluorine.

For extreme cases of cavitation or high hydrodynamic loads, Inconel 718 is recommended; this material can be cast, and shrouded impellers of complex geometry can be fabricated.

Inconel 718 and the aluminum alloy 7075 are suitable for use with LF_2 as well as with many other propellants. However, when 7075 A1 is used, it should be heat-treated and given special processing to alleviate its susceptibility to stress corrosion and to improve its strength.

3.4 HOUSING

3.4.1 Hydrodynamic Design

3.4.1.1 CASING

The casing interior wall shall not adversely affect pump efficiency or impeller axial thrust.

The casing interior contour should follow closely the exact contour of the impeller; this relation is particularly important for open-face impellers, since the casing wall establishes the tip clearance. The wall surface finish should be about 63 μ in./in. and free from fasteners, attachment points, and any surface protuberances; necessary fasteners should be located close to the pump centerline.

If recommended conditions of contour and smoothness cannot be met, tests should be made to evaluate the influence of surface roughness on the radial pressure gradient and thereby on axial thrust.

3.4.1.2 DIFFUSION SYSTEM

3.4.1.2.1 Vaneless Diffuser

The length of a vaneless diffuser (the impeller-to-stator spacing) shall result in the highest efficiency attainable without producing unacceptable discharge-pressure oscillations.

The empirical curve in figure 24 should be used as a guide to achieve high performance with acceptable oscillations in pump discharge pressure. Reference 65 presents the influence of impeller diffusion and clearance. Pressure losses in the vaneless diffuser can be calculated by the procedures given in reference 66.

3.4.1.2.2 Vaned Diffuser

A vaned diffuser shall minimize impeller radial loads over wide flow ranges and maximize pump efficiency at low specific speed.

For minimum radial loads, the vaned diffuser discharge velocity should match the volute velocity and the flow angle should match the volute tongue angle.

For maximum flow range, design the vaned diffuser so the efficiency at maximum flow rate is equivalent to that with the impeller discharging directly into a volute. Design the diffuser vane width equal to or smaller than the impeller tip width (100 percent to 90 percent) and provide well-rounded or faired side walls to permit misalignment without flow separation. Allow for wear-ring leakage flow with shrouded impellers, because the leakage reduces the width of the flow sheet entering the diffuser.

Good proportions for the diffuser channel should be established by an iteration between a minimum hydraulic radius for the required area and the number of diffuser vanes (usually, the prime number nearest to the number of impeller blades). The diffuser throat dimensions for the pump best-efficiency operating point should provide an area adequate for the passage flowrate and for the velocity at the diffuser throat mean radius, calculated by the conservation-of-momentum method from the velocity at the impeller discharge radius (fig. 25).

If a conical diffuser is used downstream, the vaned diffuser and volute tongue should be separated by a radius ratio greater than 1.05 or the tongue should virtually touch the diffuser; otherwise, pump discharge pressures may become unstable and degrade engine performance by introducing fluctuations in thrust.

Use vaned diffusers to reduce the velocity in the volute when the pump overall head coefficient is greater than 0.5, when $N_s < 1000$, and when maximum efficiency or low weight is important.

Select the number of diffuser vanes to diffuse efficiently when the requirements for inlet flow angle, radius ratio, and velocity ratio are satisfied; the number should be compatible with the number of impeller vanes. The diffuser should not exceed the equivalent-cone-angle diffusion rates indicated by figure 26; the diffusion factor for a single stage should not exceed 0.6.

Avoid boundary-layer growth, which limits further diffusion. The exit radius of a ring of diffuser vanes should not be greater than 1.4 times the inlet radius. If necessary, use more than one ring to achieve the required velocity ratio.

3.4.1.2.3 Interstage Flow Passage

The inlet of an interstage flow passage shall accept the impeller discharge flow, and the outlet of the passage shall provide the flow necessary for the following impeller – all without unacceptable pressure or flow oscillations.

The practices discussed in references 66 and 72 should be observed in designing interstage flow passages. When a vaned radial diffuser is followed by a volute, equation (20) or (21)

should be used to establish the parameters so that reinforcement of pressure waves generated by the impeller blade wakes is precluded.

To avoid excessive diffusion in any one stage, use staged diffusion (e.g., a vaned diffuser followed by a multiple-outlet volute with conical exit diffusers, or vaned radial diffusers followed by axial diffusers and crossover passages) between stages of a multiple-stage pump. It is recommended that external high-pressure flange joints be avoided.

3.4.1.3 VOLUTE

The volute shall enhance maximum downstream conical diffuser efficiency and prevent bi-stable pump head/flow characteristics.

The volute cross section should be asymmetrical so that it produces a single vortex, which improves conical diffuser performance. Use the asymmetrical volute to provide a stable pump characteristic. With a vaned diffuser, provide a stable characteristic by fairing one diffuser vane into the volute tongue or by leaving a large clearance between the vane discharge and the tongue. Both means avoid interaction with the volute-exit conical diffuser.

The divergence angle of volute-exit conical diffusers, expressed as included angle, should be as follows (ref. 71): for circular cross sections, 7° to 9°; for square cross sections, 6°; and for two parallel walls, 11°.

3.4.1.3.1 Cross-Sectional Area

The volute cross-sectional area shall result in minimum impeller radial load at the design point.

The constant-moment-of-momentum method adjusted for friction loss will produce minimum design-point impeller radial loads. The procedures presented in reference 74 may be followed for this analysis.

3.4.1.3.2 Off-Design Radial Load

In variable-flow pumps, the volute shall not impose additional radial loads on the impeller.

Any of several methods of radial-load control that have proven effective over a wide flow range of a pump may be used: multiple-tongue volute, vaned diffuser, double-outlet volute, and combinations of these (figs. 28(b), (c), and (d)).

To minimize radial thrust loads, particularly at off-design flow conditions, employ double-outlet volutes without vaned diffusers. When single outlets are required, use vaned diffusers to minimize the radial loads caused by nonuniform circumferential static pressures. It is recommended that the design of the pump discharge housing be similar to an existing design that produces minimum radial thrust over the flow range desired and that potential-flow analysis be used to estimate the radial thrust.

3.4.2 Structural Design

The housing shall withstand all predicted loads and stresses without rupture or unacceptable amounts of deflection.

Housing stresses and deflections may be calculated by procedures presented in references 61 and 76. Stress levels and deflections should be compatible with the selected materials. The factors of safety used for the housing design should be consistent with the material-control procedures and the accuracy of the calculated or measured stress levels.

Critical-speed effects, in terms of housing stiffness, should be evaluated as part of the housing analysis to ensure adequate spring rate of bearing supports.

It is recommended that machined integral-diffuser vanes serve as main structural members of high-pressure volutes and that the volute assembly reduce the influence of pressure- and line-load-induced deflections on critical clearances. Housing pressure loads should not pass through the leading edges of a vaned diffuser.

The volute tongue forms a stiff, highly loaded point in a flexible system. For this reason the tongue leading edge should be smoothly finished and shot peened if required to improve fatigue life. The ratio of volute fillet radius to web thickness should be as large as possible; a ratio greater than 1.0 will result in a minimum stress concentration.

It is recommended that volutes be sized to maintain safety factors as shown in table III when material properties are compared with primary effective stresses.

If the calculated elastic peak stress and corresponding peak strain is greater than twice the elastic limit strain, then cyclic plastic strain will occur. The volute must then be checked to ensure adequate safety factor against low-cycle fatigue failure. The low-cycle fatigue safety factor should be based on cycles to failure and should be no less than 4, i.e., the number of cycles to failure should be 4 times the number of predicted operating cycles.

Mounting loads should be minimized by designing the structure to prevent distortions of the mount points on the engine from inducing pump loads. Use hinged mounts and flexible duct

connections as required. Provide volute and housing strength to accept mounting loads.

Minimize volute and housing deflections to maintain running clearance and bearing loads within allowable limts. It is recommended that shear webs (box structure) be employed to reduce housing deflections, and that the pressure-induced loads be balanced to reduce the forces. It is also recommended that axial ties, across the volute, be incorporated to reduce these deflections. Diffuser vanes, through-bolts, and flow splitters can be used for this purpose.

Provide adequate wall thickness and space for instrumentation bosses, probes, line routing, terminals, and brackets, along with a capability for replacing such hardware during testing.

3.4.3 Mechanical Design

3.4.3.1 JOINTS AND STATIC SEALS

Joints and static seals shall be free from unacceptable leakage during storage and operation, including repeated operation.

Minimize the number of external joints. Each joint should be evaluated for effect upon assembly sequence and reliability, manufacturing ease and cost, material availability, and inspectability.

Joints and static seals should be free from yielding under load and should not relax to a permanently deformed shape under prolonged storage. A static seal should operate in its elastic range over all conditions. Joint deflections should not exceed the conformance capability of the mating static seals.

Avoid the use of materials or designs for static seals that lead to loss of ability to seal after prolonged periods of storage. Use metallic seals or composite seals in which the metal provides the spring force. Manufacturer's claims of static-seal performance should be carefully evaluated against the specific application. Tests in the correct environment prior to design commitment are recommended.

Seal surfaces should be hard, so that they will not be marred by mating surfaces under load; hard surface coatings or hard materials may be used. Design so that external seal surfaces are not easily damaged in handling; use protruding rings, studs, or other devices that prevent accidental contact of seal surfaces with tables, floors, or wrenches.

Welded joints and dual seals with inert-buffer-fluid pressurization or leakage bleed-off should be considered for zero-leakage joints. All high-pressure dual seals should be vented to internal low-pressure cavities.

For a flanged joint, verify that under thermal, mechanical, or pressure loads

(1) Flange alignment is maintained by piloting.

(2) The flange does not rotate.

(3) The joint is not distorted or opened.

(4) There is no unacceptable change in radial or axial fit.

It is recommended that flange deflection or rotation analyses be based on maximum operating pressures and the most severe interface thermal gradients established by a finite-element heat-transfer program. Through-holes and nuts or oversize high-strength inserts are recommended if stresses in the flange are excessive. The elastic deformation of the joint elements should be included in the analysis.

Thin flange joints with many small, closely-spaced bolts are superior to thicker flanges with few large bolts. Bolt-and-nut flange attachments are preferred over threaded-hole flanges. Provide adequate space for wrenches in the design of flanges and joints to avoid the possibility of easy stud-bolt damage.

Control of the configuration by an interface control drawing with a check of mating faces is recommended.

3.4.3.2 FASTENERS AND ATTACHMENTS

Fasteners and attachments for centrifugal pump assembly

- *Shall maintain critical fits and clearances, with controlled preload.*
- *Shall withstand repeated use.*
- *Shall have positive locking devices.*
- *Shall not contaminate the system or react with the service or test fluid.*

Conduct a thermal analysis based upon predicted duty cycles and test conditions. Then, superimpose these thermal conditions on a stress analysis that includes deflections induced by operating dynamics. Thus, the adequacy of fits and attachments can be assessed upon the basis of combined effects. A special configuration, or revised duty cycle, or test procedures may be required. Good fastener design practice (e.g., control of load and preload, avoidance of stress raisers, smooth transition, and proper material selection) is recommended.

A direct determination of preload is recommended. This should be done by measuring the increase in depth of a longitudinal hole in the bolt and comparing it with the desired preload expressed as strain or by measuring the force required to obtain the preload.

It is recommended that wrench clearances provide space for accurate determination of torque values; therefore, accessibility and non-awkward positioning for standard wrenches are necessary.

Materials for fasteners and attachments should be those that resist galling. Sufficient material should be present in the housing to permit repair by installation of thread inserts or oversize studs.

Tab washers, cup washers, and lock-wire are preferred locking devices; however, lock-wire is not recommended for rotating attachments. When lock-wire is used, take special care to avoid failure of the wire or contamination by the ends cut off during assembly. Tab-on-tong or cup-on-slot lockwashers are recommended for critical attachments.

Provide a large safety margin on tab stress so that the tabs retaining the washer to the stationary part will not be sheared. It is recommended that the face of the bolt or nut be relieved to prevent axial contact, false torque, or damage of the bolt or nut face by the sharp-edge washer tabs. Ductile washer material should be used.

If snap rings are mandatory, careful evaluation of groove detail, installation procedure, material selection, and loading is necessary; positive locking against creepout is required.

Fastener and attachments should be designed to permit thorough cleaning; blind holes should be avoided wherever possible. Material surfaces should resist fretting, which can cause contamination. Propellant-compatible coatings may be used to eliminate base-material fretting.

Thread lubricants for liquid-oxygen service should be tested for compatibility with the propellant (ref. 84).

3.4.3.3 ASSEMBLY PROVISIONS

3.4.3.3.1 Housing Liners

Housing liners shall not be damaged by pressure behind the liner.

Pressure relief holes should be used to vent the liner/housing cavity to the main stream to prevent distortion and damage.

3.4.3.3.2 Prevention of Errors in Assembly

Design provisions shall prevent errors in assembly.

A buildup sheet with required dimensions and method of measurement clearly specified is recommended to ensure recording of appropriate dimensions, torques, runouts, and serial numbers. Gross checks, including visual inspection, simple measurements, leak checks, and breakaway-torque checks, should be specified. Visual checks and direct measurements rather than deduced dimensions are recommended.

When only one orientation for a part is permissible, preclude misassembly in one of the following ways:

(1) Stepped land sizes on studs

(2) Missing tooth (and mating space) on splines

(3) Nonsymmetrical hole patterns for multiple bolt or stud fastening

(4) Fixed dowel pins or keys (used mostly for stationary parts or lightly loaded rotary parts)

Unique part numbers should be applied to all parts and noninterchangeable configurations of the same part. Serialization of all parts, particularly for the performance-sensitive or structurally critical components, is necessary.

It is recommended that dimensioning be based upon identifiable, accessible datum planes and diameters such as the diffuser-wall inner surface and diffuser-vane leading edges or base circle.

3.4.4 Fabrication

Housing fabrication shall not result in brittleness, stress concentrations, or degraded material properties.

Use adequate chills in tongue regions of cast volutes to maximize the ductility. Heat treat to relieve local stresses and thereby produce ductility combined with strength while avoiding susceptibility to stress corrosion. Preyielding of the housing structure by pressurizing to levels greater than operating values should be part of the fabrication process; this practice will reduce stress concentrations. Proof-test fixtures and procedures must be designed to simulate loading.

Strength, ductility, dimensional accuracy and finish, porosity, repairability, weight, deformation or deflection characteristics, and quality assurance requirements should be assessed before a cast housing is selected.

3.4.5 Materials

Housing materials shall be compatible with the propellant and shall possess properties that satisfy structural and fabrication requirements.

Materials that have given satisfactory service and are therefore recommended are presented in table IV.

It is recommended that material for test bars be added to each forging and casting so that material properties of each lot can be evaluated, particularly for high-strength applications. If it is not feasible to add this material in a high-stress area, the test data from accessible positions should be combined with forging and casting control information and with remote-position test-bar data, so that all of this information can be correlated to guarantee integrity.

In accordance with established procedures (refs. 85 and 86), evaluate the environment and conditions leading to stress corrosion.

Titanium should not be used for service with liquid oxygen. Inconel 718 or aluminum alloys A357, 6061, 7075, and 7079 are recommended.

For use with cryogenics, A357, alloy 713C, or Inconel 718 possess good properties and are therefore recommended.

It is recommended that chills be used in volute-tongue regions of aluminum castings and other areas requiring maximum strength and ductility. Manufacturing parameters such as forgeability, machineability, weldability, and heat-treat requirements, as well as cost, should be evaluated. Alternative configurations, strength levels, and fabrication processes should be evaluated in terms of loss of performance or increase in weight.

3.5 THRUST BALANCE SYSTEM

The thrust balance system shall limit unbalanced forces to values that the bearings can sustain.

The forces that thrust bearings can sustain and the bearing coolant flow rates required should be determined by procedures presented in reference 43. The unbalanced forces should be determined as described below. It is recommended that bearing-coolant and thrust-balance flow circuits be designed for minimum thermal lag by utilizing short flow passages and structural designs with minimum cross-sectional areas.

3.5.1 Unbalanced Forces

Evaluation of thrust balance system forces shall include forces imposed by both the turbine and the pump.

The calculation of the unbalanced forces should allow for

(1) Propellant compressibility effects

(2) Changes in fluid properties as a result of speed

(3) The effect of fluid heating

The affinity relationship, in which thrust varies with speed squared, should be used with caution over a wide speed range, because changes in pump-fluid density and the compressibility effects of the turbine gas will alter the familiar pump affinity relationships for an incompressible fluid.

The pressure/area and momentum change forces produced by the turbine may be calculated by procedures presented in reference 42.

The pressure gradients on smooth impeller shrouds and disks may be calculated by procedures presented in reference 79. The pressure gradients on the open face of an impeller may be calculated by procedures presented in references 52, 53, and 87. Pressure gradients induced by balance ribs on the impeller may be calculated by procedures presented in reference 80. The pressures that result in axial forces and the bearing loads should be measured early in the turbopump development program.

On large pumps with toroidal discharge housings or single volutes, average circumferential pressures at the impeller discharge must be included in calculations of axial thrust. Large pumps with toroidal discharge housings or a single-outlet volute should be provided with more than one circumferential pressure tap per angular location to obtain a radial distribution of average pressures. The use of local static pressures that are not representative of the average circumferential pressure at any radius leads to substantial errors in the calculation of the axial thrust.

3.5.2 Methods of Thrust Balance

3.5.2.1 IMPELLER WEAR RINGS

The balancing capability of an impeller wear ring shall be insensitive to tolerances on operating clearances.

The pressure in the low-pressure region of the impeller should be reduced and made insensitive to seal-clearance tolerances by using leakage flow areas approximately four times the seal-clearance area. Anti-vortex ribs may be used in the same region to control the pressure gradient. The anti-vortex ribs may be trimmed as necessary to adjust the axial force without changing the impeller seal diameters. Impeller wear rings are recommended over balance ribs since wear rings are not subject to force changes caused by cavitation or by changes in axial clearance.

3.5.2.2 IMPELLER BALANCE RIBS

Balance ribs shall not introduce the possibility of cavitation in the low-pressure regions.

Cavitation due to work-induced heating or trapped gases should be minimized by the use of holes through the impeller to vent the region prior to start and to provide a positive coolant flow to reduce heating during operation. Cavitation reduces the fluid density and thereby changes the pressure gradient on the back disk near the rib. An additional control is to size the inner diameter to adjust the minimum pressure to avoid cavitation. The impeller in the balance-rib region should be shaped to avoid trapping of gases prior to start.

For oxidizer pumps, cavitation or the presence of vapor in the cavity at the impeller backface must be avoided under all operating conditions. The pressure in the cavity on the back face of the impeller can be maintained above vapor pressure by proper sizing of the back ribs or labyrinth system feeding the back face. Cavitation in the cavity also can be avoided without affecting the balancing capability of the system or without raising the cavity pressure by supplying colder fluid (e.g., flow that bypasses the bearings) to the cavity.

When balance ribs are used for balancing axial thrust, it is recommended that the ribs be sized so that the desired minimum thrust load can be achieved by simple diametral trimming of the ribs or by modifying wear-ring surfaces.

Balance ribs should provide thrust balance over the required flow range. Evaluate the change in axial force due to the different pressure-vs-flow characteristics of the impeller and the balance ribs, and verify that the balance ribs will be effective under the expected flow conditions.

3.5.2.3 BALANCE PISTONS AND HYDROSTATIC BEARINGS

When axial thrust loads are beyond the capability of wear rings or balance ribs, a balance piston or hydrostatic bearing shall maintain the bearing loads within acceptable limits.

Self-compensating axial-thrust balance pistons are recommended for turbopumps for which prediction uncertainties and component tolerances result in excessively large variations in bearing loads at design or at off-design conditions. Load prediction should include the effect of hydraulic loading, rotor dynamics, bearing stiffness, thermal effects, and turbine effects including overspeed conditions.

It is recommended that spring-loaded axial stops be incorporated in the bearing carrier adjacent to the balance-piston assembly to locate the rotor statically and to minimize the contact force of the orifice and rotor at low speeds when the pump pressure may not be sufficient for the balance piston to overcome transient forces. Bearing load capability is greater at low speeds, making bearing load sharing or light orifice rubbing at low speeds safe for startup transients. The balance-piston position is evaluated after installation by means of static push-pull tests.

Balance pistons should have adequate uprating capability; piston chamber pressures and clearances must be selected so that the load capacity of the balance piston can be adjusted by modifying clearances or controlling inlet pressure. It is recommended that the excess load-carrying capacity of the thrust balance device be at least 100 percent of the balance force required at the design-point neutral position in both directions. For stability of balance pistons, it is recommended that balance piston pocket volume (volume between inner and outer orifices) be kept to a minimum (ref. 81).

3.5.2.4 BALL BEARINGS

Ball bearings alone shall sustain unbalanced thrust loads whenever the loads are within bearing capabilities.

Observe the bearing DN, load, bearing type, size, and bearing cooling recommendations presented in reference 43.

Avoid designs that result in restricted bearing mount or bearing travel as this restriction can cause loss of bearing preload and allow ball skidding. Bearing loads can be controlled to the level required to prevent skidding by the use of preload springs that load one bearing in a dual set against the other. The bearings are mounted freely in the housing to eliminate the possibility of sustaining shaft forces.

Use materials adjacent to bearing outer races and bearing carriers with compatible thermal contraction rates to allow for shrink differentials.

When loads are produced by springs, insure that changes in dimensions due to chilling and pressure deflections do not exceed design spring compression.

When bearing loads are produced by fluid pressure forces on pump impellers or turbines, ensure that the direction of force does not change during operation and that the force is consistent with the operating speed.

3.5.3 Materials

Materials for thrust balance systems shall be compatible with the propellant and capable of providing the required life.

Satisfactory materials and their uses are presented in table V. For oxidizer service, the materials and installation should permit thorough cleaning.

Materials for impeller seals and balance-piston orifices should minimize heat buildup and galling if lightly rubbed. In particular, the stationary orifices of the thrust balance device should be made of material that will not shatter or gall or produce galling of a mating rotating surface on contact. As shown in table V, leaded bronze is recommended as the stationary orifice material for use with a titanium, K-monel, or Inconel 718 rotor.

APPENDIX A
GLOSSARY

Symbol	Definition
A	flow area
a	velocity of sound in liquid
b	blade or vane width
c	absolute fluid velocity
D	diameter; diffusion factor
D_s	specific diameter, $D_s = \frac{DH^{1/4}}{Q^{1/2}}$
D_v	average distance from center of pump to center of volute passage
DN	bearing speed-capability index, the product of bearing bore size (D) in mm and rotation speed (N) in rpm
E	material modulus of elasticity
ELI	extra-low-interstitial (content of interstitial elements)
F_e	material endurance limit strength
F_{tu}	material ultimate tensile strength
F_{ty}	material yield tensile strength
G	impeller suction-surface relative-velocity gradient
g	acceleration due to gravity
H	head or headrise
H_i	ideal headrise
Hz	cycles per second
j	order of the harmonic of fundamantal wave

Symbol	Definition
K	impeller-seal flow coefficient
K_{adm}	admissible roughness
L	length of flow passage
L_m	meridional length of flow passage
M	slip coefficient
m	reinforcement index, used in equations (20) and (21)
N	rotating speed, rpm
N_s	specific speed, $N_s = \frac{NQ^{1/2}}{H^{3/4}}$
NPSH	net positive suction head, $NPSH = \frac{P_t - P_v}{\rho}$
P_a	power available for hydrodynamic work
P_h	hydraulic output horsepower
P_s	static pressure
P_{sh}	input shaft horsepower
P_t	total pressure
P_v	vapor pressure
Q	flowrate (volumetric)
Q'	corrected flowrate, $Q' = \frac{Q}{1 - \nu^2}$
Q_L	leakage flowrate
R	radius
RC	radial clearance

Symbol	Definition
Re_L	Reynolds number based on length
S	blade spacing, $S = \frac{\pi D}{Z}$
S_s	suction specific speed, $S_s = \frac{NQ^{1/2}}{(NPSH)^{3/4}}$
S'_s	corrected suction specific speed, $S'_s = \frac{S_s}{(1-\nu^2)^{1/2}}$
S'_s*	characteristic suction specific speed (determined in cold water)
T	fluid bulk temperature
TSH	thermodynamic suppression head
t	blade thickness
u	rotor tangential velocity (blade tip speed)
W	relative velocity of fluid
W_v	relative velocity of fluid in volute
w	fluid velocity relative to blade
X	balance piston or hydrostatic bearing orifice displacement
X_L	$\frac{\text{axial distance from midpoint of impeller inlet to impeller discharge}}{\text{impeller discharge diameter}}$
Z	number of impeller blades
Z_d	number of diffuser vanes
z	axial coordinate
α	incidence angle
β	blade angle
δ	ratio of inlet tip diameter to discharge tip diameter

Symbol	Definition
η	efficiency
θ	diffuser equivalent cone angle
ν	inlet hub-to-tip diameter ratio
ρ	density
σ_{CF}	stress caused by centrifugal force
σ_{FF}	stress caused by fluid forces
$\sigma_{allowable}$	allowable stress
σ_{alt}	alternating stress, $\sigma_{alt} = \frac{\sigma_{max} - \sigma_{min}}{2}$
σ_{mean}	average stress, $\sigma_{mean} = \frac{\sigma_{max} + \sigma_{min}}{2}$
φ	flow coefficient, $\varphi = \frac{c_m}{u}$
ψ	head coefficient, referred to impeller tip blade speed, $\psi = \frac{gH}{u^2_{t2}}$

SUBSCRIPTS

1	impeller inlet or station 1
2	impeller discharge or station 2
3	vaned diffuser inlet
4	vaned diffuser outlet
5	volute inlet
6	volute discharge
7	volute conical diffuser discharge
a	axial component; annulus

bl	blade
burst	burst speed
d	design value
h	hub; hydraulic
LE	leading edge
m	meridional; mechanical
ms	mean or rms station
op	operating conditions
opt	optimum
rms	root mean square
S	suction
TE	trailing edge
t	tip
test	test conditions
u	tangential component
v	vapor; volumetric
yield	yield speed
∞	infinite number of blades

Material[1]	Identification
A356 A357	aluminum alloys per MIL-A-21180
alloy 713C	austenitic nickel-base casting alloy per AMS 5391
AM350	semi-austenitic stainless steel per QQ-S-763

[1] Additional information on metallic materials herein can be found in the 1972 SAE Handbook, SAE, Two Pennsylvania Plaza, New York, NY; and in MIL-HDBK-5B, Metallic Materials and Elements for Aerospace Vehicle Structures, Dept. of Defense, Washington, DC, Sept. 1971.

Material	Identification
fiberglas	trade name of Owens-Corning Fiberglas Corp. for products made of or with glass fibers or glass flakes
FLOX	mixture of liquid fluorine and liquid oxygen
hydrazine	N_2H_4, propellant grade per MIL-P-26536B
Inconel 718	trade name of International Nickel Co. for precipitation-hardening nickel-chromium-iron alloy (specification AMS 5663)
IRFNA	inhibited red fuming nitric acid, propellant grade per MIL-P-7254
Kel-F	trade name of 3M Corp. for a high-molecular-weight polymer of chlorotrifluorethylene
"K" Monel	trade name of International Nickel Co. for a wrought age-hardenable alloy containing nickel, copper, and aluminum
"KR" Monel	"K" Monel that has had its machining qualities enhanced by a controlled carbon content
leaded bronze	copper alloy containing zinc and lead
LF_2	liquid fluorine
LH_2	liquid hydrogen, propellant grade per MIL-P-27201A
LOX	liquid oxygen, propellant grade per MIL-P-25508D
N_2O_4	nitrogen tetroxide, propellant grade per MIL-P-26539
RP-1	kerosene-base high-energy hydrocarbon fuel, propellant grade per MIL-P-25576
Teflon	trade name of E. I. duPont, Inc. for a polymer of tetrafluoroethylene
UDMH	unsymmetrical dimethylhydrazine, propellant grade per MIL-P-25604D
304L	austenitic stainless steel per QQ-S-763, Class 304L
310	austenitic stainless steel
347	austenitic stainless steel per QQ-S-763, Class 347
2014; 2014-T6	aluminum alloy per QQ-A-200/2; temper T6

Material	Identification
2024	aluminum alloy per QQ-A-200/3
6061; 6061-T6	aluminum alloy per QQ-A-225/8; temper T6
7075; 7075-T73	heat-treated aluminum alloy per QQ-A-250/12; temper T73
7079	aluminum alloy per QQ-A-200/12

Pumps, Engines, and Vehicles Designation	Identification
Atlas	launch vehicle using MA-5 engine system
Atlas booster engine	165/185 000 lbf-thrust engine in MA-5 engine system
Atlas sustainer engine	60 000 lbf-thrust engine in MA-5 engine system
Centaur	high-energy upper stage for Atlas and Titan; uses 2 RL10 engines
F-1	engine for S-IC; 1 500 000 lbf thrust; uses LOX/RP-1; manufactured by Rocketdyne Division, Rockwell International Corp.
H-1	engine for S-IB; 200 000 lbf thrust; uses LOX/RP-1; manufactured by Rocketdyne
J-2	engine for S-II; 200 000 lbf thrust; uses LOX/LH_2; manufactured by Rocketdyne
J-2S	uprated J-2; 250 000 lbf thrust; uses LOX/LH_2; designed and developed by Rocketdyne
M-1	1 500 000 lbf thrust engine designed and developed by Aerojet Liquid Rocket Co.; used LOX/LH_2
MA-5	five-engine system for Atlas vehicle containing 2 booster, 2 vernier, and 1 sustainer engines; boosters provide 330 000 to 370 000 lbf thrust; sustainer, 60 000 lbf thrust; uses LOX/RP-1; manufactured by Rocketdyne
Mark 3, Mark 10, Mark 14	LOX/RP-1 turbopumps developed by Rocketdyne
Mark 9, Mark 15, Mark 19, Mark 25, Mark 29	liquid-hydrogen turbopumps developed by Rocketdyne

Designation	Identification
Mark III	liquid-hydrogen turbopump developed by Aerojet Liquid Rocket Co.; used in NERVA program
MB-3	engine system for Thor vehicle; 170 000 lbf thrust; uses LOX/RP-1; manufactured by Rocketdyne
NERVA	Nuclear Engine for Rocket Vehicle Application developed by Aerojet Liquid Rocket Co.; 750 000 lbf thrust; uses H_2 as working fluid
Redstone	launch vehicle using Rocketdyne A-7 engine system providing 78 000 lbf thrust; engine used LOX/alcohol
RL10	engine for Centaur; 15 000 lbf thrust; uses LOX/LH_2 ; manufactured by Pratt & Whitney Aircraft Division of United Aircraft Corp.
Saturn V	launch vehicle for Apollo manned mission to the moon
S-IB	booster using a cluster of eight H-1 engines
S-IC	first stage (booster) of the Apollo Saturn V vehicle; uses five F-1 engines
S-II	second stage of the Apollo Saturn V vehicle; uses a cluster of five J-2 engines
S-IVB	third stage of the Apollo Saturn V vehicle; uses a single J-2 engine
Thor	launch vehicle using MB-3 engine system
Titan I, II, III	family of launch vehicles using the LR-87-AJ and LR-91-AJ series of rocket engines developed by Aerojet Liquid Rocket Co.
X-8	experimental throttleable rocket engine; 90 000 lbf thrust; uses LOX/LH_2 ; developed by Rocketdyne
LR-87-AJ-3, -5, -7, -9	Aerojet engines for the first stage of the Titan vehicles • the -3 uses LOX/RP-1, and develops 150 000 lbf thrust • the -5, -7, -9 use N_2O_4/A-50, and develop 215 000 lbf thrust
LR-91-AJ-3, -5, -7, -9	Aerojet engines for the second stage of the Titan vehicles • the -3 uses LOX/RP-1, and develops 90 000 lbf thrust • the -5, -7, -9 use N_2O_4/A-50, and develop 100 000 lbf thrust
XLR-129	rocket engine developed by the Pratt & Whitney Aircraft Division of United Aircraft Corp.; 250 000 lbf thrust; uses LOX/LH_2

APPENDIX B

Conversion of U.S. Customary Units to SI Units

Physical quantity	U.S. customary unit	SI unit	Conversion factor[a]
Force	lbf	N	4.448
Head or headrise	ft	m	0.3048
	$\frac{\text{ft-lbf}}{\text{lbm}}$	J/kg	2.989
Length	ft	m	0.3048
	in.	cm	2.54
Mass	lbm	kg	0.4536
	oz	kg	0.02835
Power	hp	W	745.7
Pressure	psi ($lbf/in.^2$)	N/m^2	6895
Rotational speed	rpm	rad/sec	0.1047
Temperature	°R	K	5/9
Viscosity, absolute	$\frac{\text{lbf-sec}}{\text{ft}^2}$	$N\text{-sec}/m^2$	47.88
Volume	gal	m^3	3.785×10^{-3}

[a]Multiply value given in U.S. customary unit by conversion factor to obtain equivalent value in SI unit. For a complete listing of conversion factors, see Mechtly, E. A.: The International System of Units. Physical Constants and Conversion Factors, Second Revision. NASA SP-7012, 1973.

REFERENCES

1. Anon.: Turbopump Systems for Liquid Rocket Engines. NASA Space Vehicle Design Criteria Monograph, NASA SP-8107 (to be published).

2. Anon.: High Pressure Pumping Technology. Final Report R-5833, Rocketdyne Div., North American Rockwell Corp., 1964.

3. Wislicenus, G. F.: Fluid Mechanics of Turbomachinery. Vols. 1 and 2. Dover Publ., 1965.

4. Balje, O. E.: Study of Turbine and Turbopump Design Parameters. Vol. IV – Low Specific Speed Turbopump Study. S/TD No. 1735, No. 20, The Sundstrand Corp. (Rockford, IL), 1959.

5. Balje, O. E.: A Study on Design Criteria and Matching of Turbomachines. J. Eng. Power, Trans. ASME, Series A, vol. 84, 1962, pp. 83-114.

6. Severud, L. K.; and Reeser, H. G.: Analysis of the M-1 Liquid Hydrogen Turbopump Shaft Critical Whirling Speed and Bearing Loads. NASA CR-54825, Aerojet-General Corp., 1965.

7. Finkelstein, A. R.: Myklestad's Method of Predicting Whirl Velocity as a Function of Rotational Velocity for Flexible Multimass Rotor Systems. J. Appl. Mech., Trans. ASME, Series E, vol. 87, 1965, pp. 589-591.

8. Ludwig, G. A.: Vibration Analysis of Large High-Speed Rotating Equipment. J. Eng. Ind., Trans. ASME, Series B, vol. 88, 1966, pp. 201-210.

9. Lund, J. W.: Rotor-Bearing Dynamics Design Technology, Part V – Computer Program Manual for Rotor Response and Stability. AFAPL-TR-65-45, Air Force Aero Prop. Lab. (WPAFB, OH), May 1965.

10. Lund, J. W.; and Sternlicht, B.: Rotor-Bearing Dynamics with Emphasis on Attenuation. J. Basic Eng., Trans. ASME, Series D, vol. 84, 1962, pp. 491-502.

11. Lund, J. W.: The Stability of an Elastic Rotor in Journal Bearings with Flexible Damped Support. J. Appl. Mech., Trans. ASME, Series E, vol. 87, 1965, pp. 911-920.

12. Lund, J. W.; and Orcutt, F. K.: Calculations and Experiments on the Unbalanced Response of a Flexible Rotor. J. Eng. Ind., Trans. ASME, Series B, vol. 89, 1967, pp. 785-796.

13. Dimentberg, F. M.: Flexural Vibrations of Rotating Shafts. Butterworth & Co. (London), 1961.

14. Yamamoto, T.: On the Critical Speeds of a Shaft. Memoirs of the Faculty of Engineering, Nagoya Univ. (Japan), vol. 6, no. 2, Nov. 1954.

15. Yamamoto, T.: On the Vibrations of a Rotating Shaft. Memoirs of the Faculty of Engineering, Nagoya Univ. (Japan), vol. 9, no. 1, May 1957.

16. Yamamoto, T.: On Critical Speeds of a Shaft Supported by Ball Bearings. J. Appl. Mech., Trans. ASME, Series E, vol. 81, 1959, pp. 199-204.

17. Wirt, L. A.: An Introduction to the Works of Toshio Yamamoto Which Treat the Vibration Problems Encountered in High-Speed Rotating Machinery. Strain Gage Readings, vol. V, no. 1, April-May 1962, pp. 7-20.

18. Rieger, N. F.: Rotor-Bearing Dynamics Design Technology. Part I – State of the Art. AFAPL-TR-64-45, Air Force Aero.Prop. Lab. (WPAFB, OH), May 1965.

19. Poritsky, H.: Rotor-Bearing Dynamics Design Technology. Part II – Rotor Stability Theory. AFAPL-TR-64-45, Air Force Aero. Prop. Lab. (WPAFB, OH),May 1965.

20. Lund, J. W.; et al.: Rotor-Bearing Dynamics Design Technology. Part III – Design Handbook for Fluid Film Type Bearings. AFAPL-TR-65-45, Air Force Aero. Prop. Lab. (WPAFB, OH), May 1965.

21. Lewis, P.; and Malanoski, S. B.: Rotor-Bearing Dynamics Design Technology. Part IV – Ball Bearing Design Data. AFAPL-TR-65-45, Air Force Aero. Prop. Lab. (WPAFB, OH), May 1965.

22. Hamburg, G.; and Parkinson, J. P.: Gas Turbine Shaft Dynamics. Paper 382B, SAE Summer Meeting (St. Louis, MO), June 5-9, 1961.

23. Alford, J. S.: Protecting Turbomachinery from Self-Excited Whirl. J. Eng. Power, Trans. ASME, Series A, vol. 87, 1965, pp. 333-344.

24. Ehrich, F.: The Influence of Trapped Fluids on High Speed Rotor Vibrations. J. Eng. Ind., Trans. ASME, Series B, vol. 89, 1967, pp. 806-812.

25. Ehrich, F. F.; Subharmonic Vibration of Rotors in Bearing Clearance. ASME paper 66-MD-1, ASME Design Engineering Conference and Show (Chicago, IL), May 9-12, 1966.

26. Macchia, D.: Acceleration of an Unbalanced Rotor Through the Critical Speed. Paper 63-WA-9, ASME Winter Annual Mtg., Nov. 17-22, 1963.

27. Baker, J. G.: Mathematical-Machine Determination of Vibration of an Accelerated Unbalanced Rotor. J. Appl. Mech., Trans. ASME, Series E, vol. 61, 1939, pp. A-145 through A-150.

28. McCann, G.D. Jr.; and Bennett, R. R.: Vibration of Multifrequency Systems During Acceleration through Critical Speeds. J. Appl. Mech., Trans. ASME, Series E, vol. 71, 1949, pp. 375-382.

29. Mironenko, G.: Titan III M-87 High Speed Shaft Critical Speed and Bearing Load Analysis. SA-MOL-TPA-223, Aerojet-General Corp. (Sacramento, CA), July 15, 1966.

30. Howitt, F.: Accelerating a Rotor Through a Critical Speed. The Engineer, vol. 212, no. 5518, Oct. 27, 1961, pp. 691-692.

31. Linn, F. C.; and Prohl, M. A.: The Effect of Flexibility of Support Upon the Critical Speeds of High Speed Rotors. Trans. Soc. Naval Arch. and Marine Engrs., vol. 59, 1951.

32. Anon.: Liquid Rocket Engine Turbopump Shafts and Couplings. NASA Space Vehicle Design Criteria Monograph, NASA SP-8101, Sept. 1972.

33. Anon.: Liquid Rocket Engine Turbopump Inducers. NASA Space Vehicle Design Criteria Monograph, NASA SP-8052, May 1971.

34. Meng, P. R.; and Connelly, R. E.: Investigation of Effects of Simulated Nuclear Radiation Heating on Inducer Performance in Liquid Hydrogen. NASA TMX-1359, 1967.

35. Anon.: Evaluation of NPSH Performance of the Model Mark-3 Lox Turbopump Used in the Thor MB-3 Propulsion System. R-6995, Rocketdyne Div., North American Rockwell Corp., Apr. 21, 1967.

36. Saleman, V.: Cavitation and NPSH Requirements of Various Liquids. J. Basic Eng., Trans. ASME, Series D, vol. 81, 1959, pp. 167-173.

37. James, J. B.: Development of the Liquid Hydrogen Turbopump for the J-2 Rocket Engine (U). Paper presented at AIAA Propulsion Specialists Conference, Air Force Academy (Colorado Springs, CO), June 14-18, 1965. (Confidential).

38. Stepanoff, A. J.: Cavitation in Centrifugal Pumps with Liquids Other than Water. J. Eng. Power., Trans. ASME, Series A. vol. 83, 1961, pp. 79-90.

39. James, J. B.: J-2X Turbomachinery Report for 1967. Report TSM 8115-2005, Rocketdyne Div., North American Rockwell Corp., Feb. 1968.

40. King, J. A.: Design of Inducers for Two-Phase Operation, Final Report. R-8283, Rocketdyne Div., North American Rockwell Corp., July 1970.

41. Ruggeri, R. S.; and Moore, R. D.: Method for Prediction of Pump Cavitation Performance for Various Liquids, Liquid Temperatures, and Rotative Speeds. NASA TN D-5292, 1969.

42. Anon.: Liquid Rocket Engine Turbines. NASA Space Vehicle Design Criteria Monograph, NASA SP-8110 (to be published).

43. Anon.: Liquid Rocket Engine Turbopump Bearings. NASA Space Vehicle Design Criteria Monograph, NASA SP-8048, Mar. 1971.

44. Anon.; Liquid Rocket Engine Turbopump Rotating Shaft Seals. NASA Space Vehicle Design Criteria Monograph (to be published).

45. Williams, F. B.: Design, Fabricate and Test Breadboard Liquid Hydrogen Pump (U). Final Report July 1, 1966 – July 15, 1967, PWA FR-2184, Pratt & Whitney Aircraft, Div. of United Aircraft Corp. (West Palm Beach, FL), 1967. (Confidential).

46. Ball, C. L.; Meng, P. R.; and Reid, L.: Cavitation Performance of 84° Helical Pump Inducer Operated in 37° and 42° Liquid Hydrogen. NASA TM X-1360, Feb. 1967.

47. Bullock, R. O.: Analysis of Reynolds Number and Scale Effects on Performance of Turbomachinery. J. Eng. Power, Trans. ASME, Series A, vol. 86, 1964, pp. 247-256.

48. Hildebrand, P.; et al.: Centrifugal Pump (High Pressure) for Power Transmissions. Rep. No. AFAPL-TR-66-12 (AD-480108), The Garrett Corporation, 1966.

49. Stepanoff, A. J.: Volute vs Diffuser Casings for Centrifugal Pumps. Proceedings National Conference on Industrial Hydraulics, Oct. 18-19, 1950, pp. 55-74. Publ. Armour Research Foundation, Chicago, IL, 1951.

*50. Hansen, O.: Untersuchungen Uber den Einfluss des Endlichen Schaufelabstandes in Radialen Kreiselradern. Verlag Kanrad Triltsh, (Wurzburg, Germany), 1937.

51. Anisimov, S. A.; et al.: Study of the Efficiency of Centrifugal Compressor Wheels with a Two-Stage Vane Cascade. Translation from Russian Periodical, Energomashinostroenie, No. 221, 1962; AD-400535, Wright Patterson Air Force Base, OH, 1963, pp. 44-68.

52. Vavra, M. H.: Aero-Thermodynamics and Flow in Turbomachines. John Wiley & Sons, Inc., 1960.

53. Katsanis, T.: Use of Arbitrary Quasi-orthogonals for Calculating Flow Distribution in the Meridional Plane of a Turbomachine. NASA TN D-2546, 1964.

54. Katsanis, T.; and McNally, W. D.: Fortran Program for Calculating Velocities and Streamlines on a Blade-to-Blade Stream Surface of a Tandem Blade Turbomachine. NASA TN D-5044, 1969.

55. Anon.: Rotating and Positive-Displacement Pumps for Low-Thrust Rocket Engines. Vol. 1 – Evaluation and Design; Vol. 2 – Fabrication and Testing. NASA CR-72965 and CR-72966, Rocketdyne Div., Rockwell International (to be published).

56. Wiesner, F. J.: A Review of Slip Factors for Centrifugal Impellers. J. Eng. Power, Trans. ASME, Series A, vol. 89, 1967, p. 558.

57. Wood, G. M.; Welna, H.; and Lamers, R. P.: Tip Clearance Effects in Centrifugal Pumps. Paper No. 64-WA/FE-17, ASME Winter Annual Mtg. (New York, NY), 1964.

58. Hoshide, R. K.; and Nielson, C. E.: Study of Blade Clearance Effects on Centrifugal Pumps. NASA CR-120815, Rocketdyne Div., North American Rockwell Corp., Nov. 1972.

59. Wolf, J. E.: Fabrication Techniques for Shrouded Titanium Impeller – Final Report. R-8061, Rocketdyne Div., North American Rockwell Corp., 1969.

*Dossier for design criteria monograph "Liquid Rocket Engine Centrifugal Flow Pumps." Unpublished, 1968. Collected source material available for inspection at NASA Lewis Research Center, Cleveland, Ohio.

60. Wolf, J. E.: Titanium Pump Impeller Testing – Final Report. TMR 0115-3141, Rocketdyne Div., North American Rockwell Corp., 1971.

61. Radowski, P. P.; Davis, R. M.; and Bolduc, M. R.: A Numerical Analysis of the Equations of Thin Shells of Revolution. Paper presented at ARS 15th Annual Mtg. (Washington, DC), Dec. 5-8, 1960.

62. Anon.: Design, Fabricate and Test Breadboard Liquid Hydrogen Pump (U). PWA-FR-1461, NASA CR-82289, Pratt & Whitney Aircraft, Div. of United Aircraft Corp. (West Palm Beach, FL), July 30, 1965. (Confidential)

63. Kovats, A.: Investigation of Volute – Impeller Interaction in Pumps. ASME Paper No. 66-FE-14, ASME-EIC Fluids Eng. Conf., Apr. 25-28, 1966.

64. Lazarkiewicz, S.; and Troskolanski, A. T.: Impeller Pumps. Pergamon Press, 1965.

65. Jackson, E. D.: Study of Pump Discharge Pressure Oscillations. Final Report, R-6693-2, Rocketdyne Div., North American Rockwell Corp., Oct. 1966.

66. Eckert, B.; and Schnell, E.: Axial und Radial Kompressoren. Springer-Verlag (Berlin), 1961.

67. Stepanoff, A. J.: Centrifugal and Axial Flow Pumps. Revised, John Wiley & Sons, Inc., 1960.

68. Pfleiderer, C.: Die Kreiselpumpen fur Flussigkeiten und Gase. Springer-Verlag (Berlin), 1961.

69. Patterson, G. N.: Modern Diffuser Design. Aircraft Eng., vol. 10, no. 115, Sept. 1938, pp. 267-273.

*70. Jakobsen, J. K.: Hydrodynamic Design of the Mark 22 Diffuser and Scroll Section. Internal Report, TAMR 6115-5, Rocketdyne Div., North American Rockwell Corp., June 1966.

71. McDonald, A. T.; and Fox, R. W.: An Experimental Investigation of Incompressible Flow in Conical Diffusers. International Journal of Mechanical Sciences, vol. 8, Feb. 1966, pp. 125-139.

72. Rutschi, K.: The Effect of Guide Arrangements on the Output Efficiency of Centrifugal Pumps. British Hydromechanics Res. Assoc., (Cranfield, Eng.). Trans. into English from Schweizerische Bauzeitung (Zurich), vol. 79, no. 15, Apr. 1961.

73. Strub, R. A.: Pressure Fluctuations and Fatigue Stresses in Storage Pumps and Pump Turbines. J. Eng. Power, Trans. ASME, Series A, vol. 86, 1964, pp. 191-194.

74. Brown, W. B.; and Bradshaw, G. R.: Design and Performance of Family of Diffusing Scrolls with Mixed-Flow Impeller and Vaneless Diffuser. NACA Report 936, 1949.

75. Knapp, R. T.: Centrifugal-Pump Performance as Affected by Design Features. Trans. ASME, vol. 63, 1941, pp. 251-260.

*Dossier for design criteria monograph "Liquid Rocket Engine Centrifugal Flow Pumps." Unpublished, 1968. Collected source material available for inspection at NASA Lewis Research Center, Cleveland, Ohio.

76. Becker, E. B.; and Brisbane, J. J.: Application of the Finite-Element Method to Stress Analysis of Solid Propellant Rocket Grains. Rep. S-76, Rohm & Haas Co., vol. I (AD 474031), Nov. 1965; vol II, part 1 (AD 476515); vol. II, part 2 (AD 476735), Jan. 1966.

77. Anon.: Liquid Rocket Disconnects, Couplings, Fittings, Joints, and Seals. NASA Space Vehicle Design Criteria Monograph (to be published).

78. Anon.: Aerospace Structural Metals Handbook. AFML-TR-68-115, vols. 1, 2, and 3. Air Force Materials Laboratory (WPAFB, OH), 1969.

79. Due, H. F. Jr.: An Empirical Method for Calculating Radial Pressure Distribution on Rotating Discs. J. Eng. Power, Trans. ASME, Series A, vol. 88, 1966, pp 188-196.

80. Young, W. E.; and Due, H. F.: Investigation of Pressure Prediction Methods for Low-Flow Radial Impellers, Phase III. PWA FR-1761, Pratt & Whitney Aircraft, Div., United Aircraft Corp. (West Palm Beach, FL), Jan. 13, 1966.

81. Watters, W. E.; and Luehr, L.: Development of Steady-State and Dynamic Performance Prediction Methods for Turbopump Self-Compensating Thrust Balance Systems. NASA CR-72630, Aerojet-General Corp., (Sacramento, CA), Mar. 1970.

82. Anon.: Mechanical Design Aspects of Centrifugal Impellers with High Tip Speed Capability (U). Rep. 7446-01F (AD 350716), Aerojet-General Corp., Mar. 1963. (Confidential).

83. Anon.: Mechanical Design Aspects of Centrifugal Impellers with High Tip Speed Capability: The Results of Experimental Program (U). Phase II Final Rep. 7446-01F (AD 340146), Aerojet-General Corporation, Aug. 1963. (Confidential).

84. Anon.: Testing Compatibility of Materials for Liquid Oxygen Systems. MSFC-Spec-106A, Marshall Space Flight Center (Huntsville, AL), Sept. 1966.

85. Uhlig, H. H.: Corrosion and Corrosion Control. Second ed., John Wiley & Sons, Inc. (NY), 1971.

86. Fontana, M. G.; and Greene, N. D.: Corrosion Engineering. McGraw-Hill Book Co. (NY), 1967.

87. Young, W. E., et al: Investigation of Pressure Prediction Methods for Low Flow Radial Impellers, Phase II. UAC-PFR-1276, United Aircraft Corporation (E. Hartford, Conn.), Mar. 1965.

NASA SPACE VEHICLE DESIGN CRITERIA MONOGRAPHS ISSUED TO DATE

ENVIRONMENT

SP-8005	Solar Electromagnetic Radiation, Revised May 1971
SP-8010	Models of Mars Atmosphere (1967), May 1968
SP-8011	Models of Venus Atmosphere (1972), Revised September 1972
SP-8013	Meteoroid Environment Model–1969 (Near Earth to Lunar Surface), March 1969
SP-8017	Magnetic Fields–Earth and Extraterrestrial, March 1969
SP-8020	Mars Surface Models (1968), May 1969
SP-8021	Models of Earth's Atmosphere (90 to 2500 km), Revised March 1973
SP-8023	Lunar Surface Models, May 1969
SP-8037	Assessment and Control of Spacecraft Magnetic Fields, September 1970
SP-8038	Meteoroid Environment Model–1970 (Interplanetary and Planetary), October 1970
SP-8049	The Earth's Ionosphere, March 1971
SP-8067	Earth Albedo and Emitted Radiation, July 1971
SP-8069	The Planet Jupiter (1970), December 1971
SP-8084	Surface Atmospheric Extremes (Launch and Transportation Areas), May 1972
SP-8085	The Planet Mercury (1971), March 1972
SP-8091	The Planet Saturn (1970), June 1972
SP-8092	Assessment and Control of Spacecraft Electromagnetic Interference, June 1972

SP-8103	The Planets Uranus, Neptune, and Pluto (1971), November 1972
SP-8105	Spacecraft Thermal Control, May 1973

STRUCTURES

SP-8001	Buffeting During Atmospheric Ascent, Revised November 1970
SP-8002	Flight-Loads Measurements During Launch and Exit, December 1964
SP-8003	Flutter, Buzz, and Divergence, July 1964
SP-8004	Panel Flutter, Revised June 1972
SP-8006	Local Steady Aerodynamic Loads During Launch and Exit, May 1965
SP-8007	Buckling of Thin-Walled Circular Cylinders, Revised August 1968
SP-8008	Prelaunch Ground Wind Loads, November 1965
SP-8009	Propellant Slosh Loads, August 1968
SP-8012	Natural Vibration Modal Analysis, September 1968
SP-8014	Entry Thermal Protection, August 1968
SP-8019	Buckling of Thin-Walled Truncated Cones, September 1968
SP-8022	Staging Loads, February 1969
SP-8029	Aerodynamic and Rocket-Exhaust Heating During Launch and Ascent May 1969
SP-8030	Transient Loads From Thrust Excitation, February 1969
SP-8031	Slosh Suppression, May 1969
SP-8032	Buckling of Thin-Walled Doubly Curved Shells, August 1969
SP-8035	Wind Loads During Ascent, June 1970
SP-8040	Fracture Control of Metallic Pressure Vessels, May 1970
SP-8042	Meteoroid Damage Assessment, May 1970
SP-8043	Design-Development Testing, May 1970

SP-8044	Qualification Testing, May 1970
SP-8045	Acceptance Testing, April 1970
SP-8046	Landing Impact Attenuation for Non-Surface-Planing Landers, April 1970
SP-8050	Structural Vibration Prediction, June 1970
SP-8053	Nuclear and Space Radiation Effects on Materials, June 1970
SP-8054	Space Radiation Protection, June 1970
SP-8055	Prevention of Coupled Structure-Propulsion Instability (Pogo), October 1970
SP-8056	Flight Separation Mechanisms, October 1970
SP-8057	Structural Design Criteria Applicable to a Space Shuttle, Revised March 1972
SP-8060	Compartment Venting, November 1970
SP-8061	Interaction with Umbilicals and Launch Stand, August 1970
SP-8062	Entry Gasdynamic Heating, January 1971
SP-8063	Lubrication, Friction, and Wear, June 1971
SP-8066	Deployable Aerodynamic Deceleration Systems, June 1971
SP-8068	Buckling Strength of Structural Plates, June 1971
SP-8072	Acoustic Loads Generated by the Propulsion System, June 1971
SP-8077	Transportation and Handling Loads, September 1971
SP-8079	Structural Interaction with Control Systems, November 1971
SP-8082	Stress-Corrosion Cracking in Metals, August 1971
SP-8083	Discontinuity Stresses in Metallic Pressure Vessels, November 1971
SP-8095	Preliminary Criteria for the Fracture Control of Space Shuttle Structures, June 1971
SP-8099	Combining Ascent Loads, May 1972

SP-8104	Structural Interaction With Transportation and Handling Systems, January 1973

GUIDANCE AND CONTROL

SP-8015	Guidance and Navigation for Entry Vehicles, November 1968
SP-8016	Effects of Structural Flexibility on Spacecraft Control Systems, April 1969
SP-8018	Spacecraft Magnetic Torques, March 1969
SP-8024	Spacecraft Gravitational Torques, May 1969
SP-8026	Spacecraft Star Trackers, July 1970
SP-8027	Spacecraft Radiation Torques, October 1969
SP-8028	Entry Vehicle Control, November 1969
SP-8033	Spacecraft Earth Horizon Sensors, December 1969
SP-8034	Spacecraft Mass Expulsion Torques, December 1969
SP-8036	Effects of Structural Flexibility on Launch Vehicle Control Systems, February 1970
SP-8047	Spacecraft Sun Sensors, June 1970
SP-8058	Spacecraft Aerodynamic Torques, January 1971
SP-8059	Spacecraft Attitude Control During Thrusting Maneuvers, February 1971
SP-8065	Tubular Spacecraft Booms (Extendible, Reel Stored), February 1971
SP-8070	Spaceborne Digital Computer Systems, March 1971
SP-8071	Passive Gravity-Gradient Libration Dampers, February 1971
SP-8074	Spacecraft Solar Cell Arrays, May 1971
SP-8078	Spaceborne Electronic Imaging Systems, June 1971
SP-8086	Space Vehicle Displays Design Criteria, March 1972

SP-8096	Space Vehicle Gyroscope Sensor Applications, October 1972
SP-8098	Effects of Structural Flexibility on Entry Vehicle Control Systems, June 1972
SP-8102	Space Vehicle Accelerometer Applications, December 1972

CHEMICAL PROPULSION

SP-8087	Liquid Rocket Engine Fluid-Cooled Combustion Chambers, April 1972
SP-8081	Liquid Propellant Gas Generators, March 1972
SP-8052	Liquid Rocket Engine Turbopump Inducers, May 1971
SP-8048	Liquid Rocket Engine Turbopump Bearings, March 1971
SP-8101	Liquid Rocket Engine Turbopump Shafts and Couplings, September 1972
SP-8094	Liquid Rocket Valve Components, August 1973
SP-8097	Liquid Rocket Valve Assemblies, November 1973
SP-8090	Liquid Rocket Actuators and Operators, May 1973
SP-8080	Liquid Rocket Pressure Regulators, Relief Valves, Check Valves, Burst Disks, and Explosive Valves, March 1973
SP-8064	Solid Propellant Selection and Characterization, June 1971
SP-8075	Solid Propellant Processing Factors in Rocket Motor Design, October 1971
SP-8076	Solid Propellant Grain Design and Internal Ballistics, March 1972
SP-8073	Solid Propellant Grain Structural Integrity Analysis, June 1973
SP-8039	Solid Rocket Motor Performance Analysis and Prediction, May 1971
SP-8051	Solid Rocket Motor Igniters, March 1971
SP-8025	Solid Rocket Motor Metal Cases, April 1970
SP-8041	Captive-Fired Testing of Solid Rocket Motors, March 1971

☆ U.S. GOVERNMENT PRINTING OFFICE: 1974—739-161/135

NATIONAL AERONAUTICS AND SPACE ADMINISTRATION
WASHINGTON, D.C. 20546

OFFICIAL BUSINESS
PENALTY FOR PRIVATE USE $300

SPECIAL FOURTH-CLASS RATE BOOK

POSTAGE AND FEES PAID
NATIONAL AERONAUTICS AND
SPACE ADMINISTRATION
451

POSTMASTER: If Undeliverable (Section 158 Postal Manual) Do Not Return